BENEMÉRITA UNIVERSIDAD AUTÓNOMA DE PUEBLA

INSTITUTO DE FÍSICA “LUIS RIVERA TERRAZAS”

“NUMERICAL STUDY OF PROPAGATION AND INTERACTION OF SPATIAL SOLITONS IN NONLINEAR AND NONLOCAL MEDIA”

THESIS

TO OBTAIN THE DEGREE OF

DOCTOR OF PHILOSOPHY (PhD) (PHYSICS)

PRESENTED BY:

MAJID HESAMI

SUPERVISORS:

MARCELA MARIBEL MENDEZ OTERO

J. JESUS ARRIAGA RODRIGUEZ

JANUARY 2020

PUEBLA, MEXICO

BENEMÉRITA UNIVERSIDAD AUTÓNOMA DE PUEBLA

INSTITUTO DE FÍSICA “LUIS RIVERA TERRAZAS”

“NUMERICAL STUDY OF PROPAGATION AND INTERACTION OF SPATIAL SOLITONS IN NONLINEAR AND NONLOCAL MEDIA”

TESIS

PARA OBTENER EL GRADO DE

DOCTOR EN CIENCIAS (FÍSICA)

PRESENTA:

MAJID HESAMI

ASESOR(ES):

MARCELA MARIBEL MÉNDEZ OTERO
J. JESUS ARRIAGA RODRIGUEZ

ENERO 2020
PUEBLA, MEXICO

Acknowledgments

This research was carried out with the financial support of CONACYT (Consejo Nacional de Ciencia y Tecnología).

Agradecimientos

Este trabajo se ha realizado con apoyo financiero del CONACYT (Consejo Nacional de Ciencia y Tecnología). Se agradece a la Vicerrectoría de Investigación y Estudios de Posgrado por el apoyo otorgado para la conclusión de esta tesis dentro del programa IV. Investigación y Posgrado. Apoyar a los Programas de posgrado para lograr su incorporación al Padrón Nacional de Calidad. Indicador establecido en el plan de Desarrollo Institucional 2017-2021. Y también agradezco a todos los integrantes del jurado revisor por sus correcciones y comentarios, Dr. Felipe Pérez Rodríguez, Dr. José Antonio Méndez Bermúdez, Dr. Julio Villanueva Cab, Dr. José Javier Sánchez Mondragón, y Dra. Marcela Maribel Méndez Otero.

If you fall in love with the road,
you will forget the destination
(Zen Saying)

ABSTRACT

The main objective of this thesis is to perform a numerical study of the generation and propagation of space optical solitons in a nonlocal medium as a realistic media. The nonlocality of the medium is considered numerically through different symmetric functions, where its width is considered as the degree of nonlocality. So, the propagation of arbitrary beam profile in a nonlocal medium is studied. Amazingly, by choosing appropriate beam-width, the intensity profile, can be confined in direction of propagation with small oscillation, called quasi-soliton. Some arbitrary initial beam profiles are investigated to propagate in nonlocal medium with appropriate initial beam-width, resulting in quasi-solitons (The quasi-soliton is a soliton-like beam that propagates similar to a soliton but demonstrates some oscillations in its intensity profile and beam-with). These quasi-solitons after some initial distance of propagation, reshape to a Gaussian profile, where their profiles are obtained analytically and are simulated for comparison with the final intensity profile.

For this purpose, in this thesis, the propagation of the paraxial center of an intense beam in different media is investigated. First, we demonstrate the spatial propagation of a Gaussian beam in a linear medium, where the Helmholtz equation is governing the medium. The Fourier transform method is employed, and by using the obtained Transfer Function in the Fourier domain, the propagation is simulated numerically by a MATLAB program. It is showed that the beam suffers pure diffraction during the propagation. Then to study the propagation of a beam in a third order nonlinear medium, also known as Kerr medium, the Nonlinear Schrodinger (NLS) equation is obtained from Maxwell equations. Two solitary solutions of the NLS equation are analytically obtained. These two solutions correspond to beams spatially confined in direction of perpendicular

to the direction of propagation and are called bright and dark spatial solitons. The Self-focusing and self-defocusing effects for positive and negative Kerr medium respectively are explained. These effects conflict with the diffraction effects and produce solitons. The soliton propagation in Kerr medium is obtained by solving the NLS equation using the Split-Step method and numerical simulation by a MATLAB program. The propagation of intensity profile of the soliton, which propagates with a constant profile, is simulated. The interaction between two spatial solitons, when they are propagating, either initially parallel trajectory or at some angles, is discussed. The interaction by considering different relative phases between two solitons is presented. It is demonstrated that the "force" between the solitons varies smoothly from maximum attractive at $\Delta\phi$=0, to maximum repulsive at $\Delta\phi=\pi$. The results show that, when two bright solitons propagate with a big angle, after the collision, they never return to each other and continue their own modified paths. Furthermore, the beam propagation for nonlocal medium is investigated. The response of the nonlocal medium at a point is not determined solely by the wave intensity at that point (as in local media) but also depends on the wave intensity in its vicinity.

Preface

In recent years, Photonics has enabled the introduction of new science and technology areas based on the nonlinear propagation and interaction of light beams. Although the propagation of optical beams is actively investigated, still there is a larger variety of studies to be made on realistic and new media and new beams where they will exhibit different and new properties. Those properties and new phenomena, which occur due to beam propagation and in particular soliton propagation in different media, has allowed us to get to the point to consider back applications such as transferring of data through fiber optics, telecommunication, all-optical switching and optical circuits [96] [25]. A significant part of these mentioned applications corresponds to the confining of the beam intensity in the propagation direction, and this cannot comprehensively be achieved if the soliton definition is not in the circle of our knowledge [2].

Although the soliton definition and their properties are well known, a first step on this thesis is to make a review on the topic. Soliton propagation, and interaction phenomena, is the backbone for constructing our beam propagation discussion on realistic properties media. Properties, such as nonlocality, are the central topics of this thesis [15][26][3][48][49]. In addition, starting the thesis from the basics, and from there reaching the thesis goal, is a convenient approach to introduce new readers who are not familiar with the soliton propagation and interaction topics [20][24]. As such, the initial soliton definition is that of a localized wave that propagates without a intensity profile change through a third order nonlinear medium. This localized wave forms when the dispersion, or associated diffraction, is compensated by the nonlinear effect induced by the wave itself. Depending on the type of nonlinearity, the nonlinear media may support either bright or dark solitons [52][53]. While bright spatial solitons are just finite-size beams formed in media with self-focusing nonlinearity, dark spatial solitons are more complex objects and they represent an intensity dip in an otherwise constant background with nontrivial phase profile. Spatial bright (dark) solitons have been observed and studied in media with a positive (negative) or self- focusing (-defocusing) nonlinearity [45].

The novelty and key topic of this thesis lies on the nonlocal concept. The nonlocal nonlinearity nature results from the influence of the transport process such as atom diffusion or heat transfer [7], [8],[9]. It can originate from long-range molecular interactions as in a nematic liquid crystals [37] with an orientational nonlocal nonlinearity [12]. Nonlocality appears naturally in a large variety of physical systems, including thermal media, and also Bose-Einstein condensates [13] [29]. It implies that the response of the medium at a particular point is not solely determined by the wave intensity at that point (as in a local media case) but also depends on the wave intensity in its vicinity [16] [17].

Nonlocality plays an important role on the generation and dynamics of self-trapped optical beams. Studies of spatially nonlocal nonlinearities reveal several interesting effects. Perhaps most important one, nonlocality tends to suppress the modulational instability (MI) [48] [104] of plane waves propagating in self-focusing media [26]. While the suppression is the case, it is worth noting that certain types of nonlocality may promote MI, even in defocusing media. It is well-known that localized multi-dimensional waves [4] in media with a focusing nonlinearity may exhibit strong self-focusing which can lead to a catastrophic increase (blow-up, or collapse) of the intensity over finite time (i.e.in temporal soliton), or propagation distance (i.e. in spatial soliton) [24]. However, nonlocality can prevent catastrophic collapse of beams and stabilize multidimensional solitons as was first shown by Turitsyn for a restricted class of models and more recently for general nonlocal models. As the result nonlocality has been proved to stabilize optical beams that would otherwise become unstable in a pure local nonlinear medium (such as propagation of two-dimensional optical soliton [3][31][38]).

In local medium, while bright solitons may attract, repel, or even form bound states, depending on their relative phase; dark solitons always repel each other [90]. This has been confirmed in numerous theoretical and experimental works. [91]. However, when availability of nonlocality is the case, spatial nonlocality provides stabilization of bright solitons and induces their attraction even if they are out-of-phase. The nature of dark soliton interaction can be drastically altered by the spatially nonlocal character of nonlinearity, and it has been shown that nonlocality induces attraction leading to the formation of their bound states as degree of nonlocality grows in both manner of numerically and experimentally [3].

Although there are many of materials that shows the nonlocality, as the example the paraffin oil dyed with iodine, Nematic liquid crystal, and composite materials with metallic nanoparticles can be mentioned that recently have been used for conducting the related investigation.

In this thesis, in addition of simulation for beam propagation in linear and third order nonlinear (Kerr) medium, the numerical nonlocal medium beam propagation has been conducted from a low to a high degree of nonlocality for positive and negative Kerr media. Although a variety of symmetric nonlocal response functions have been considered, at the end, we have concluded that there is not such a difference for considering different responses.

Quasi-soliton pulses are soliton-like pulses in lasers or fiber-optics links, where true solitons cannot exist. In this thesis, Spatial quasi-soliton refers to a soliton-like beam that includes some small inherent oscillation on its intensity profile and beam-width through propagation. Although the quasi-soliton has some differences from perfect soliton, it has many characteristics of the soliton, such as making a self-waveguide and having the ability to send a low intense prob beam in the provided waveguide [82].

The central work of this thesis is at the nonlocality characteristic, where the arbitrary initial beam profiles ((hyperbolic secant, exponential and gaussian) have been considered. We have amazingly obtained the way how to confine the intensity of the beam on the path direction into the so-called quasi-soliton. Different degrees of nonlocality and different nonlocal response functions have been chosen for both of positive and negative Kerr medium. In all these different situations, the quasi-soliton has been obtained by just simply adjusting the best initial beam-width. Another interesting point that has been demonstrated for a nonlocal medium is that the beam profiles evolves into a gaussian profile for positive Kerr medium and reversed-Gaussian profile for negative Kerr medium; regardless of the nonlocal response function, the degree of nonlocality, and the initial beam profile.

Later, we didn't limit our self to just nonlocal media and we have obtained the quasi-soliton in local medium as well by arbitrary initial beam profiles (from exponential and triangular, to super-Gaussian and rectangular) in positive and negative Kerr media. Additional interesting points have been obtained in a local medium, where all the arbitrary initial beam profiles evolve into a hyperbolic secant and hyperbolic tangent in positive and negative Kerr medium respectively.

We have included this preface, since we wanted to stand out the important part of this research. The included references also are used in the text.

Contents

List of Tables:

List of Figures:

Chapter 1: **Introduction**

Self-trapped optical beams, or more precisely spatial optical solitons [1], propagate without change through nonlinear media. They can be generated in media that present an intensity-dependent refractive index [2], where diffraction is compensated by the nonlinear effects. While in the local medium limit, the change of refractive index in one point depends on the intensity in that point; in nonlocal medium, the change of refractive index depends on the intensity in the vicinity points [3]. Analytical solutions for such solitons have been obtained from the equations that describe the beam evolution in local [4] and nonlocal media [5][6].

In optics, nonlocality can be due to different physical mechanism [7], such as long-range forces [8], transport [9], or many body interaction [10], [11]. Nonlocality naturally appears In many media or physical systems, such as Nematic liquid crystal [12], Bose-Einstein condensates [13], thermal media [14], etc. The most accepted mathematical model to describe the nonlocality of a medium is considering that the change of induced refractive index Δn, in the (1+1)-Dimensional Nonlinear Schrödinger (NLS) equation, must be written by a convolution integral between the medium nonlocal response function R(X) and the beam intensity I(X) according to [3]:

$$\Delta \mathrm{n(I)} = \int_{-\infty}^{+\infty} \mathrm{R}(X' - X) I(X', Z) dX' \qquad (1.1)$$

where the medium response function $\mathrm{R}(X)$ has the property of being real, localized, and symmetric. The Response function width is associated to the degree of nonlocality and can go from a narrow value as Dirac delta function which describes a local medium up to a highly nonlocal situation. It is well known that the hyperbolic secant (Sech) initial profile is adequate to obtain spatial optical soliton in a local medium [4]. However, for a nonlocal medium with different degree of nonlocality the exact analytical solutions [3], [5], [6] can be very complicated. In reference [15], a numerical method was developed to obtain soliton solutions in media with an arbitrary degree of nonlocality for two types of response functions: Gaussian and exponential. The authors obtained that, in media with Gaussian response function for high nonlocality the soliton profile must be Gaussian. However, for very low nonlocality the Sech profile is the adequate profile for soliton. However, for the case of media with an exponential response function, even in the case of high nonlocality, Gaussian beam profile is not the adequate for a soliton behavior.

Little attention has been given to analyze what happens when an arbitrary initial beam profile is propagated in one-dimensional nonlinear media with any degree of nonlocality. In spite that exist methods (see for example [16], [17] and references therein) to find the adequate initial soliton profile for any degree of nonlocality.

1.1 Local medium

An optical material that exhibits third order non-linearity (local), generates nonlinear optical interactions such as: Third Harmonic Generation (THG), Self-Phase Modulation, Sum and Difference Frequency Generation, Four wave mixing, Optical Phase Conjugation, and Optical Rectification [18], [19]. In the nonlinear optical interaction in Self-Phase-Modulation, there are optical phenomena such as Optical Kerr Effect, Self-Focusing, Self-Defocusing, Spatial Solitons, and Raman Effect.

When an intense optical beam travels through a homogenous non-linear medium of a certain thickness, the refractive index is altered in a non-uniform manner, so that, the medium can act as a graded-index waveguide. In this way, the beam can create its own waveguide. If the intensity of the beam has the same spatial distribution in the transverse plane as one of the modes of the waveguide that the beam self-creates, the beam propagates without changing its spatial distribution. Under such conditions, diffraction is compensated by the non-linear effect and the beam is confined to its self-created waveguide [20]. Such self-guided beams are called spatial solitons. Nonlinear effects in optics have become accessible after the invention of the laser by Mainman and his collaborators 1960 [21], who made available light intensities strong enough to excite a nonlinear behavior. The first experimental demonstration of nonlinear phenomena in optics was the Second Harmonic Generation (SHG) by Franken et al. in 1961[22]. Ever since many kinds of nonlinearities have been discovered. The simplest nonlinearity is the Kerr one, which entails a nonlinear polarization P_{NL} given by $P_{NL} = x^{(3)}E^3$ in isotropic media. Using the latter in the electric field ruling equations, nonlinear change in the refractive index Δn is given by $\Delta n = n_2 I$, I being the beam intensity and n_2 the Kerr coefficient [23]. Therefore, propagating fields modulate their own phase: for spatially finite beams propagating in homogeneous media, self-focusing (self-defocusing) effect [20][24] occurs if $n_2 > 0$ ($n_2 < 0$) and frequency nonlinear chirp happens [25] for finite pulses propagating in guides (for example fibers).

The paraxial evolution of a (1+1)-Dimensional beam, propagating along the z-direction in a local Kerr medium ($\Delta n(I) = n_2 I$) is described by the Nonlinear Schrodinger (NLS) equation given by:

$$-i\frac{\partial A(X,Z)}{\partial Z} = \frac{1}{4}\frac{\partial^2 A(X,Z)}{\partial X^2} + \frac{L_D}{L_{NL}}|A(X,Z)|^2 A(X,Z) \qquad (1.2)$$

where $A(X,Z)$ is the field amplitude given by $E = E(x,z)\exp(ikz)$ normalized to the maximum intensity $I_m^{1/2}$, $L_D = (n_0 k_0 \omega_0^2)/2$ is the Rayleigh distance or diffraction length, with n_0 the linear refractive index, $k_0 = 2\pi/\lambda$ the wave vector, λ the wavelength, ω_0 is the initial beam width, $L_{NL} = (n_2 k_0 I_m)^{-1}$ the self-focusing distance, n_2 the nonlinear refractive index, $X = x/\omega_0$ and $Z = z/L_D$ are the normalized lengths along transversal axis and direction of propagation. When $L_D/L_{NL} = 1$ and n_2 is positive, equation (1.2), allows an analytical solution known as a fundamental soliton described by hyperbolic secant (Sech) profile called bright spatial soliton.

1.2 Nonlocal medium

In recent years, the study of non-linear effects in non-local media has attracted great interest in some areas of physics including non-linear optics [26][27]. In a non-local environment, the non-linear response induced at a certain point, depends on the surrounding region. In this way, a narrow-localized wave can induce a wide spatial response in the medium. The important role of nonlocality appears in many areas of nonlinear physics, including plasma physics [11], BEC [28] [29], fluid mechanics [30] and optics [31]. In general, the non-locality that appears in many optical systems are consequence of, for example, the transport process, the conduction of heat in thermal media [32][33], diffusion in atomic vapors [34][35][36], or due to long-range interaction as in the Nematic liquid crystals [37]. A spatial nonlocal response can deeply affect the propagation of nonlinear waves, e.g. stabilizing two-dimensional self-guided beams [3][31][38], or even more complicated structures [39][40][41][42][43]. The nature and extent of nonlocality substantially depend on materials, i.e. in optics, thermo-optic media [32][33][44], photorefractive [45], soft-matter [27], semiconductor amplifier [36], atomic or molecules diffusion in vapors [35] and liquid crystals [46][47]. Propagation of beams in nonlinear media can be dramatically modified due to nonlocality [3][48][49], i.e. changes in soliton interactions [50][51][39][44]. This is due to the non-local response resulting in the formation of an effective potential, which produces an attractive

force acting between distant solitons [33],[31]. The effect is particularly dramatic in the case of self-defocusing and interactions of dark solitons, which is in contrast to local environment [52][53], can exhibit attraction and similarly generates bound states [39][44]. To date, there are several published works regarding the propagation of bright and dark spatial solitons, uni-dimensional and bi-dimensional, in nonlinear and non-local media [3][31][54][8][55][56].

The NLS equation for nonlocal case [57], can be written as equation (1.3), where the positive (negative) signs correspond to a focusing (defocusing) nonlinearity and r and Z denote transverse and propagation-normalized coordinates, respectively. It is assumed, that the refractive index change $\Delta n(I)$, induced by the beam, with intensity $I(r,z) = |q(r,z)|^2$ can be described by the phenomenological nonlocal model (1.4).

$$-i\frac{\partial q(r,z)}{\partial Z} = \frac{1}{4}\left(\frac{\partial^2 q(r,z)}{\partial X^2} + \frac{\partial^2 q(r,z)}{\partial Y^2}\right) \pm \Delta n(\mathrm{I}) * q(r,z) \qquad (1.3)$$

$$\Delta n(I)(r,Z) = \int_{-\infty}^{+\infty} R(r'-r)I(r',Z)dr' \qquad (1.4)$$

In equation (1.4), the induced refractive index change, $\Delta n(I)$, is the convolution between local intensity and $R(r)$, the response function of the medium. The integral $\int dr'$ is over all transverse dimension. The response function $R(r)$ is assumed to be real, localized and symmetric.

We have considered the following three normalized response functions, and in the chapter of nonlocality it is demonstrated that there is not difference between considering these response functions:

$$\begin{cases} R_g(X) = \dfrac{1}{\alpha_g\sqrt{\pi}}\exp\left(-\left(\dfrac{X}{\alpha_g}\right)^2\right) & \rightarrow \text{Normalized gaussian nonlocal response} \\ R_S(X) = \dfrac{1}{\int_{-\infty}^{+\infty} Sech\left(\dfrac{X}{\alpha_s}\right)dX}\, Sech\left(\dfrac{X}{\alpha_s}\right) & \rightarrow \text{Normalized Sech nonlocal response} \\ R_e(X) = \dfrac{1}{2*\alpha_e}\exp\left(-\dfrac{|X|}{\alpha_e}\right) & \rightarrow \text{Normalized exponential nonlocal respons} \end{cases} \qquad (1.5)$$

Where $\alpha_s, \alpha_g, \alpha_e$ are the widths related with the degree of nonlocality of Sech, Gaussian and Exponential nonlocal response functions respectively.

1.3 Method of propagation in local and nonlocal medium in this thesis

In this thesis, beginning from Maxwell's equations, the Helmholtz equation is rederived. By considering the Polarization in linear medium, a general wave equation is derived to study the light propagation. The obtained wave equation just shows pure diffraction. The propagation of collimated one- and two-dimensional Gaussian beams is studied. Then the Nonlinear Schrodinger (NLS) equation is obtained by substituting the third-order nonlinear Polarization in the wave equation. The NLS equation contains the diffraction effect and the Self-focusing (or Self-defocusing) effect. The situation when these two effects are compensated, is investigated. The analytical solution is determined to obtain the exact solution of the NLS equation. Numerical simulations are developed in the MATLAB programming software package. Those techniques included Fast Fourier Transform (FFT) and the Split-Step propagation algorithm [58]. The split-step method was introduced by Fisher [59], and it is also known as the Split-Step Fourier method. The method calculates the propagation of an optical field in dispersive and nonlinear medium considering small segments in which one of the two properties is absent [60], and has been widely used to solve the NLS equation in optical fibers (see for example [61]). The method is reliable, versatile and allows the study of new problems [62] [63].

For the next step, the nonlocality effect in the NLS equation is considered. Three different (Gaussian, Exponential, Hyperbolic Secant) nonlocal response functions of medium with different degree of nonlocality are considered, from low up to high nonlocality. The effect of nonlocality in the NLS equation is considered by substituting the change of induced refractive index by the mathematical convolution between local intensity and nonlocal response function. By doing this, the modified NLS equation for the nonlocal medium is obtained. The result of beam propagation demonstrates that, in local medium, arbitrary shape symmetric beam profile with the adequate initial beam-width can propagate as a quasi-soliton and the propagated intensity profile takes the form of square hyperbolic secant. On the other hand, in nonlocal medium with arbitrary nonlocal response function and with any degree of nonlocality a similar behavior can be obtained: any initial beam profile with suitable initial beam-width can give rise to a quasi-soliton. In this case the propagated intensity profile takes the form of square Gaussian.

1.4 Thesis Objectives

1.4.1 General objective

Numerical study of the behavior and properties of the propagation and interaction of spatial optical solitons in non-linear and non-local media.

1.4.2 Specific objectives

1- Analyze the equation that governs the propagation of an optical field in a non-linear medium.
2- Determine the initial conditions for the generation of spatial optical solitons, as well as how to introduce the non-locality of the medium into the model.
3- Implement a numerical method to solve the nonlinear equation that governs the propagation of spatial optical solitons.
4- Develop the numerical program that allows the propagation and interaction of spatial solitons in a non-linear non-local optical medium.
5- Obtain the numerical results of the propagation and interaction of spatial solitons in non-linear non-local media.
6- Determine the influence of the non-locality of the medium in the generation of spatial solitons.

1.5 Thesis outline:

Chapter 2: Beam Propagation. In this chapter the beam propagation in both linear and third-order nonlinear (Kerr) medium is investigated. First, we started from Maxwell equations and by considering linear and third order nonlinear polarization, and paraxial approximation, the Paraxial Helmholtz Equation, and Nonlinear Schrödinger equation for the linear and nonlinear medium are obtained respectively. In the linear medium, the Fourier Transform is applied to the equation to change the spatial coordinates to spatial frequencies and obtain the Transfer function. A Numerical MATLAB program is used to simulate the propagation of a Gaussian beam as an initial condition in the linear medium. For testimony of the numerical MATLAB program results, the initial and the obtained final intensity profile for the propagation along one Rayleigh distance are compared

with those reported in many nonlinear books such as reference [18]. The NLS equation in third order (Kerr medium) nonlinearity, depends on the Kerr coefficient sign ($n_2 > 0, n_2 < 0$), and allows two different solutions, bright and dark spatial solitons respectively. Analytically NLS equation is solved to obtain the exact solution for bright and dark solitons. Thereafter, by using the Split-Step method and the MATLAB program, the beam propagation in Kerr medium is numerically simulated.

Chapter 3:Interactions and Collision,

In this chapter, the soliton interaction in a third order nonlinear medium is reviewed. We discussed the interaction between two initially parallel trajectories bright spatial solitons (Sech) when the different initial relative phases are chosen. For the case of zero relative phase between two Sech beams ($\Delta\phi = 0$), the two beams are absorbing and repelling each other periodically by propagation. However, repulsion is observed for the $\Delta\phi = \pi$. Then, the interaction of two initially parallel trajectories dark solitons is discussed, with the same initial condition as bright solitons. For the interaction of two dark solitons, it is observed that by considering any relative phase, just repulsion is demonstrated. In addition, in the case of the collision between two symmetric bright spatial solitons in ta Kerr medium. If we consider the two beams approaching at each other by a big angle, at the colliding point and depending on the relative phase, different values of energy are released into the medium. After the collision, the two beams continue their propagation with the same intensity profile as initial, just with a wider path angle.

Chapter 4:Quasi-solitons in nonlocal and local medium: In this chapter, the effect of nonlocality over the beam propagation is investigated. The nonlocality concept in Optics comes from the issue that the response of the medium, at a point, is not solely determined by the wave intensity at that point (as in local media), but also depends on the wave intensity in its vicinity. Different nonlocal response functions are considered, and for any nonlocal response function, a parameter (α) plays the role of nonlocality degree. From weak up to high nonlocality, the convolution between local intensity and nonlocal response function is used to define the induced change of the refractive index (Δn) in the NLS equation. A numerical MATLAB simulation of the propagation of a Sech profile bright spatial soliton in nonlocal medium with different degrees of nonlocality is presented. It is observed that by increasing the degree of nonlocality, more diffraction and intensity decay

occurs. For a better intensity confinement, its is necessary a reinforcement of the self-focusing part in the NLS equation as it is shown by the Sech beam propagation in the nonlocal medium with different degrees of nonlocality. To avoid such diffraction, some changes on the initial beam-width of the Sech beam are applied, until it is obtained the smallest on-axis intensity propagation variation. Different initial beam profiles are propagated in a nonlocal medium with different nonlocal response functions and degrees of nonlocality. For all these cases, the best initial beam-width is obtained for a beam propagating in a solitary way, and with the smallest on-axis intensity oscillation. Those beams that propagate in a solitary way, and with small intensity oscillation, are the so-called quasi-soliton. The arbitrary initial beam profiles, different from those of a local medium Sech beam, propagation is tested by changing the initial beam-width. The beam intensity profile almost becomes confined in the direction of propagation and a quasi-soliton in a local medium is observed.

Chapter 2: **Beam Propagation**

In this chapter, the theory of beam propagation in a linear medium with the Fourier Transform method will be presented. Next, the beam propagation in third order nonlinear (Kerr) medium, with the Split-Step method is discussed. Then we introduce the spatial solitons as the solitary solution of Nonlinear Schrodinger (NLS) equation. Bright and dark spatial soliton as exact analytical solutions of the NLS equation for positive and negative Kerr medium will be presented respectively. In addition, the soliton propagation is numerically simulated by a MATLAB program. The results of the simulation are shown and discussed.

2.1 Beam Propagation in a Linear Medium

Before invention of the laser beam, predominant thoughts were on the issue that all the media have linear response for an incident light beam. The considered medium is Linear, Homogeneous, Isotropic, Non-magnetic, Non-dispersive and does not have any free charge. Definition of mentioned media is presented below:

Linear Medium: The medium is linear if it satisfies the linearity properties. If we can write $\vec{P} = \epsilon_0 \vec{E}$. It means that the polarization is proportional to the electric field and then the medium is linear.

Homogeneous Medium: The medium is homogeneous if its permittivity (ϵ) is constant throughout the region of propagation.

Nondispersive Medium: The medium is nondispersive if its permittivity (ϵ) is independent of wavelength over the wavelength region occupied by the propagating wave, in other words in Nondispersive medium the refractive index is not dependent on frequency.

Dispersive Medium: The medium is dispersive if the refractive index is dependent on the frequency of the wave, this means that waves of different frequencies travel at different velocities [64].

Nonmagnetic Medium: The medium is nonmagnetic, when the magnetic permeability (μ) is equal to (μ_0) the vacuum permeability.

Isotropic Medium: The medium is isotropic if its properties are independent of the direction of polarization of the wave. This means that in the equation $\vec{D} = \epsilon_0\vec{E} + \vec{P} = \epsilon_0\left(1 + x^{(1)}\right)\vec{E}$, $\vec{D}$ and $\vec{E}$ are parallel to each other and $x^{(1)}$ is a scalar.

Anisotropic Medium: The medium is anisotropic if $\vec{D}$ and $\vec{E}$ are not parallel to each other. In general, in equation $\vec{D} = \epsilon\vec{E}$, ϵ is not scalar. So, in general ϵ is a tensor and the displacement vector can be written as follows:

$D_x = \epsilon_{xx}E_x + \epsilon_{xy}E_y + \epsilon_{xz}E_z$

$D_y = \epsilon_{yx}E_x + \epsilon_{yy}E_y + \epsilon_{yz}E_z$

$D_z = \epsilon_{zx}E_x + \epsilon_{zy}E_y + \epsilon_{zz}E_z$

The epsilon matrix always is a symmetric matrix. It means that $\epsilon_{xy} = \epsilon_{yx}, \epsilon_{xz} = \epsilon_{zx}$ and $\epsilon_{yz} = \epsilon_{zy}$. Always it is possible to choose a coordinate system where this matrix becomes diagonal and consequently, all off-diagonal elements become zero and the coordinate system is called principal axis.

$$\begin{pmatrix} D_x \\ D_y \\ D_z \end{pmatrix} = \begin{pmatrix} \epsilon_{xx} & 0 & 0 \\ 0 & \epsilon_{yy} & 0 \\ 0 & 0 & \epsilon_{zz} \end{pmatrix}\begin{pmatrix} E_x \\ E_y \\ E_z \end{pmatrix}$$

Therefore, in the principal axis, it can be written as:

$D_x = \epsilon_{xx}E_x$

$D_y = \epsilon_{yy}E_y$

$D_z = \epsilon_{zz}E_z$

Different Media are defined according to the value of the matrix elements by:

$$\begin{cases} 1 \rightarrow \epsilon_{xx} = \epsilon_{yy} = \epsilon_{zz} & Isotropic\ media \\ 2 \rightarrow \epsilon_{xx} = \epsilon_{yy} \neq \epsilon_{zz} & Uniaxial\ media\ (Anisotropic) \\ 3 \rightarrow \epsilon_{xx} \neq \epsilon_{yy} \neq \epsilon_{zz} & Biaxial\ media\ (Anisotropic) \end{cases}$$

In general, if we write $\vec{D} = \epsilon\vec{E}$, where ϵ is scalar and independent of position, it corresponds to the linear, homogenous, and isotropic medium. To study the beam propagation in Linear, Homogeneous, Isotropic, Non-magnetic and Non-dispersive medium, the Maxwell's equations in International System of units as are written as:

Faraday's law of induction,

$$\vec{\nabla} \times \vec{E} = -\frac{\partial \vec{B}}{\partial t} \tag{2.1}$$

Ampere's Law,

$$\vec{\nabla} \times \vec{B} = \mu_0 \vec{J_f} + \mu_0 \frac{\partial \vec{D}}{\partial t} \tag{2.2}$$

Gauss's law for magnetism,

$$\vec{\nabla} \cdot \vec{B} = 0 \tag{2.3}$$

Gauss's law for electricity,

$$\vec{\nabla} \cdot \vec{D} = \rho \tag{2.4}$$

In order to find the corresponding wave equation, we can proceed by taking the curl of Faraday's law equation (2.1),

$$\vec{\nabla} \times \left(\vec{\nabla} \times \vec{E}\right) = \vec{\nabla} \times \left(-\frac{\partial \vec{B}}{\partial t}\right)$$

$$\vec{\nabla}\left(\vec{\nabla} \cdot \vec{E}\right) - \nabla^2 \vec{E} = -\frac{\partial}{\partial t}(\vec{\nabla} \times \vec{B})$$

Since there is no free charge $\vec{\nabla} \cdot \vec{D} = 0$ and $\vec{D} = \epsilon_0 \vec{E} + \vec{P} = \epsilon_0\left(1 + x^{(1)}\right)\vec{E}$. In general, the divergence of the electric field ($\vec{\nabla} \cdot \vec{E}$) is not zero but in an isotropic medium where it is zero ($\vec{\nabla} \cdot \vec{E} = 0$). By using Ampere's law (2.2), and taking into account non-magnetic materials;

$-\nabla^2 \vec{E} = -\frac{\partial}{\partial t}\left(\mu_0 \vec{J}_{\mathrm{f}} + \mu_0 \frac{\partial \vec{D}}{\partial t}\right) \rightarrow \vec{J}_{\mathrm{f}} = 0 \rightarrow$ There is no free current density.

$$-\nabla^2 \vec{E} = -\mu_0 \frac{\partial^2 \vec{D}}{\partial t^2} = -\mu_0 \frac{\partial^2}{\partial t^2}(\epsilon_0 \vec{E} + \vec{P}) = -\mu_0 \epsilon_0 \frac{\partial^2 \vec{E}}{\partial t^2} - \mu_0 \frac{\partial^2 \vec{P}}{\partial t^2}$$

The wave equation is obtained as follow:

$$\begin{cases} \nabla^2 \vec{E} - \frac{1}{c^2}\frac{\partial^2 \vec{E}}{\partial t^2} = \mu_0 \frac{\partial^2 \vec{P}}{\partial t^2} \\ \nabla^2 \vec{E} = \mu_0 \frac{\partial^2 \vec{D}}{\partial t^2} \end{cases} \tag{2.5}$$

In general, the polarization is expressed in a Taylor expansion as:

$$P = E\frac{\partial P}{\partial E} + \frac{1}{2}E^2 \frac{\partial^2 P}{\partial E^2} + \frac{1}{6}E^3 \frac{\partial^3 P}{\partial E^3} + \cdots \tag{2.6}$$

This can be written as:

$$P = \epsilon_0 x^{(1)} E + \epsilon_0 x^{(2)} E * E + \epsilon_0 x^{(3)} E * E * E + \cdots \quad (2.7)$$

Where $x^{(1)}$ is the first order, $x^{(2)}$ the second order, and $x^{(3)}$ the third order of susceptibility, and so on. For the case of free space ($P = 0$) the wave equation (2.5) is,

$$\nabla^2 \vec{E} - \frac{1}{c^2} \frac{\partial^2 \vec{E}}{\partial t^2} = 0 \quad (2.8)$$

For the case of linear medium, the equations (2.5) may be viewed as the inhomogeneous term to the wave equation. In a medium with an isotropic, and linear optical response, the polarization is:

$$\vec{P} = \epsilon_0 x^{(1)} \vec{E} \quad (2.9)$$

And the wave equation in the linear medium becomes:

$$\nabla^2 \vec{E} - \frac{1}{c^2} \frac{\partial^2 \vec{E}}{\partial t^2} = \mu_0 \frac{\partial^2}{\partial t^2} (\epsilon_0 x^{(1)} \vec{E})$$

$$\nabla^2 E - \frac{(1 + x^{(1)})}{c^2} \frac{\partial^2 E}{\partial t^2} = 0$$

$$D = \epsilon_0 E + P = \epsilon_0 E + \epsilon_0 x^{(1)} E = \epsilon_0 \left(1 + x^{(1)}\right) E = \epsilon_0 \epsilon_r E$$

$where\ n = \sqrt{\epsilon_r} = \sqrt{1 + x^{(1)}} \rightarrow n$ is the refractive index

$$\nabla^2 E - (n^2/c^2) \frac{\partial^2 E}{\partial t^2} = 0$$

and c/n is the velocity of the light in the medium.

$$\nabla^2 E - \left(\frac{1}{v^2}\right) \frac{\partial^2 E}{\partial t^2} = 0 \quad (2.10)$$

It is clear that there is not too much difference between the wave equation in the free space (2.8) and the linear medium (2.10), just the velocity of light in free space and in the medium is different.

Since the vector wave equation is obeyed by both $\vec{E}$ and $\vec{B}$, an identical scalar wave equation is defined by all components of those vectors. In general;

$\nabla^2 U(\vec{r}, t) - \frac{1}{v^2} \frac{\partial^2 U(\vec{r}, t)}{\partial t^2} = 0$,

where $U(\vec{r}, t)$ is any component of $\vec{E}$ or $\vec{B}$. A solution of this equation has the general form:

$$E(r, t) = E(r) e^{i(\vec{K}_0 . \vec{r} - \omega t + \phi_0)} \quad (2.11)$$

From electromagnetic theory the light is a wave composed of an electric field and a magnetic field, which are perpendicular to each other. In the mathematical representation of a wave, it suffices to

specify only the instantaneous value of the electric field as a function of time t. The electric field or magnetic field can be represented by:

$$U(\vec{r},t) = U(\vec{r})e^{-i\omega t} \;\rightarrow\; U(\vec{r}) = A(\vec{r})e^{in\vec{K}_0.\vec{r}} \tag{2.12}$$

In equation (2.12), $U(r,t)$ is separated in spatial $U(r)$ and temporal parts $e^{-i\omega t}$. $U(r)$ is a complex amplitude of the wave and its amplitude $A(r)$. Since the phase is constant, therefore, for a wave-front, $n\vec{K}_0.\vec{r} = \vec{k}.\vec{r}$ is constant. By substituting the general wave function (2.12) in the wave equation (2.10):

$$\nabla^2 U(\vec{r},t) - \frac{1}{v^2}\frac{\partial^2 U(\vec{r},t)}{\partial t^2} = 0$$

$$[\nabla^2 - \frac{1}{v^2}\frac{\partial^2}{\partial t^2}]\, U(\vec{r})e^{-i\omega t} = 0$$

$$\nabla^2 U(\vec{r}) + \frac{\omega^2}{v^2}U(\vec{r}) = 0$$

$$\frac{\omega^2}{v^2} = \left(\frac{\omega}{c/n}\right)^2 = \left(\frac{n2\pi\nu}{c}\right)^2 = \left(\frac{n2\pi}{c/\nu}\right)^2 = \left(\frac{n2\pi}{\lambda_0}\right)^2 = (nk_0)^2 = k^2$$

The Helmholtz equation in the medium is obtained:

$$[\ \nabla^2 + n^2k_0^2\ ]U(\vec{r}) = 0 \tag{2.13}$$

Two very simple solutions for equation (2.13) in homogeneous medium are “Plane waves” and “Spherical waves”. However, of our interest are those of the so-called paraxial approximation, (defined as a wave where normal wave fronts are paraxial rays). The complex amplitude of the wave function, propagating in the z-direction, can be written as:

$$U(\vec{r}) = A(\vec{r})e^{ink_0z} \tag{2.14}$$

By substituting (2.14) in Helmholtz equation (2.13):

$$[\ \nabla^2 + n^2k_0^2\ ]U(\vec{r}) = [\ \nabla^2 + n^2k_0^2\ ]\, A(\vec{r})e^{ink_0z} = 0 \tag{2.15}$$

$$\frac{\partial^2}{\partial x^2}[A(\vec{r})e^{ink_0z}] = \frac{\partial^2 A(\vec{r})}{\partial x^2}e^{ink_0z}$$

$$\frac{\partial^2}{\partial y^2}[A(\vec{r})e^{ink_0z}] = \frac{\partial^2 A(\vec{r})}{\partial y^2}e^{ink_0z}$$

$$\frac{\partial^2}{\partial z^2}\left[A(\vec{r})e^{ink_0z}\right] = \left[\frac{\partial^2 A(\vec{r})}{\partial z^2} + 2ink_0\frac{\partial A(\vec{r})}{\partial z} - n^2k_0^2A(\vec{r})\right]e^{ink_0z}$$

Since the complex envelope $A(\vec{r})$ varies slowly along the z-axis, within a wavelength distance $\Delta Z = \lambda$, it is possible to neglect the second partial derivative of A with respect to z.

$$\frac{\partial^2 A(\vec{r})}{\partial z^2} \ll \frac{\partial A}{\partial z}$$

Then the Paraxial Helmholtz Equation is obtained:

$$\nabla_T^2 A(\vec{r}) + 2ink_0 \frac{\partial A(\vec{r})}{\partial z} = 0 \qquad (2.16)$$

The Paraxial Helmholtz equation is a partial differential equation that resembles the Schrödinger equation of quantum physics. This equation describes the diffraction of an optical field as a function of the propagation distance. One solution to this equation is a Gaussian beam. To numerically study the propagation, we normalize the Paraxial Helmholtz Equation using parameters of the Gaussian beam: ω_0 and Z_R. ω_0 is the beam width or waist radius of the Gaussian beam at z=0, and Z_R is the Rayleigh range. The Rayleigh range or the Rayleigh distance, is the distance along the propagation direction of a beam measured from the waist to a distance where the area of the cross-section is doubled. The complex amplitude of the Gaussian beam [18] is given by:

$$U(\vec{r}) = A_0 \frac{\omega_0}{\omega(z)} \exp\left(-\frac{x^2+y^2}{\omega(z)^2}\right) \exp\left(-ink_0 z - ink_0 \frac{x^2+y^2}{2R(z)} + i\epsilon(z)\right) \qquad (2.17)$$

ω_0 is the beam width or waist radius of a Gaussian beam in z=0, and $\omega(z)$ is the width of the Gaussian beam at an axial distance z, which increases with the axial distance z as illustrated in Figure 2-1, and $R(z)$ is the radius of curvature of the wave-front.

$$\omega(z) = \omega_0 \left[1 + \left(\frac{z}{z_R}\right)^2\right]^{\frac{1}{2}}$$

$$R(z) = z\left[1 + \left(\frac{z_R}{z}\right)^2\right]$$

$$\epsilon(z) = \arctan\left(\frac{z}{z_R}\right)$$

$$\omega_0 = \left(\frac{\lambda_0 z_R}{n\pi}\right)^{\frac{1}{2}} \rightarrow z_R = \frac{n\,\pi\omega_0^2}{\lambda_0}$$

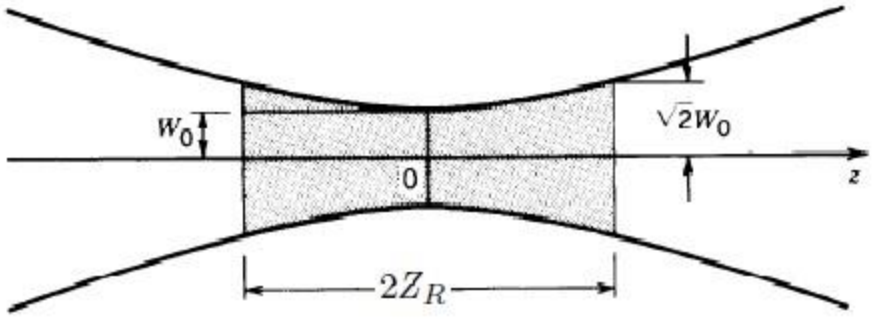

Figure 2-1: Gaussian beam [18]

Defining the normalized coordinate parameters $X, Y,$ and Z as,

$$X = \frac{x}{\omega_0}, \qquad Y = \frac{y}{\omega_0}, \qquad Z = \frac{z}{z_R}$$

$$\frac{\partial^2}{\partial x^2} = \frac{\partial}{\partial x}\left(\frac{\partial}{\partial x}\right) = \frac{\partial}{\partial x}\left(\frac{\partial X}{\partial x}\frac{\partial}{\partial X}\right) = \frac{\partial}{\partial x}\left(\frac{1}{\omega_0}\frac{\partial}{\partial X}\right) = \frac{1}{\omega_0^2}\frac{\partial^2}{\partial X^2}$$

With a similar result for the y-component. For the z component we have: $\frac{\partial}{\partial z} = \frac{1}{z_R}\frac{\partial}{\partial Z}$

We finally obtain the Normalized Paraxial Helmholtz Equation:

$$\frac{1}{\omega_0^2}\frac{\partial^2 A(X,Y,Z)}{\partial X^2} + \frac{1}{\omega_0^2}\frac{\partial^2 A(X,Y,Z)}{\partial Y^2} + \frac{2ink_0}{z_R}\frac{\partial A(X,Y,Z)}{\partial Z} = 0 \qquad (2.18)$$

The coefficient of the third term of this equation can be simplified as, $\frac{2ink_0}{z_R} = \frac{2in2\pi/\lambda_0}{n\pi\omega_0^2/\lambda_0} = \frac{4i}{\omega_0^2}$

And we obtain:

$$\frac{\partial A(X,Y,Z)}{\partial Z} = \frac{i}{4}\left[\frac{\partial^2 A(X,Y,Z)}{\partial X^2} + \frac{\partial^2 A(X,Y,Z)}{\partial Y^2}\right] \qquad (2.19)$$

To solve this equation, the two-dimensional Fourier transform on both sides of the equation is done.

$$F.T_{XY}\left[\frac{\partial A(X,Y,Z)}{\partial Z}\right] = F.T_{XY}\left[\frac{i}{4}\left[\frac{\partial^2 A(X,Y,Z)}{\partial X^2} + \frac{\partial^2 A(X,Y,Z)}{\partial Y^2}\right]\right] \qquad (2.20)$$

Where the Fourier transform is defined as,

$$\hat{A}(\omega_X, \omega_Y, Z) = \iint_{-\infty}^{+\infty} A(X,Y,Z)e^{i\omega_X X}e^{i\omega_Y Y}dX\,dY \qquad (2.21)$$

Here ω_X *and* ω_Y are the spatial angular frequencies (radians per unit length), where

$\omega_X = k_X = 2\pi\nu_X$, $\omega_Y = k_Y = 2\pi\nu_Y$ and $k_Z = 2\pi\nu_Z$.

k_X, k_Y and k_Z are the components of the wave vector $\vec{k} = k_X\hat{\imath} + k_Y\hat{\jmath} + k_Z\hat{k}$. And $k = |\vec{k}|$ is the wave number $k = |\vec{k}| = \sqrt{k_X^2 + k_Y^2 + k_Z^2} = \frac{2\pi}{\lambda}$. The elements ν_X and ν_Y are known as spatial frequencies -cycle per unit length- in X and Y directions respectively. It is worth to mention that spatial frequency does not exceed the inverse wavelength $(1/\lambda)$.

Let's analyze some of the basic characteristics of the solutions of these paraxial equations. Based on the properties mentioned in appendix (6.5) about Fourier transform of the first and second derivative of a function:

$$F.T\left[\frac{df(x)}{dx}\right] = \int_{-\infty}^{+\infty} \frac{df(x)}{dx} e^{-i\omega x} dx = (i\omega) F.T[f(x)]$$

$$F.T\left[\frac{d^2f(x)}{dx^2}\right] = \int_{-\infty}^{+\infty} \frac{d^2f(x)}{dx^2} e^{-i\omega x} dx = (i\omega)^2 F.T[f(x)] = -\omega^2 F.T[f(x)]$$

The equation (2.20) becomes:

$$\frac{\partial}{\partial Z}\hat{A}(\omega_X, \omega_Y, Z) = \frac{i}{4}[(i\omega_X)^2 + (i\omega_Y)^2]\,\hat{A}(\omega_X, \omega_Y, Z) \tag{2.22}$$

Integrating both sides:

$$\int \frac{\partial \hat{A}(\omega_X, \omega_Y, Z)}{\hat{A}(\omega_X, \omega_Y, Z)} = \int_0^{\mathrm{Z}} -\frac{i}{4}[\omega_X^2 + \omega_Y^2]\, dZ$$

$$\hat{A}(\omega_X, \omega_Y, Z) = \hat{A}(\omega_X, \omega_Y, 0) \exp\left[-\frac{i}{4}(\omega_X^2 + \omega_Y^2)\mathrm{Z}\right] \tag{2.23}$$

Equation (2.23) can propagate any initial function in the Fourier domain until the required distance Z. Just the initial beam profile in the Fourier domain must be multiplied with Transfer function $H(\omega_X, \omega_Y, Z)$ as,

$$H(\omega_X, \omega_Y, Z) = \frac{\hat{A}(\omega_X, \omega_Y, Z)}{\hat{A}(\omega_X, \omega_Y, 0)} = \exp\left[-\frac{i}{4}(\omega_X^2 + \omega_Y^2)\mathrm{Z}\right] \tag{2.24}$$

To obtain the propagated beam profile in space coordinates, the inverse Fourier transformation from the final wave function is required.

$$A(X, Y, Z) = I.F.T\left[\hat{A}(\omega_X, \omega_Y, Z)\right] \tag{2.25}$$

To implement numerically the beam propagation, it is necessary to do the Fourier transforms known as the discrete Fourier transforms. As is mentioned in the appendix (Program 6-1) a MATLAB program for the propagation of a Gaussian beam with the initial condition of $A(X) = \exp(-X^2)$ is written. One result of the MATLAB program is displayed in Figure 2-2. Figure 2-2a, is the top view of a Gaussian beam, launched from the downside into a linear medium, and Figure 2-2b demonstrates the normalized intensity of a one-dimensional Gaussian beam propagating in linear medium for one Rayleigh Range. We can observe that the beam gets broader as it propagates, due only to the diffraction effect. The Figure 2-3, compares the initial and final intensity profile after one Rayleigh range. Therefore, due to the beam diffraction, the intensity profile broadens due to propagation. In this figure, the blue line corresponds to the incident beam intensity, with a normalized maximum value of initial intensity equal to one ($I_0 = 1$), and the red line corresponds to the final propagated beam intensity profile, and the normalized maximum value of propagated intensity is $I_0/\sqrt{2} = I_0 * 0.7071$. This difference is reported in many nonlinear books such as reference [18]. Since here the linear medium with refractive index $n_0 = 1.5$ is considered, with $\lambda_0 = 600\ nm$ and $\omega_0 = 1000\ \mu m$, the value of Rayleigh Range is $z_R = \frac{n_0\,\pi\omega_0^2}{\lambda_0} = 7.8540$ meters. For the same condition but considering the free space ($n_0 = 1$), the value of the Rayleigh Range becomes $z_R = \frac{n_0\,\pi\omega_0^2}{\lambda_0} = 5.2360$ meters. It means, by propagation in linear medium $n = 1.5$, it reaches the same behavior for a 7.8540-meter propagation distance than when the propagation is done for a 5.236-meter propagation distance in free space. So, by increasing the refractive index, the same broadening on an intensity profile happens at long-distance.

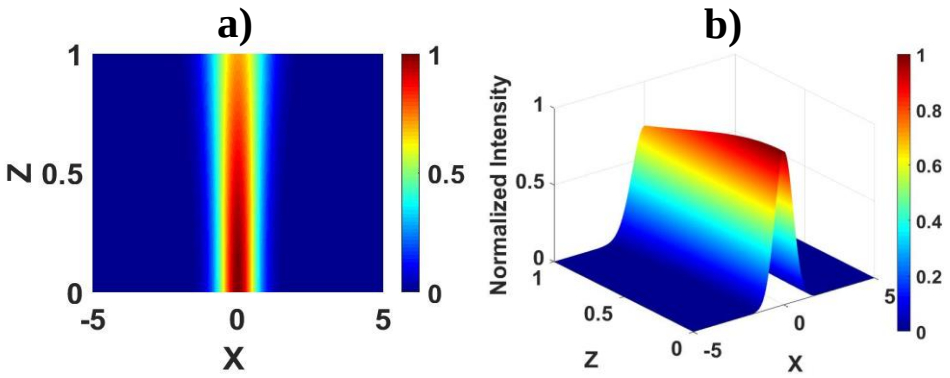

Figure 2-2: (a) top view of a Gaussian beam launched from the downside into a linear medium, (b) normalized intensity of one-dimensional Gaussian beam propagating in a linear medium for one Rayleigh Range. The beam gets broader as it propagates.

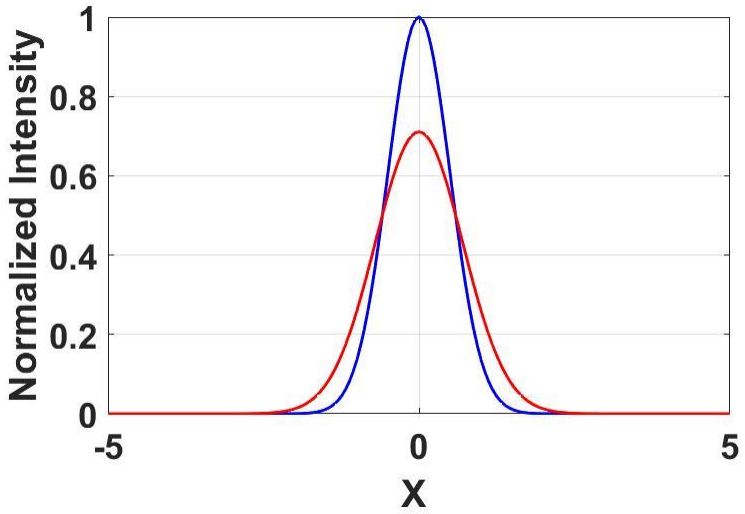

Figure 2-3: Comparison between initial (blue) and final (red) intensity profile of a gaussian beam for one Rayleigh Range propagation in linear medium

The MATLAB program for the simulation of the propagation of a two dimensional Gaussian beam $A(X,Y) = \exp\left(-(X^2 + Y^2)\right)$ appears in the appendix (Program 6-2). The comparison between initial intensity profile and the propagated intensity profile after one Rayleigh range appears in Figure 2-4. In Figure 2-4 (a & c), the initial intensity is figured out, while in Figure 2-4 (b & d) the intensity profile after one Rayleigh Range is plotted. In the down row of the figure, the area occupied by beam intensity is simulated and the color value referred to color bar shows the intensity value, whereas in the top row of the figure, intensity value as well as by color value, is

plotted in the perpendicular axis. Form Figure 2-4 the maximum value of initial normalized intensity at the center (X=0,Y=0) of the beam is 1, and after the one Rayleigh Range (1Z) propagation, the maximum value of normalized intensity comes to 0.5, which has similar rate as mentioned in reference [18]. For comparison between our result and the one reported in reference [18], Figure 2-5 shows the result of that reference. In this figure, the intensity value of a two-dimensional transverse Gaussian beam, before and after one Rayleigh range propagation in a linear medium, is demonstrated. The maximum value of final intensity is decreased to half value, same as our simulation result.

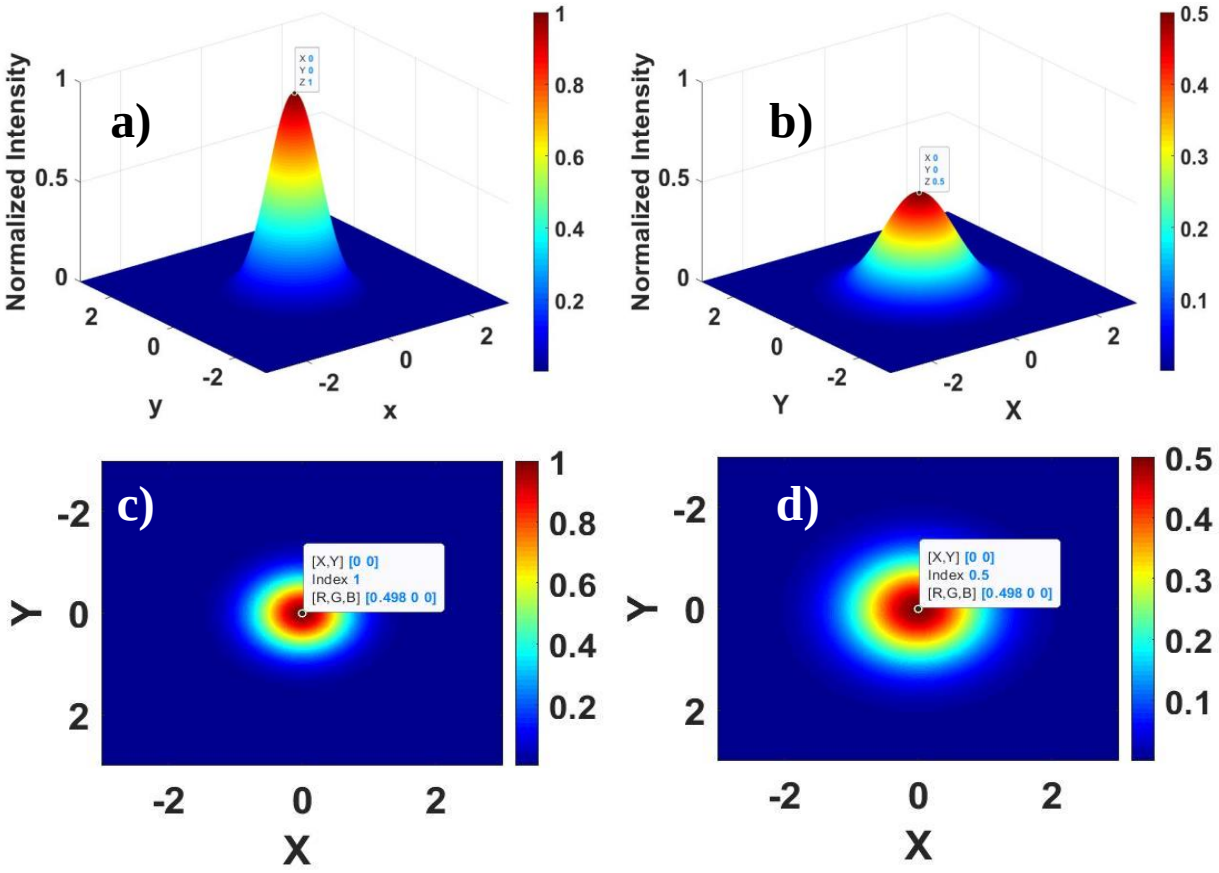

Figure 2-4: (a) initial, and (b) final intensity distribution, for propagation of a two dimensional Gaussian beam in linear medium for one Rayleigh range. (c) initial, and (d) final cross-section.

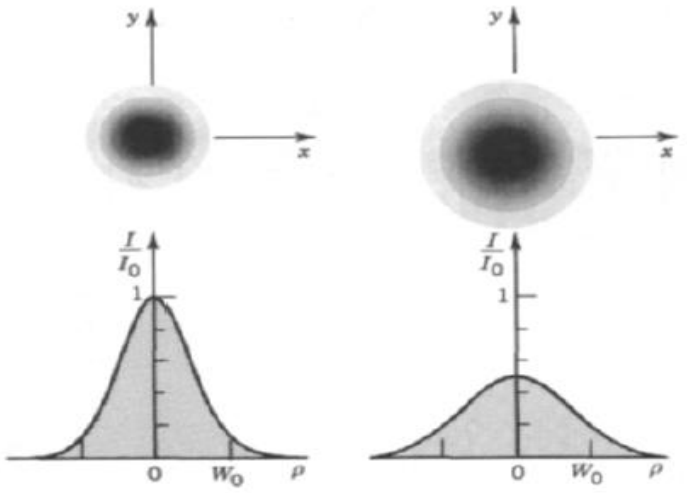

Figure 2-5: Intensity value of two-dimensional transverse Gaussian beam before and after one Rayleigh range propagation [18].

2.2 Beam propagation in a third-order non-linear medium (Kerr medium)

Throughout the long history of optics, it was thought that all optical media were linear. That was before intense laser beam generation and therefore until relatively recently. The assumption of linearity of the optical medium has far-reaching consequences: refractive index and absorption coefficient are independent of light intensity; the superposition principle, a fundamental tenet of classical optics and many other areas of physics, were thought as valid for all media. Also, it was a principle that the frequency of light cannot be changed by travelling through the medium. Even light could not interact with light; two beams of light in the same region of a linear optical medium cannot affect each other [18]. However, by the invention of the laser beam in 1960, it enabled us to observe the behavior of light in optical materials at higher intensities. Many of the experiments made it clear that optical media in fact exhibit nonlinear behavior, as listed by the following: the refractive index, and consequently the speed of light in an optical medium, does change with the light intensity. The principle of superposition is violated. Light can alter its frequency as it passes through a nonlinear optical material. Light can control light; photons do interact. Nonlinear behavior is not exhibited when light travels in free space. Light interacts with light via the medium. The presence of an optical field modifies the properties of the medium which, in turn, modify another optical field or even the original field itself [18]. One of the fascinating effects of nonlinearity is in third order nonlinearity that occurs due to high intense beam. The self-focusing

effect raises against of diffraction or dispersion, and the beam makes their own induced waveguide, or the beam becomes self-trapped. One of the commonly used methods to eliminate spatial spreading (diffraction) is to use wave-guiding. In a waveguide, the propagation behavior of the beam in a high index medium is modified by the total internal reflection from boundaries with media of lower refractive index, and under conditions of constructive interference between the reflections, the beam becomes trapped between these boundaries and thus, forms a `guided mode'[65].

In this section, the third order nonlinearity is discussed. In this case, the induced refractive index of medium has dependency on intensity, where the light induces its own waveguide, and can be self-trapped, so the medium can act like a graded-index medium. These self-trapped beams are called spatial solitons. In this section, two kind of spatial solitons are considered: bright and dark solitons. As an example of a crystal that has a high nonlinear coefficient is the LITHIUM NIOBATE ($LiNbO_3$). Propagation or spatial evolution of light beams in nonlinear media is a central topic of nonlinear optical dynamics. There has been a continuous interest in this topic since the initial investigations of self-trapping of light beams in nonlinear media [66][67]. The analysis of the stability and nonlinear evolution of solitary-wave solutions of nonlinear propagation equations is one of the most crucial parts of the problem of self-trapping of optical beams.

In this section, polarization for third order nonlinear medium is considered, the analytical calculation to obtain the Nonlinear Schrodinger (NLS) equation, and the necessary criteria to obtain self-trapping for an incident beam is reviewed and discussed. Afterwards, the initial condition for incident beam profile in order to be confined in direction of propagation is presented. These confined beams called bright and dark solitons, which are obtained when Kerr coefficient n_2 is positive or negative respectively. Then, the exact analytical calculation to obtain these solitons are discussed. Followed by some definition about the Split-Step method to solve the NLS equation, we implement the corresponding MATLAB program. Finally, the simulation for solving the NLS equation is presented for both cases: bright and dark solitons.

In the case of a small electric field, in an isotropic medium $\vec{P} = \epsilon_0 x \vec{E}$ the polarization and electric field are parallel to each other. But in anisotropic medium $\vec{P} = \epsilon_0 \bar{\bar{x}}\, \vec{E}$ where $\bar{\bar{x}}$ is not scalar, is a tensor. $P_i = \sum_j \epsilon_0 x_{ij} E_j = \epsilon_0 x_{i1} E_1 + \epsilon_0 x_{i2} E_2 + \epsilon_0 x_{i3} E_3$. However, in the principal axis, $\bar{\bar{x}}$ just has orthogonal nonzero elements and other elements are zero. In both cases it is considered that displacement of atomic dipoles is very small, and oscillations are harmonic, this is true because

the electric field is not very large. On the other hand, when the electric field becomes large comparable to the interatomic electric field in the medium, this linear approximation fails, and the oscillation is no more harmonic. Therefore the relation between polarization and electric field in the case of Isotropic medium becomes $P = \epsilon_0 x^{(1)} E + \epsilon_0 x^{(2)} E * E + \epsilon_0 x^{(3)} E * E * E$. Consequently for anisotropic medium this relation is $P_i = \sum_j \epsilon_0 x_{ij}^{(1)} E_j + \sum_j \sum_k \epsilon_0 x_{ijk}^{(2)} E_j E_k + \sum_j \sum_k \sum_l \epsilon_0 x_{ijkl}^{(3)} E_j E_k E_l + \cdots$.

Since in this thesis isotropic medium is considered, the following polarization is valid.

$$P = \epsilon_0 x^{(1)} E + \epsilon_0 x^{(2)} E * E + \epsilon_0 x^{(3)} E * E * E$$

$x^{(2)}$: is the second order susceptibility representing second order nonlinearity, $x^{(3)}$: is the third order susceptibility representing third order nonlinearity

In media possessing centro-symmetry, the second-order nonlinear term is absent. It is worth to mention that as a property of a centro-symmetry medium, the polarization is reversed when the electric field is reversed. The dominant nonlinearity is then of third order, and the material is called a Kerr medium. Kerr media responds to optical fields generating third harmonics and sums and differences of triplets of frequencies [18]. Then in Kerr medium $x^{(2)} = 0$, and $x^{(3)} \neq 0$, and the polarization response becomes as mentioned in (2.26), which is used to modify the wave equation (2.27):

$$P_{Total} = \epsilon_0 x^{(1)} E + \epsilon_0 x^{(3)} E * E * E \tag{2.26}$$

$$\nabla^2 E - \frac{1}{c^2} \frac{\partial^2 E}{\partial t^2} = \mu_0 \frac{\partial^2 P_{Total}}{\partial t^2} \tag{2.27}$$

By separating the total polarization in linear and nonlinear terms,

$P_{Total} = P_L + P_{NL}$

$P_L = \epsilon_0 x^{(1)} E$

$P_{NL} = \epsilon_0 x^{(3)} E * \mathrm{E} * \mathrm{E}$

It is often easier to carry out mathematical operations with complex numbers, so the wave function $u(\vec{r}, t)$ which is the real part of a complex function $U(\vec{r}, t)$ is used,

$$u(\vec{r}, t) = \mathrm{Re}\{\, U(\vec{r}, t) \,\} \tag{2.28}$$

Where $U(r,t) = A(r)e^{in_0\vec{K}_0.\vec{r}}e^{-i\omega t} = U(r)e^{-i\omega t}$

Using this in,

$$[\nabla^2 - \frac{1}{c^2}\frac{\partial^2}{\partial t^2}]\, u(r,t) = \mu_0 \frac{\partial^2 P_{Total}}{\partial t^2} \tag{2.29}$$

The P_L and P_{NL} are:

$$P_L = \epsilon_0 x^{(1)} u(r,t) = \epsilon_0 x^{(1)} Re\left[\frac{U(r)e^{-i\omega t} + U^*(r)e^{i\omega t}}{2}\right]$$

$$P_{NL} = \epsilon_0 x^{(3)} u(r,t) * u(r,t) * u(r,t)$$

This term can be written as:

$$P_{NL} = \frac{3}{4}\epsilon_0 x^{(3)} |U(\omega)|^2 \left[\frac{U(r)e^{-i\omega t} + U^*(r)e^{i\omega t}}{2}\right] + \frac{1}{4}\epsilon_0 x^{(3)} \left[\frac{U(r)^3 e^{-i3\omega t} + U^*(r)^3 e^{-i3\omega t}}{2}\right]$$

The presence of a component of polarization $P_{NL}(3w)$ at the frequency $3w$ indicates, that the Third Harmonic Generation (THG), is generated. The THG term requires phase matching condition, and in most cases the energy conversion efficiency is very low and generally is negligible. Then just the first term of P_{NL}, is considered.

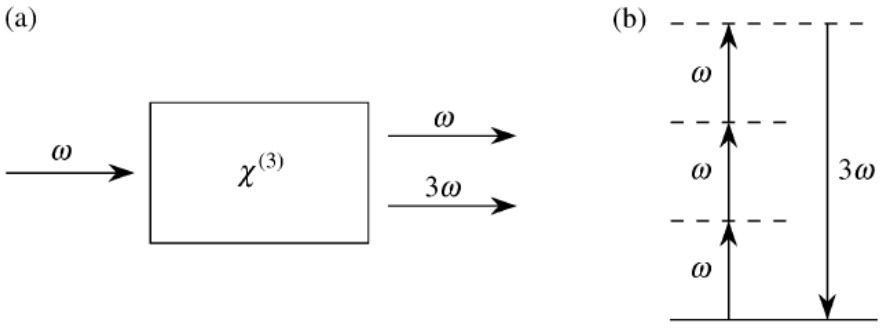

Figure 2-6: Third Harmonic Generation (THG) [18]

This term can be written as,

$$P_{NL}(\omega) = \frac{3}{4}\epsilon_0 x^{(3)} |U(r)|^2 \left[\frac{U(r)e^{-i\omega t} + U^*(r)e^{i\omega t}}{2}\right] = \frac{3}{4}\epsilon_0 x^{(3)} |U(r)|^2 * Re\left[U(r)e^{-i\omega t}\right]$$

$$P_{NL}(\omega) = \frac{3}{4}\epsilon_0 x^{(3)} |U(r)|^2 * Re\left[U(r)e^{-i\omega t}\right] \tag{2.30}$$

By substituting P_L and P_{NL} in equation (2.29):

$$\left[\nabla^2 + \frac{\omega^2}{c^2}\left(1 + x^{(1)}\right)\right] Re\left[U(r)e^{-i\omega t}\right] = \mu_0 \frac{3}{4}\epsilon_0 x^{(3)}|U(r)|^2 \frac{\partial^2}{\partial t^2} Re\left[U(r)e^{-i\omega t}\right]$$

Once the second derivative of $Re\left[U(r)e^{-i\omega t}\right]$ is calculated, the time part can be eliminated,

$$\left[\nabla^2 + \frac{\omega^2}{c^2}\left(1 + x^{(1)} + \frac{3}{4}x^{(3)}|U(r)|^2\right)\right] * Re\left[U(r)e^{-i\omega t}\right] = 0 \qquad (2.31)$$

The refractive index in a nonlinear medium is,

$n^2 = 1 + x^{(1)} + \frac{3}{4}x^{(3)}|U(r)|^2$

$n^2 = \mathrm{n}_0^2 + \frac{3}{4}x^{(3)}|U(r)|^2$, where $n_0^2 = 1 + x^{(1)}$ is the refractive index in linear medium.

By factorizing n_0 , and considering that the second term is small we obtain the expression due to binomial approximation:

$$n = n_0\left(1 + \frac{3}{4n_0^2}x^{(3)}|U(r)|^2\right)^{\frac{1}{2}} = n_0\left(1 + \frac{3}{8n_0^2}x^{(3)}|U(r)|^2\right)$$

The **binomial approximation** is useful for approximately calculating powers of sums of 1 and a small number x. It states that: $(1+x)^\alpha = 1 + \alpha x$. It is valid when $|x| < 1$ and $|\alpha x| \ll 1$ where x and α may be real or complex numbers.

$$n = n_0 + \frac{3}{8n_0}x^{(3)}|U(r)|^2$$

$n = n_0 + \Delta n$

$$\Delta n = \frac{3}{8n_0}x^{(3)}|U(r)|^2$$

By introducing the impedance $\eta = \sqrt{\frac{\mu}{\epsilon}}$ where $\mu = \mu_r\mu_0, \epsilon = \epsilon_0\epsilon_r = \epsilon_0 n^2$ and $\mu_r = 1$

Then:

$\eta = \sqrt{\frac{\mu_r\mu_0}{\epsilon_0 n_0^2}} = \frac{\sqrt{\frac{\mu_0}{\epsilon_0}}}{n_0} = \frac{\eta_0}{n_0}$, where $\eta_0 = \sqrt{\frac{\mu_0}{\epsilon_0}}$ is the impedance of free space.

The intensity of the wave I, can be put as,

$$I = \frac{|U(r)|^2}{2\eta} = \frac{n_0|U(r)|^2}{2\eta_0} \Rightarrow |U(r)|^2 = \frac{2\eta_0 I}{n_0}$$

Therefore Δn is,

$\Delta n = \frac{3}{8n_0}x^{(3)}|U(r)|^2 = \frac{3x^{(3)}\eta_0}{4n_0^2}I = n_2 I$ where $n_2 = \frac{3x^{(3)}\eta_0}{4n_0^2}$ is the Kerr coefficient.

The Kerr effect is a phenomenon where an applied electrical field induces a change in the refractive index of a material. What distinguishes the Kerr effect from others of this kind (e.g. the Pockel's effect) is that the change in refractive index is directly proportional to the square of the electric field or in other words, directly proportional to the intensity. The refractive index is then described by the following equation:

$$n(I) = n_0 + \frac{3x^{(3)}\eta_0}{4n_0^2} I \;\rightarrow\; n(I) = n_0 + n_2 I \tag{2.32}$$

By substituting $\mathrm{n}^2(I) = 1 + x^{(1)} + \frac{3}{4}x^{(3)}|U(r)|^2$ in equation (2.31), the following Helmholtz equation in nonlinear medium is obtained, which is completely dependent on spatial coordinates and the time part has been eliminated.

$$[\nabla^2 + \mathrm{k}_0^2\mathrm{n}^2(\mathrm{I})]\, Re[U(r)] = 0 \tag{2.33}$$

If we substitute the spatial part of wave function $U(r,t) = A(r)e^{in_0k_0z}e^{-i\omega t} = U(r)e^{-i\omega t}$, then

$$[\nabla^2 + k_0^2 n^2(I)]\, A(r)e^{in_0k_0z} = 0 \tag{2.34}$$

$$\frac{\partial^2}{\partial z^2}\left[A(r)e^{in_0k_0z}\right] = \left[\frac{\partial^2 A(r)}{\partial z^2} + 2in_0k_0\frac{\partial A(r)}{\partial z} - {n_0}^2k_0^2A(r)\right]e^{in_0k_0z}$$

Assuming that the complex envelope $A(r)$ varies slowly along the z-axis (within a wavelength λ), then it follows that $\frac{\partial^2 A(r)}{\partial z^2} \ll \frac{\partial A(r)}{\partial z}$, the second partial derivative of $A(r)$ with respect to z can be neglected, so then the Helmholtz equation becomes:

$$\frac{\partial^2 A(r)}{\partial x^2} + \frac{\partial^2 A(r)}{\partial y^2} + 2in_0k_0\frac{\partial A(r)}{\partial z} + (n^2(I) - n_0^2)\, k_0^2 A(r) = 0 \tag{2.35}$$

Since the nonlinear effect is small ($n_2 I \ll n_0$), and $n(I) = n_0 + n_2 I$ the following is valid:

$\mathrm{n}^2(I) - \mathrm{n}_0^2 = (n(I) - n_0)(n(I) + n_0) = (n_0 + n_2 I - n_0)(n_0 + n_2 I + n_0) = (n_2 I)(2n_0)$

For realizing how much the magnitude of the coefficient n_2 is small, it is worth to mention that the magnitude order of n_2 (in units of cm^2/w) is 10^{-16} to 10^{-14}in glasses, 10^{-14} to 10^{-7} in doped glasses, 10^{-10} to 10^{-8} in organic materials, 10^{-10} to 10^{-2} in semiconductors (see chapter 3 in ref [18]).

Then the following Non-linear Schrödinger (NLS) equation is obtained,

$$-i\frac{\partial A(r)}{\partial z}=\frac{1}{2n_0k_0}\left(\frac{\partial^2A(r)}{\partial x^2}+\frac{\partial^2A(r)}{\partial y^2}\right)+n_2Ik_0A(r) \qquad (2.36)$$

that can be further reduced to its standard form by doing the normalization process by the two factors, Rayleigh Range Z_R and initial beam-width ω_0 ,

$$X=\frac{x}{\omega_0}\,,\qquad Y=\frac{y}{\omega_0},\qquad Z=\frac{z}{Z_R}$$

$$Z_R=\frac{n_0\pi\omega_0^2}{\lambda_0}=\frac{n_0\omega_0^2k_0}{2}$$

The second partial derivatives are,

$$\frac{\partial^2}{\partial x^2}=\frac{\partial}{\partial x}\left(\frac{\partial}{\partial x}\right)=\frac{\partial}{\partial x}\left(\frac{\partial X}{\partial x}\frac{\partial}{\partial X}\right)=\frac{\partial}{\partial x}\left(\frac{1}{\omega_0}\frac{\partial}{\partial X}\right)=\frac{1}{\omega_0^2}\frac{\partial^2}{\partial X^2}$$

And the same for the y-axis is valid, whereas for the z_partial derivative,

$$\frac{\partial}{\partial z}=\frac{\partial Z}{\partial z}\frac{\partial}{\partial Z}=\frac{1}{Z_R}\frac{\partial}{\partial Z}$$

Replacing these in the NLS equation, the next normalized equation is obtained.

$$-i\frac{\partial A(r)}{\partial Z}=\frac{1}{4}\left(\frac{\partial^2A(r)}{\partial X^2}+\frac{\partial^2A(r)}{\partial Y^2}\right)+Z_Rn_2Ik_0A(r) \qquad (2.37)$$

The next normalization step is for the initial amplitude $A(r)=\sqrt{I_m}q(r)$ with the maximum initial intensity (I_m), where $q(r)$ is a dimensionless normalized function.

$I=\frac{n_0\,|A(r)|^2}{2\eta_0}=\frac{n_0}{2\eta_0}I_m|q(\vec{r})|^2$, if we substitute $A(r)$ in equation (2.37), then

$$-i\frac{\partial q(\vec{r})}{\partial Z}=\frac{1}{4}\left(\frac{\partial^2q(\vec{r})}{\partial X^2}+\frac{\partial^2q(\vec{r})}{\partial Y^2}\right)+Z_Rn_2\frac{n_0}{2\eta_0}k_0I_m|q(\vec{r})|^2q(\vec{r})=0$$

This equation can be further reduced using the parameter of Non-linear diffraction length or self-focusing distance or nonlinear length $L_{NL}=\frac{2\eta_0}{n_0|n_2|I_mk_0}$. L_{NL} is a distance over which the nonlinear index change introduces a phase change of 1 radian. When an electric field propagates for this length, the nonlinear effects cannot be neglected anymore, and the previous equation is,

$$-i\frac{\partial q(\vec{r})}{\partial Z}=\frac{1}{4}\left(\frac{\partial^2q(\vec{r})}{\partial X^2}+\frac{\partial^2q(\vec{r})}{\partial Y^2}\right)+\frac{Z_R}{L_{NL}}|q(\vec{r})|^2q(\vec{r}) \qquad (2.38)$$

In the normalized Non-linear Schrödinger equation (2.38) the constants L_{NL} and Z_R are the key to the formation of a spatial soliton. Therefore, the different situations for these parameters are evaluated as bellow:

- In the case $Z_R \ll L_{NL}$, the effect of nonlinear part can be neglected so that the field will be affected by the linear effect (diffraction) much earlier than the nonlinear effect, it will just diffract without too much effect from nonlinear.
- In the opposite case if $L_{NL} \ll Z_R$, the nonlinear effect will be more evident than the diffraction, and the Kerr effect is predominating. By the effect of the phase modulation, the beam experiments a self-focusing if n_2 is bigger than zero ($n_2 > 0$) or a self-defocusing if n_2 is less than zero ($n_2 < 0$).
- However, for the case of $L_{NL} = Z_R$, the effect of beam broadening by diffraction phenomena is compensated by the spectral broadening produced by Kerr effect, the intensity profile of the beam propagates without suffering diffraction or self- focusing or defocusing, that generates the spatial soliton.

For a positive Kerr medium or positive nonlinear refractive index material ($n_2 > 0$) the soliton type solution of Equation (2.38) with ($L_{NL} = Z_R$) is given by [68]:

$$q(X, Z) = \operatorname{sech}\left(\sqrt{2}X\right) \exp\left(\frac{iZ}{2}\right) \tag{2.39}$$

Physically, this equation represents a beam whose cross-section does not change as it propagates in the medium, which is known as bright spatial soliton. For a negative Kerr medium or negative nonlinear refractive index material ($n_2 < 0$) the soliton type solution of equation (2.38) with ($L_{NL} = Z_R$) is given by [68] :

$$q(X, Z) = \tanh\left(\sqrt{2}X\right) \exp(iZ) \tag{2.40}$$

This is a dark spatial soliton and represents a dark region immersed in the uniform background of the transverse beam profile. Different numerical methods have been implemented to carry out the solution of the NLS equation. However, the numerical Split-Step method, in this thesis is applied. In the following section, the numerical method of Split-Step to solve the Non-linear Schrödinger equation is discussed.

2.3 Split-Step Method

The Split-Step Method algorithm, is an iterative stable numerical method to solve the NLS equation, introduced in the year of 1975. The split-step method was introduced by Fisher [59], also known as Split-Step Fourier method, to calculate the propagation of an optical field in dispersive and nonlinear media; considering small segments in which one of the two properties is absent [60]. It has been widely used to solve the NLS equation in optical fibers [61]. The method is based on dividing the medium into many steps. Any step is divided into 2 halves, in the first half, the function feels diffraction effects, in the second half, the function feels non-linear effects. To apply the Split-Step method, the NLS equation (2.38) is considered in terms of operators as follow:

$$-i\frac{\partial}{\partial Z}q(X,Z) = \left(\widehat{D} + \widehat{N}\right)q(X,Z) \tag{2.41}$$

Where the operator $\widehat{D} = \frac{1}{4}\left(\frac{\partial^2}{\partial X^2} + \frac{\partial^2}{\partial Y^2}\right)$ describes linear diffraction effect (or dispersion effect if the pulse is propagating in time). Whereas, the operator $\widehat{N} = \frac{Z_R}{L_{NL}}|q(r)|^2 = Z_R n_2 \frac{n_0}{2\eta_0} k_0 I_m |q(\mathrm{r})|^2$ describes the nonlinear effect.

One of the particular solutions for equation (2.41) is that the diffraction operator ($\widehat{D}$) becomes fully compensated by nonlinearity ($\widehat{N}$) and the right-hand side of the equation becomes zero. This particular solution is invariant along propagation in Z and describes a soliton that maintains its shape and energy along propagation. In general, diffraction and nonlinearity act together during propagation. An important approximation is: in propagation over small distance, the diffraction and non-linear effects can act independently. We start by writing NLS in terms of operators as follows:

$$-i\frac{\partial}{\partial Z}q(X,Z) = \widehat{D}q(X,Z) + \widehat{N}q(X,Z) = \left(\widehat{D} + \widehat{N}\right)q(X,Z)$$

$$\int_Z^{Z+h} \frac{\partial q(X,Z)}{q(X,Z)} = \int_Z^{Z+h} i\left(\widehat{D} + \widehat{N}\right)dZ$$

$$Log[q(X,Z+h)] - Log[q(X,Z)] = i\left(\widehat{D} + \widehat{N}\right)h$$

$$Log\left[\frac{q(X,Z+h)}{q(X,Z)}\right] = i\left(\widehat{D} + \widehat{N}\right)h$$

$$q(X,Z+h) = \exp\left[i\left(\widehat{D} + \widehat{N}\right)h\right]q(X,Z) = \exp\left[i\widehat{D}h\right]\exp\left[i\widehat{N}h\right]q(X,Z)$$

Since the two operators act independently, it is possible to consider Diffraction effects by operator $\widehat{D}$ in half part, and in the other half part, just nonlinear effect measured by operator $\widehat{N}$. Both the linear and the nonlinear parts have their own analytical solutions. For solving Nonlinear Schrödinger equation containing both parts, a 'small' step h is taken along z, then, the two operators can be treated separately. For example, for half step $h/2$ the diffraction operator $\widehat{D}$ is applied, and for the other half $h/2$ the nonlinear operator $\widehat{N}$ (as demonstrated in Figure 2-7). Then,

1-when linearity or diffraction acts: $\widehat{D} \neq 0, \widehat{N} = 0$

$$q\left(X, Z + \frac{h}{2}\right) = \exp\left[i\left(\widehat{D} + \widehat{N}\right)\frac{h}{2}\right] q(X, Z) = \exp\left[i\widehat{D}\,\frac{h}{2}\right] q(X, Z)$$

2-when nonlinearity acts: $\widehat{N} \neq 0, \widehat{D} = 0$

$$q\left(X, Z + \frac{h}{2}\right) = \exp\left[i\left(\widehat{D} + \widehat{N}\right)\frac{h}{2}\right] q(X, Z) = \exp\left[i\widehat{N}\,\frac{h}{2}\right] q(X, Z)$$

When linearity or diffraction acts: $\widehat{D} \neq 0, \widehat{N} = 0$ the system is in lack of nonlinearity matter, so that the solution of the problem is the same as normal diffraction as previously solved by Fourier transform.

$$-i\frac{\partial}{\partial Z} q(X, Z) = \left(\widehat{D} + 0\right) q(X, Z)$$

$$-i\frac{\partial}{\partial Z} q(X, Z) = \frac{1}{4}\frac{\partial^2}{\partial X^2} q(X, Z)$$

$$q\left(X, Z + \frac{h}{2}\right) = I.F.T\left[H(\nu_X) * F.T[q(X, Z)]\right]$$

Where I.F.T is the Inverse Fourier Transform, and F.T is the Fourier transform, $H(\nu_X)$ is the Transform Function in Fourier domain. In the second half just, nonlinearity acts $\widehat{N} \neq 0, \widehat{D} = 0$:

$$-i\frac{\partial}{\partial Z} q(X, Z) = \left(0 + \widehat{N}\right) q(X, Z)$$

$$q(X, Z + h) = \exp\left[i\widehat{N}\,\frac{h}{2}\right] q\left(X, Z + \frac{h}{2}\right) = \exp\left[i\frac{Z_R}{L_{NL}}\left|q\left(X, Z + \frac{h}{2}\right)\right|^2 \frac{h}{2}\right] q\left(X, Z + \frac{h}{2}\right)$$

The whole of this mathematical Split-Step method is demonstrated in the flowchart of Figure 2-8.

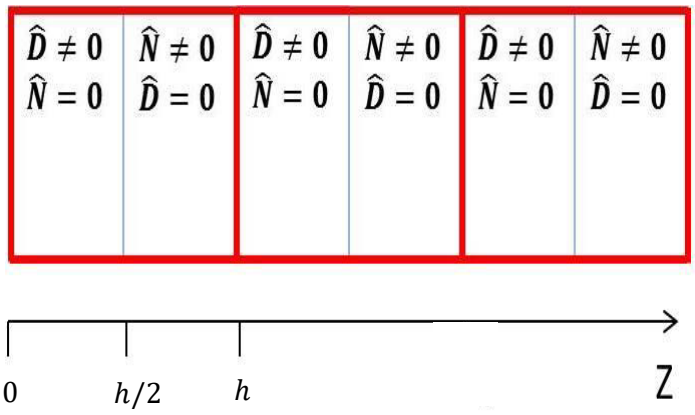

Figure 2-7: Illustration of medium division due to Split-Step method.

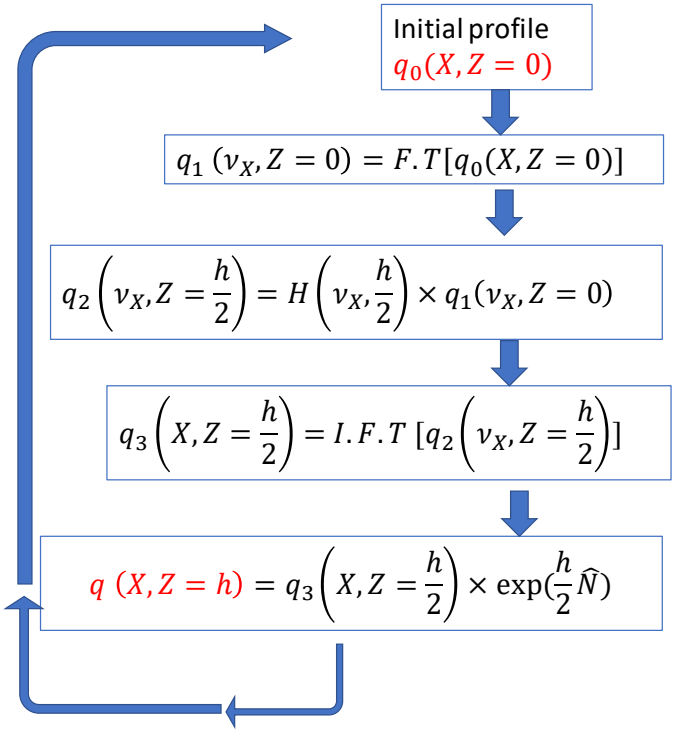

Figure 2-8: Schematic of mathematic view on Split-Step method

2.4 Spatial Solitons

Solitary waves create their own channel as they travel in a uniform medium, remaining localized and preserving their shape. But they can be dramatically altered by colliding with another one. Solitons are solitary waves that are unaltered by collisions. Solitary waves, commonly referred to

as solitons, have been the subject of intense theoretical and experimental studies in many different fields, including hydrodynamics, nonlinear optics, plasma physics, and biology [69],[70]. The history of solitons, in fact, dates to 1834, the year in which James Scott Russell observed that a heap of water in a canal propagated undistorted over several kilometers, the report was published in 1844 [71]. Such waves were later called solitary waves. However, their properties were not understood completely until appropriate mathematical models were introduced and the inverse scattering method was developed in the 1960s [72].

In the context of nonlinear optics, solitons are classified as being either temporal or spatial, depending on whether the confinement of light occurs in time or space during wave propagation. Temporal solitons represent optical pulses that maintain their shape, whereas spatial solitons represent self-guided beams that remain confined in the transverse directions orthogonal to the direction of propagation. Both types of solitons evolve from a nonlinear change in the refractive index of an optical material induced by the light intensity, the phenomenon is known as the *optical Kerr effect* in the field of nonlinear optics [46], [73]. The intensity dependence of the refractive index leads to spatial self-focusing (or self-defocusing) and temporal self-phase modulation (SPM), as two major nonlinear effects, that are responsible for the formation of optical solitons. A spatial soliton is formed when the self-focusing of an optical beam balances its natural diffraction. In contrast, it is the Self Phase Modulation (SPM) that counteracts the natural dispersion-induced, broadening of an optical pulse and leads to the formation of a temporal soliton[46]. In both cases, the pulse or the beam propagates through a medium without change in its shape and is said to be *self-localized* or *self-trapped* [74]. The earliest example of a spatial soliton corresponds to the 1964 discovery of the nonlinear phenomenon of self-trapping of continuous-wave (CW) optical beams in a bulk nonlinear medium [75]. Self-trapping was not linked to the concept of spatial solitons immediately because of its unstable nature. During the 1980s, stable spatial solitons were observed using nonlinear media in which diffraction spreading was limited to only one transverse dimension [76]. Self-focusing and self-defocusing of continuous-wave (CW) optical beams in a bulk nonlinear medium has been studied extensively [77], [78]. To briefly review the various kinds of optical spatial solitons that have been demonstrated experimentally refer to Segev M. and Kivshar Y S and Luther-Davies [79],[80].

The first spatial solitons were suggested in nonlinear optical Kerr media in the 1960s. Kerr nonlinearities are characterized by a local, instantaneous refractive index change, $\Delta n = n_2 I$,

where I is the local intensity and n_2 is a real constant. All media exhibit the optical Kerr effect at frequencies very far from any resonances so that the nonlinearity is very weak. Typical values of Δn are of the order of 10^{-4} or smaller. It became quickly clear that bright Kerr solitons are stable only in planar (1+1) D systems; bright (2+1) D solitons undergo catastrophic collapse [24]. Kerr solitons have been observed in CS_2, glass [80], semiconductor [81], and polymer waveguides [81]. In bulk (3D) media, although there is a critical power for which self-focusing balances diffraction, any fluctuations in intensity or beam shape lead to, either catastrophic self-focusing and usually material damage, or to beam spreading [24]. It was discovered some time ago [75] that the suppression effect of diffraction through a local change of the refractive index can be produced solely by the nonlinear effects if they lead to a change in the refractive index of the medium, in such a way that, it is larger in the region where the beam intensity is large. An optical beam can create its own waveguide and be trapped by this self-induced waveguide. The input beam diffracts at low power but forms a spatial soliton when its intensity is large enough to create a self-induced waveguide by changing the refractive index. This change is largest at the beam center and gradually reduces to zero near the beam edges, resulting in a graded-index waveguide. The spatial soliton can be thought as the fundamental mode of this waveguide. Such nonlinear waveguide can even guide a weak probe beam of a different frequency or polarization [82]. When very narrow optical beams propagate without affecting the properties of a medium, they undergo natural diffraction and broaden with distance. The narrower the initial beam is, the faster it diverges (diffracts). In nonlinear materials, the presence of light modifies their properties (refractive index, absorption, or conversion to other frequencies). The refractive index change, resembles the intensity profile of the beam, forming an optical lens that increases the index in the beam's center while leaving it unchanged in the beam's tails. This induced lens focuses the beam (see Figure 2-9 (A)), a phenomenon called self-focusing that is a precursor of solitons. When self-focusing exactly balances beam divergence or diffraction (see Figure 2-9 (B)), the beam becomes self-trapped at a very narrow width and is called an optical spatial soliton (Figure 2-9 (C)) [83]. Since Spatial solitons creating their own waveguide [38], it is possible to utilize the spatial solitons as optical channels for another beam in an intensity-dependent refractive-index medium [68]. Dark spatial solitons induce waveguides in self-defocusing media and these induced waveguides can support bound modes of a probe beam propagating coaxially along the soliton [84]. The spatial soliton described by the NLS equation is completely analogous to the temporal soliton in optical fibers.

Bright spatial solitons, which can be obtained in materials with a positive nonlinear refractive index, have recently been reported in multimode CS_2 waveguides [85] and single-mode glass waveguides. And dark spatial solitons are possible in materials with a negative nonlinear refractive index (n_2) [86].

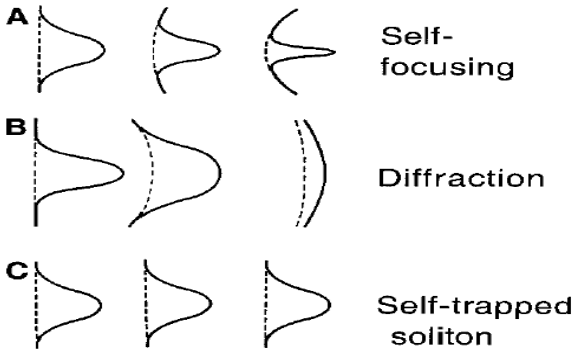

Figure 2-9: Schematic illustration of the lens analogy for spatial beam profiles (solid Lines) and phase fronts (dashed lines). Diffraction acts as a concave lens while the nonlinear medium acts as a convex lens. A soliton forms when the two lenses balance each other in such way that the phase front remains plane.[87]. (A) beam self-focusing, (B) normal beam diffraction, and (C) soliton propagation.

One can also understand the formation of spatial solitons through a lens analogy. Diffraction creates a curved wave-front like that produced by a concave lens and spreads the beam to a wider region. The index gradient created by the self-focusing effect, in contrast, acts like a convex lens that tries to focus the beam toward the beam center. A Kerr medium acts as a convex lens. As seen in Figure 2-9, the beam can become *self-trapped* and propagate without any change in its shape if the two lensing effects cancel each other [75]. Of course, the intensity profile of the beam should have a specific shape for a perfect cancellation of the two effects. These specific beam profiles associated with spatial solitons are the nonlinear analog of the modes of the linear waveguide formed by the self-induced index gradient [87]. Comparing the spatial with a simple convex lens, as shown in the Figure 2-10, an optical field approaches the lens and then it is focused. Here the refractive index is constant, but at different x the light feels different length of the lens or the light will travel in different optical path. ($\text{Optical path} = \int n\text{dL}$).

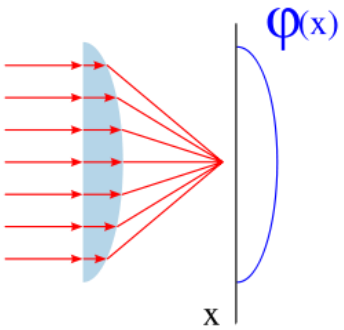

Figure 2-10: Convex lens

Since parallel optical rays before entering to the lens have constant phase, and they are perpendicular to the wave-front, during travel procedure inside the lens, optical rays which are passing through thicker part of the lens suffer more delay. So that wave-front of the beam exit from the lens, will be changed from plane wave-front to spherical wave-front. Since always the optical rays are perpendicular to the wave-front, the beam become focused. The effect of the lens is to introduce a non-uniform phase change that causes focusing. This phase change is a function of the space and can be represented with $\varphi(x)$ and is approximately represented in the Figure 2-10. The phase change can be expressed, as the product of the phase constant and the width of the path that the field has traveled. It can be written as:

$$\varphi(x) = k_0 * n * L(x)$$

Where $L(x)$ is the width of the lens that is changing in each point of x-direction, k_0 and refractive index n are constant. To get a focusing by the third order nonlinearity effect, it is not necessary to change the thickness of the lens. If we fix the thickness of the lens, and we change its refractive index, the same effect is obtained.

Spatial solitons are based on the same principle. The Kerr effect introduces a self-phase modulation changing the refractive index according to,

$$\varphi(x) = k_0 n(x) L = k_0 * \left(n_0 + n_2 I(x)\right) * \mathrm{L}$$

That's the way in which graded-index fibers work, the change in the refractive index introduces a focusing effect, and this effect is against to the natural diffraction of the field. If the two effects balance each other perfectly, then we have a confined field propagating within the fiber. In Figure 2-11 since the intensity shape of the incident beam is Gaussian, the phase changes and the field shows a self-focusing effect due to self-phase modulation. In other words, the field creates a fiber-like guiding structure while propagating. If the field becomes a mode of this fiber at the same time,

it means that the focusing nonlinear and diffractive linear effects are perfectly balanced and the field propagates forever without changing its shape as long as the medium does not change. Here it is worth to mention that the losses are neglected. To have a self-focusing effect, the medium must have a positive n_2, otherwise, the opposite effect is obtained, and the beam becomes defocused.

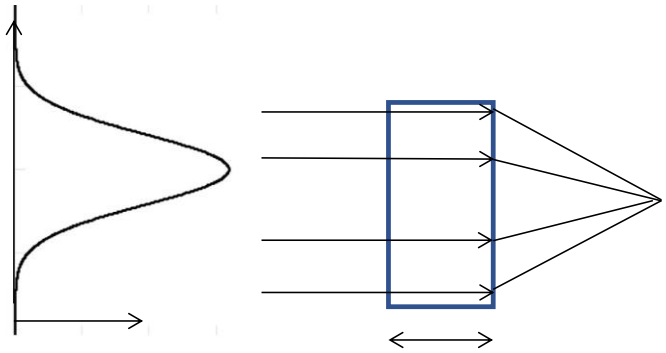

Figure 2-11: Nonlinear lens

2.5 Exact analytical solutions for spatial solitons

2.5.1 Exact analytical solutions for spatial bright solitons

For a positive Kerr medium or positive nonlinear refractive index material ($n_2 > 0$) the Nonlinear Schrodinger (NLS) equation (2.38), has the following form.

$\eta = \frac{Z_R}{L_{NL}}$, $\eta > 0$.

$$-i\frac{\partial q(r)}{\partial Z} = \frac{1}{4}\left(\frac{\partial^2 q(r)}{\partial X^2} + \frac{\partial^2 q(r)}{\partial Y^2}\right) + \eta * |q(r)|^2 q(r) \qquad (2.42)$$

Because n_2 is larger than zero, the sign behind of η in NLS is positive. Here it is tempting to solve this equation analytically, but just for one transversal dimension. The $q(X,Z)$ as the initial normalized amplitude of the beam has an analytical shape $q(X,Z) = U(X) * \exp(i\Gamma Z)$ and by substituting in NLS equation the following is obtained.

$\frac{\partial^2 U(X)}{\partial X^2} - 4\Gamma\, \mathrm{U(X)} + 4\eta\, |U(X)|^2 U(X) = 0$

Multiplying to $\frac{\partial U(X)}{\partial X}$ and integrating with respect to X ,

$$\int \frac{\partial^2 U(X)}{\partial X^2}\frac{\partial U(X)}{\partial X}dX - \int 4\Gamma\, \mathrm{U(X)}\frac{\partial U(X)}{\partial X}dX + \int 4\eta\, |U(X)|^2 U(X)\frac{\partial U(X)}{\partial X}dX = 0$$

Calculating by parts the first integral,

$$\int \frac{\partial^2 U(X)}{\partial X^2}\mathrm{dU(X)} = \int \frac{\partial^2 U(X)}{\partial X^2}\frac{\partial \mathrm{U}}{\partial \mathrm{X}}\,\mathrm{dX} == \frac{\partial \mathrm{U}}{\partial \mathrm{X}} * \frac{\partial \mathrm{U}}{\partial \mathrm{X}} - \int \frac{\partial^2 \mathrm{U}}{\partial \mathrm{X}^2}\frac{\partial \mathrm{U}}{\partial \mathrm{X}}\,\mathrm{dX} = \frac{\partial \mathrm{U}}{\partial \mathrm{X}} * \frac{\partial \mathrm{U}}{\partial \mathrm{X}} - \int \frac{\partial^2 \mathrm{U}}{\partial \mathrm{X}^2}\mathrm{dU}$$

$\Rightarrow$

$$2\int \frac{\partial^2 U(X)}{\partial X^2}\mathrm{dU} = \left(\frac{\partial \mathrm{U}}{\partial \mathrm{X}}\right)^2 \qquad (2.43)$$

$$\frac{1}{2}\left(\frac{\partial \mathrm{U}}{\partial \mathrm{X}}\right)^2 - 2\Gamma\, \mathrm{U}^2(X) + \eta \mathrm{U}^4(X) = C$$

C is an integration constant that considers the integration limits**.** For exponentially localized solutions C is equal to zero [88].

$$\left(\frac{\partial \mathrm{U}}{\partial \mathrm{X}}\right)^2 + \mathrm{U}^2(X)(2\eta \mathrm{U}^2(X) - 4\Gamma) = 0 \qquad (2.44)$$

$U(x)$ *h*as its maximum value U_0 at the center of transversal axis X=0, $\frac{\partial \mathrm{U}}{\partial \mathrm{X}}|_{X=0} = 0$. So, by substituting these values in the previous equation (2.44) for X=0,

$$0 + \mathrm{U}_0^2(2\eta U_0^2 - 4\Gamma) = 0 \rightarrow \quad \Gamma = \frac{\eta U_0^2}{2} \Rightarrow$$

Then,

$$q(X,Z) = U(X) * \exp\left(i\frac{\eta U_0^2}{2}Z\right)$$

And also substitute in equation (2.44),

$$\left(\frac{\partial \mathrm{U}}{\partial \mathrm{X}}\right)^2 + \mathrm{U}^2(X)\left(2\eta \mathrm{U}^2(X) - 4\frac{\eta U_0^2}{2}\right) = 0 \Rightarrow$$

Then, the transversal solution of the NLS equation is,

$$\frac{\partial \mathrm{U}}{\partial \mathrm{X}} = \pm \mathrm{U(X)}\sqrt{2\eta}\sqrt{U_0^2 - \mathrm{U}^2(X)} \quad \Rightarrow \quad \int \frac{dU}{\mathrm{U(X)}\sqrt{U_0^2 - \mathrm{U}^2(X)}} = \pm\int \sqrt{2\eta}\, dX \Rightarrow$$

$$\frac{1}{U_0} ArcSech\left(\frac{U(X)}{U_0}\right) = \pm\sqrt{2\eta}\; X \Rightarrow$$

$$U(X) = U_0\, Sech\left(U_0\sqrt{2\eta}\ X\right) \tag{2.45}$$

Since the $q(X,Z)$ is the normalized solution, the U_0 value is equal to one ($U_0 = 1$). So, the complete solution of the NLS equation for positive Kerr medium is,

$$q(X,Z) = U_0\, Sech\left(U_0\sqrt{2\eta}\ X\right) * \exp\left(i\frac{\eta U_0^2}{2}Z\right) \tag{2.46}$$

If we take $q(X, Z = 0)$ as the initial condition in Z=0, the bright spatial soliton in this positive Kerr medium is obtained.

2.5.2 Exact analytical solutions for spatial dark solitons

For a negative Kerr medium (negative nonlinear refractive index) the NLS equation is written as,

$$-i\frac{\partial q(\vec{r})}{\partial Z} = \frac{1}{4}\left(\frac{\partial^2 q(\vec{r})}{\partial X^2} + \frac{\partial^2 q(\vec{r})}{\partial Y^2}\right) - \eta * |q(\vec{r})|^2 q(\vec{r}) \tag{2.47}$$

In this part, the solution of the mentioned NLS equation for one transversal dimension is considered as $q(X,Z) = U(X) * \exp(i\Gamma Z)$. Where the $U(X)$ is the normalized amplitude and Γ is the normalized wave vector. By replacing the $q(X,Z)$ in NLS equation:

$$\frac{1}{4}\frac{\partial^2 U(X)}{\partial X^2} - \eta\, \mathrm{U}^2(X)U(X) - \Gamma\, \mathrm{U(X)} = 0. \tag{2.48}$$

Since the dark soliton solution has the form of a hyperbolic tangent function, the value of the amplitude in points far from the center of the transversal axis is,

When $X \to \infty \Rightarrow \begin{cases} U(X) = U(\infty) = U_0, & \mathrm{U}^3(X) = U_0^3 \\ \frac{\partial U(X)}{\partial X}|_{\mathrm{X}\to\infty} = 0, & \frac{\partial^2 U(X)}{\partial^2 X}|_{\mathrm{X}\to\infty} = 0 \end{cases}$

By replacing this in equation (2.48), the value of Γ can be obtained.

$\Gamma = -\eta U_0^2$

By replacing in the equation (2.48), the next equation is obtained.

$\frac{\partial^2 U(X)}{\partial X^2} - 4\eta\, \mathrm{U}^3(X) + 4\eta U_0^2\, \mathrm{U(X)} = 0.$

Multiplying to $\frac{\partial U(X)}{\partial X}$ and integrating with respect to X ,

$$\int \frac{\partial^2 U(X)}{\partial X^2}\frac{\partial U(X)}{\partial X}dX - \int 4\eta\, \mathrm{U}^3(X)\frac{\partial U(X)}{\partial X}dX + \int 4\eta U_0^2\, \mathrm{U(X)}\frac{\partial U(X)}{\partial X}dX = 0$$

The following integral with respect to is obtained.

$$\int \frac{\partial^2 U(X)}{\partial X^2}\mathrm{dU(X)} - \int 4\eta\, \mathrm{U}^3(X)dU(X) + \int 4\eta \mathrm{U}_0^2\, \mathrm{U(X)\ dU(X)} = C \qquad (2.49)$$

Using (2.43) in (2.49), and integrating we obtain,

$$\left(\frac{\partial \mathrm{U}}{\partial \mathrm{X}}\right)^2 - 2\eta \mathrm{U}^4(X) + \eta 4\mathrm{U}_0^2\, \mathrm{U}^2(X) = 8C \qquad (2.50)$$

C is the integration constant and can be calculated by considering the function $U(X)$ as $X \to \infty$,

$C = \frac{1}{4}\eta U_0^4$

Replacing this in (2.50),

$$\left(\frac{\partial \mathrm{U}}{\partial \mathrm{X}}\right)^2 - 2\eta \mathrm{U}^4(X) + 4\eta \mathrm{U}_0^2\, \mathrm{U}^2(X) - 2\eta U_0^4 = 0 \qquad (2.51)$$

$\frac{1}{\sqrt{2\eta}}\frac{\partial \mathrm{U}}{\partial \mathrm{X}} = \pm(\mathrm{U}^2(X) - U_0^2) \Rightarrow$

$\int \frac{dU}{U(X)^2 - \mathrm{U}_0^2} = \pm\int \sqrt{2\eta}\, dX \Rightarrow$ Since $\quad |U(X)| < U_0 \ \Rightarrow \frac{1}{U_0} Arctanh\left(\frac{U(X)}{U_0}\right) = \pm\sqrt{2\eta}X$

$U(X) = U_0 Tanh(\pm U_0\sqrt{2\eta}\, X) \Rightarrow U(X) = \pm U_0 Tanh(\pm U_0\sqrt{2\eta}\, X)$

Since the amplitude profile $q(X, Z)$ is normalized the equation (2.52) is the analytical solution of negative Kerr medium where produces dark solitons.

$$q(X, Z) = \pm Tanh(\pm\sqrt{2\eta}\, X) * \exp(-i\eta Z) \qquad (2.52)$$

If $q(X, Z = 0)$ is the initial condition in Z=0 the dark spatial soliton in the negative Kerr media is obtained.

2.6 Simulation of soliton propagation in third-order nonlinear (Kerr) medium

In this section, the propagation of hyperbolic secant (Sech) and hyperbolic tangent (Tanh) mentioned in equations (2.46) and (2.52) is simulated respectively. It is discussed that the Sech (Tanh) beam profile can be propagated as bright (dark) soliton in positive (negative) Kerr medium

correspondingly. It is considered that the intensity of the initial beam profile is sufficiently high that induces third order nonlinearity. The considered initial intensity is such that $\eta = \frac{Z_R}{L_{NL}} = 1$.

2.6.1 Bright soliton propagation in positive Kerr medium

The equation (2.53) is used as an initial condition to propagate in this positive Kerr medium. Beam intensity propagation is simulated numerically by a MATLAB program. The program is written by using the Split-Step method. In the left (right) part of Figure 2-12, we show the normalized amplitude of the real (imaginary) part of incident beam. Since the initial phase of the beam is zero, the imaginary part of the initial condition in the transversal axis is zero. The propagation simulation appears in Figure 2-13, where the Figure 2-13(a) demonstrates the top view of beam intensity propagation, initiated from the downside of the figure and propagates for 30 Rayleigh range. It explains that the transversal occupied space by the intensity of the beam is constant and is not changing by propagation, as it is one of definition of bright spatial soliton. Figure 2-13 (b) simulates the same information, and the normalized intensity is figured out on the perpendicular axis. The figure demonstrates that the intensity profile is constant in whole distance of propagation and the on-axis normalized intensity is on a constant line and value by propagation, as bright spatial soliton is. For obtaining a better view over intensity profile by propagation, Figure 2-14 compares the normalized intensity profile of incident (blue line) and propagated (red points) beam after 30Z propagation distance, and there is a good fit between them. From the Figure 2-12, Figure 2-13, and Figure 2-14, it is observed, by using the suitable initial condition with an appropriate initial intensity which induces third-order nonlinear medium, it is possible to make the balance between diffraction and self-focusing effect and propagate the beam as spatial bright soliton.

$$q(X) = Sech\left(\sqrt{2}\, X\right) \tag{2.53}$$

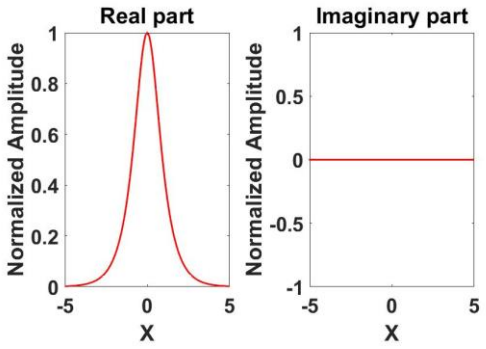

Figure 2-12: Real (left side) and imaginary part (right side) of incident Sech beam

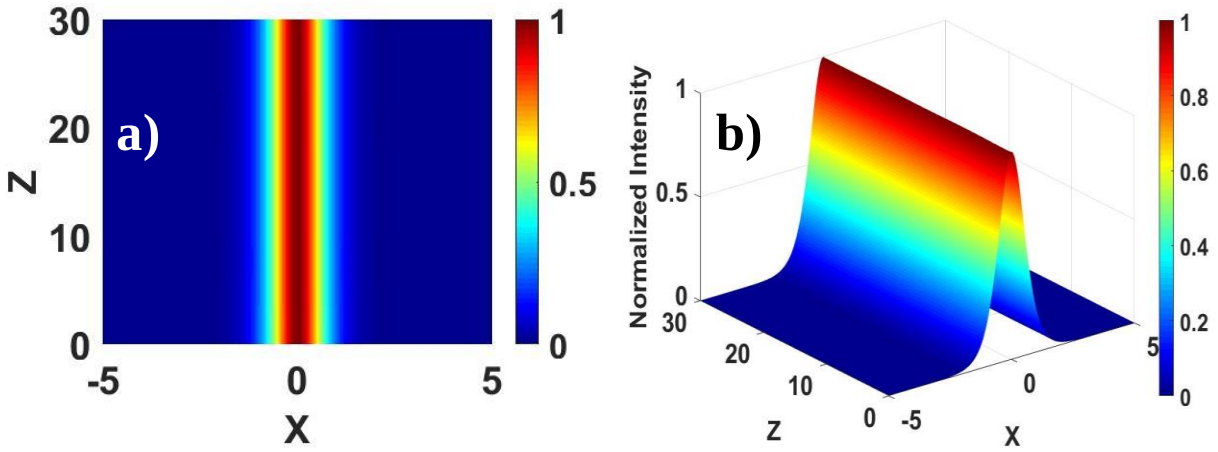

Figure 2-13: Sech intensity propagation for 30Z in, (a) two-dimensional, and (b) three-dimensional view.

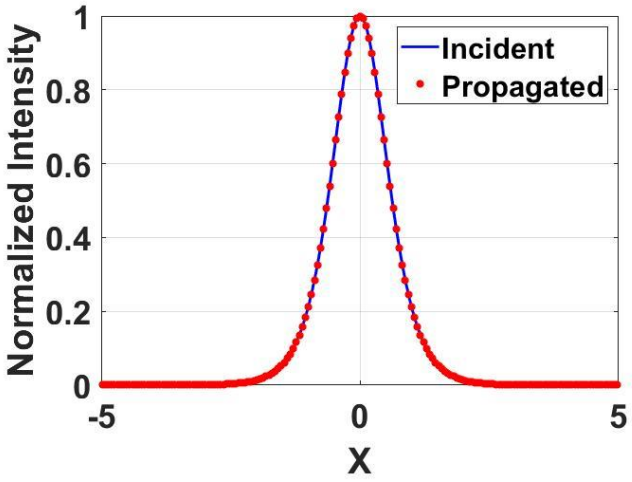

Figure 2-14: Comparing the incident (blue line) and Propagated (red points) intensity profile of the Sech beam after 30Z.

2.6.2 Dark soliton propagation in negative Kerr medium

To study numerically the propagation of a dark soliton equation (2.54) is used as an initial condition. In this part, the medium is the negative Kerr medium where the nonlinear refractive index is negative ($n_2 < 0$), which allows the dark soliton as the solution of the NLS equation. Again, the Split-Step method is used, and a suitable MATLAB program has been written to simulate the intensity propagation in negative Kerr medium.

$$A(X) = 1 * \ Tanh(\sqrt{2}\, X) \tag{2.54}$$

The exact equation that is used for calculating in MATLAB software is included with the multiplication of one super-Gaussian for eliminating the reflected intensity from the borders, which occurs just in numerical MATLAP program. So, the equation (2.55) is considered as initial condition.

$$A(X) = Tanh\left(\sqrt{2}\, X\right).* \exp\left(-\left(\frac{X}{0.80 * X_f}\right)^{20} \right) \tag{2.55}$$

For having a better view of the Tanh beam profile the Figure 2-15 is plotted, that demonstrates normalized amplitude of the real part (left side) and imaginary part (right side) of incident Tanh before propagation. Figure 2-16 shows the intensity propagation of the Tanh beam profile for 30Z distance. More precisely the Figure 2-16 (a) shows the top view of intensity propagation, and Figure 2-16 (b) demonstrates the same information, in addition, the normalized intensity is plotted in another perpendicular axis. Figure 2-16 (a & b) demonstrates that, based on the color bar, the normalized intensity value over the on-axis is zero, and the zero intensity is immersed in the normalized intensity value about 1. This issue of intensity propagation continues until the end of propagation distance. By propagation, the intensity profile is not broadening by diffraction effect nor focusing due to Self-defocusing effect, as it is the definition of spatial dark soliton. Finally, in Figure 2-17, we compare the initial and propagated normalized intensity profile before propagation (blue solid line), and after 30Z propagation (red points) distance, and it can be observed that both intensity profiles are same.

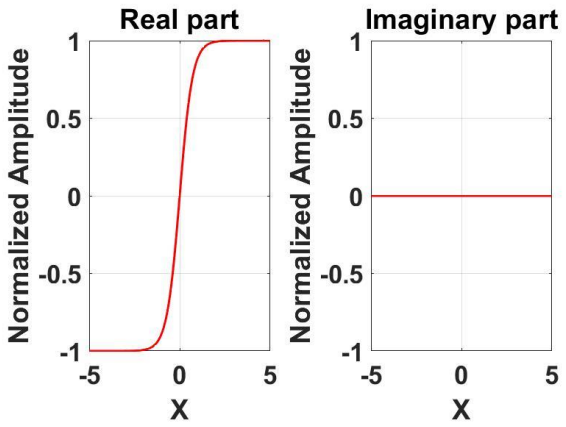

Figure 2-15: Real (left side) and imaginary part (right side) of incident Tanh beam

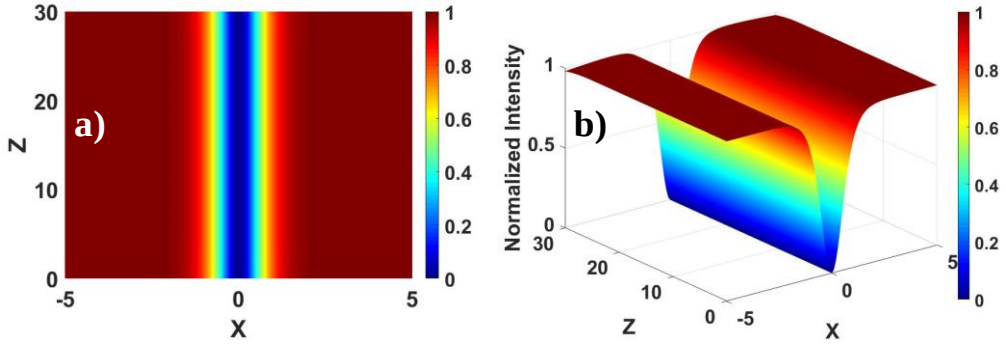

Figure 2-16: Tanh intensity propagation as dark soliton for 30Z in, (a) two-dimensional view, and (b) three-dimensional view

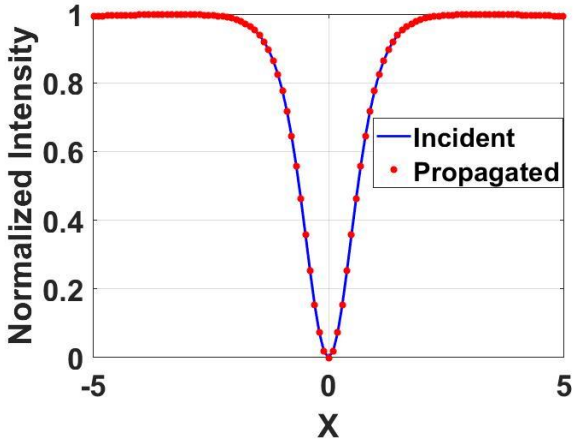

Figure 2-17: Comparing the incident (blue line) and Propagated (red points) intensity profile after 30Z propagation distance of hyperbolic tangent beam profile as dark soliton.

In the appendix appears the MATLAB program (Program 6-3), for simulate the propagation of Sech or Tanh beam in nonlinear Kerr medium. The value of parameter η (eta) in the program must be negative in the case of Tanh propagation.

2.7 Summary

In this chapter the beam propagation in the linear and third order nonlinear medium was discussed. The Fourier Transform method to simulate the propagation of a center intense beam profile in linear medium, and the Split-Step method for nonlinear medium has been introduced. The Nonlinear Schrodinger equation for the Kerr medium has been obtained. The analytical solution of the NLS equation has been demonstrated. The solitary solution of the NLS equation, the bright and dark soliton for positive and negative Kerr medium respectively, has been discussed and the propagation has been simulated.

Chapter 3: **Interactions and Collision**

In this chapter, the soliton interaction in third order nonlinear medium will be reviewed. We discussed the interaction between two bright solitons when the different initial relative phases are chosen. Also, we will describe the interaction of two dark solitons, with the same initial condition as bright soliton. In addition, the collision between two symmetric bright spatial solitons in the Kerr medium will be presented. The results will be argued.

3.1 Soliton interaction in nonlinear (Kerr) medium

Interactions between solitons are perhaps the most fascinating features of soliton phenomena. Soliton interactions are sufficiently complex that it is frequently necessary to resort to detailed numerical calculations for predictions. However, a few cases can be analyzed using inverse scattering theory for the (1+1)-D Kerr case. First, because Kerr solitons are (1+1)-D, their collisions occur in a single plane. Second, all collisions are fully elastic so that the number of solitons is always conserved. Third, the system is integrable, and therefore no energy is lost (to radiation waves). Finally, the directions and propagation velocities of the solitons recover to their initial values after each collision. This equivalence between solitons and particles was first suggested in 1965 and led to the term "soliton" [89]. The real surprise was, however, that solitons survive the collision event as self-trapped entities, even though the solitons themselves are highly nonlinear creatures. Furthermore, the collision between solitons involves "forces" [90] and they interact like real particles, exerting attraction and repulsion on one another. The simplest collisions occur for two parallel launched equivalent solitons when their relative phase is zero (in-phase, $\Delta\phi = 0$). When the solitons interfere, the intensity in the central region between the induced waveguides is increased, which leads to an increase in the refractive index in that region for $n_2 > 0$. This, in turn, attracts more light to the center, moving the centroid of each soliton towards it, and hence the solitons appear to initially attract each other. Detailed analysis of the evolution shows that the force is indeed initially attractive and there is no energy exchange between the solitons. This feature is universal for all coherently interacting solitons in isotropic nonlinear media. Collisions in Kerr slab waveguide media have been demonstrated experimentally in carbon disulfide, glass, and AlGaAs [91]. The attraction and repulsion for $\Delta\phi = 0$ and $\Delta\phi = \pi$ were

clearly observed, as was the exchange of soliton power, which is maximized at $\Delta\phi = \frac{\pi}{2}$ and $\Delta\phi = 3\pi/2$, and the reversal in power transfer direction due to change in $\Delta\phi$ of π. The universal principle unifying all solitons is that the wave-packet (beam or pulse) creates, by virtue of the nonlinearity, a potential well and captures itself in it. It becomes a bound state of its own induced potential well. Thus, interactions between solitons are just interactions between bound states of a jointly induced potential well, or between bound states of different wells located at close proximity [83]. In many aspects, solitons interact like particles despite the electromagnetic wave nature of their fields. The existence of the interaction is manifested in a change in their trajectories when a second soliton is introduced so that the soliton fields overlap significantly in their tails. As the soliton fields, by definition, modify the optical properties of the medium, the propagation characteristics of any other electromagnetic wave, a second soliton, are also affected [83]. Some methods have been reported to construct an optical switch based on the interaction of two bright spatial solitons according to their initial relative angle and although the soliton guidance properties have been carried out, the study has not been carried out fully. [84]

3.1.1 Bright solitons interaction in Kerr medium with relative phase

In nonlinear medium, particularly in Kerr medium with third order positive nonlinearity, the bright spatial soliton beam, hyperbolic secant (Sech), propagates without any diffraction. In other words, there is a balance between diffraction and self-focusing effect. In this part, the interaction between two equal paralleled bright spatial solitons is discussed. The initial condition for interaction between two bright spatial solitons is described by equation (3.1). In this equation two bright spatial solitons (Sech) profile are considered, where their center of beam are located at $X = -C$ and $X = C$. In this equation, A_0 is the normalized amplitude equal to one ($A_0 = 1$), and the relative phase between two beams, which are located at left and right-hand side of transversal axis, is measured by $\Delta\phi$. In this part of interaction, various values of relative phases are considered such as $\Delta\phi = 0, \pi/4, \pi/2, \pi, 2\pi$.

$$A(X) = A_0 Sech\left(\sqrt{2}\,(X + C)\right) * \exp(-i\Delta\phi) + A_0 Sech\left(\sqrt{2}\,(X - C)\right) \qquad (3.1)$$

First, the distance between the center of two beams is considered to be very large compared to the width of the beams, with zero relative phase ($\Delta\phi = 0$). In this case $C = 4$ is specified. Equation

(3.2) is used for the simulation of two equal and initially parallel trajectory beams which is obtained by substituting the C value and the relative phase in equation (3.1).

$$A(X) = A_0 Sech\left(\sqrt{2}\,(X+4)\right) * \exp(-i*0) + A_0 Sech\left(\sqrt{2}\,(X-4)\right) \qquad (3.2)$$

Figure 3-1 shows the initial condition of two Sech beams. Figure 3-1(a) is the initial normalized amplitudes, Figure 3-1(b) the imaginary amplitude, and Figure 3-1(c) the normalized initial intensity, where two equal Sech beams are used for propagation. From Figure 3-1b, it is obvious that, the relative phase is zero, since the imaginary part for both beams is zero. The simulation result of propagation for 40 Rayleigh range (40Z) is presented in Figure 3-2. Figure 3-2a shows the two-dimensional perspective of propagation, and the color value indicates the intensity value. Figure 3-2b shows the same information in three dimensions with the intensity value in the perpendicular axis. The results show that the two beams do not feel each other during propagation, due to their high separation distance. However, in infinity distance of propagation ($Z \to \infty$), they interact with each other, since transversal value of Sech beam does not reach to zero even in large value of X. The stated results are independent of relative phase $\Delta\phi$.

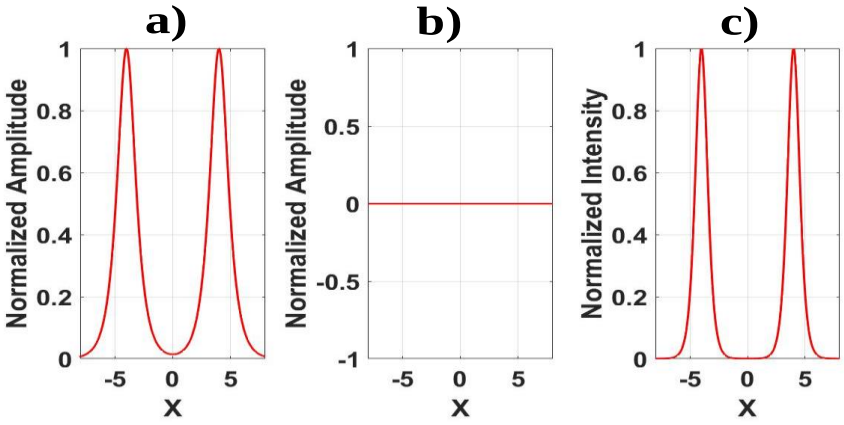

Figure 3-1: Initial normalized (a) amplitude, (b) imaginary part, and (c) intensity of two initialy parallel Sech beams at $X = \pm 4$, $\Delta\phi = 0$.

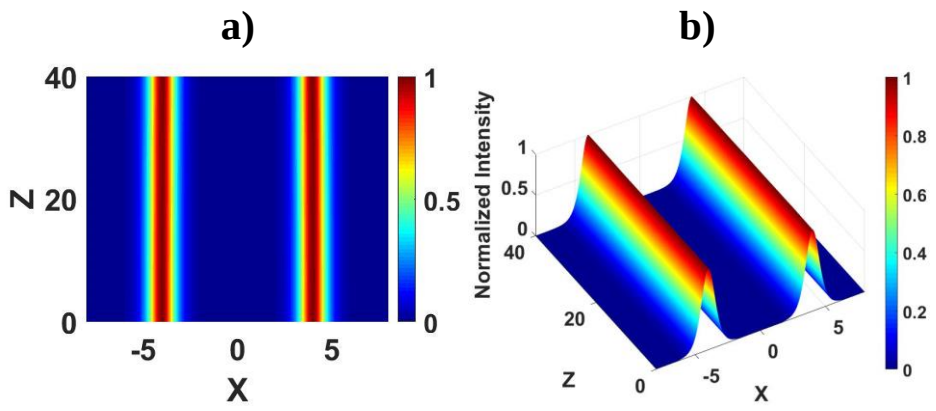

Figure 3-2: Propagation of two Sech beams, (a) 2-D, and (b) 3-D, when their center of beams are far from each other at X $= \pm 4$, $\Delta\phi = 0$.

When the transversal distance of two solitons is small, they feel the presence of each other. The simplest soliton interaction occurs for two equal paralleled propagated solitons with different phase equal to zero, giving rise to an attraction between the solitons. When these beams propagate along the Z-axis, they interfere coherently and the intensity in the central region, between the induced waveguides, is increased, which leads to an increase in the refractive index in that region. In this part the lower value of C (i.e. C=1.2), with relative phase equal to zero ($\Delta\phi = 0$), as appears in equation (3.3) is considered and the results of the simulation appears in Figure 3-3.

$$A(X) = A_0 Sech\left(\sqrt{2}\,(X + 1.2)\right) * \exp(-i * 0) + A_0 Sech\left(\sqrt{2}\,(X - 1.2)\right) \quad (3.3)$$

Figure 3-3a shows the two-dimensional perspective of the interaction, and the color value indicates the value of intensity. Whereas Figure 3-3b shows the intensity value by a perpendicular axis as well as color bar. The results from Figure 3-3 shows that, for two equivalent Kerr solitons, with initially parallel trajectories and zero relative phase, the resulting path of the centroid of each individual soliton is periodic with the solitons returning to their input condition at the end of each cycle.

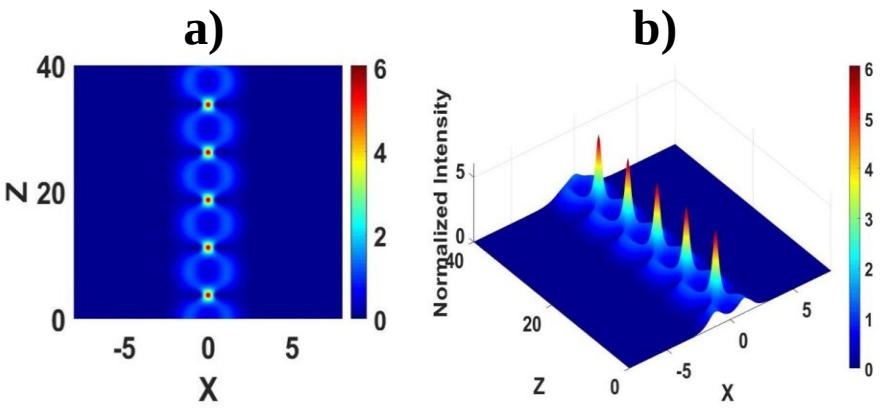

Figure 3-3: Propagation of two Sech beams, (a) 2-D, and (b) 3-D, when their center of beams are at $X = \pm 1.2$, and $\Delta\phi = 0$

The interaction between two equivalent Kerr solitons, on initially parallel trajectories, with other values of relative phase $\Delta\phi = \pi/4$, $\Delta\phi = \pi/2$, and $\Delta\phi = \pi$ is simulated in Figure 3-4. Figure 3-4 (a & b), shows the result of $\Delta\phi = \pi/4$. At the beginning of propagation some energy is transferred from the beam with retarded phase to the other beam, then, the left-hand side beam is propagating with lower intensity and continues almost with the same path, while right-hand side beam, gains energy and propagates with some angle, and its intensity profile as well as beam-width oscillates. Likewise, this issue happens for the case of $\Delta\phi = \pi/2$ (see Figure 3-4 (c & d)) just the angle of path increases more and propagates with wider angle. This semi-repelling occurs when $\Delta\phi = 3\pi/4$ and widest angles happen for the right-hand side beam. The Figure 3-4(e & f), shows interacting beams with $\Delta\phi = \pi$ out of phase from each other. They interfere destructively, and the refractive index in the central region is lowered by their overlap. Therefore, the centroid of each soliton moves outward and the solitons appear to repel each other, and the both beam paths suffer symmetric widening angle by propagation. To get fully information for the above interactions, a comparison between the initial intensity profile of two Sech beams, and propagated intensity profiles after propagation for 40 Z in Figure 3-5, is plotted. Figure 3-5 (a, b & c), are the results for $\Delta\phi = \pi/4$, $\Delta\phi = \pi/2$, and $\Delta\phi = \pi$, respectively. The results show that for $\Delta\phi = \pi/4$, the center of right-hand side beam is shifted from X=1.2 to X=5.039 after 40 Z propagation. For the case of relative phase $\Delta\phi = \pi/2$ the center of right-side beam reaches to X=8.965 while the left-hand side beam path also receives wider angle.

By increasing the relative phase $\Delta\phi$ more than $\Delta\phi = 3\pi/4$, the left-hand side, instead of losing energy, gains the energy and widen its path angle where the center of the propagated beam reaches the position of beam to $X = -11.48$. For the case of $\Delta\phi = \pi$, symmetric widening angle for both propagation path (right- and left-hand side beam) happens, this is a consequence of the repelling between both beams. The final position for center of both beams after 40Z propagation, reaches to $X = \pm 11.43$ with same symmetric normalized intensity profiles as the initial. Finally, for $\Delta\phi = 2\pi$ beams interaction occurs same as $\Delta\phi = 0$ and periodically absorb and repel each other. As the amplitudes and the relative phases of the solitons change with distance, their widths also change keeping the appropriate relation between width and peak power for Kerr solitons. Consequently, the details of the trajectories can be quite complex [83][92][93].

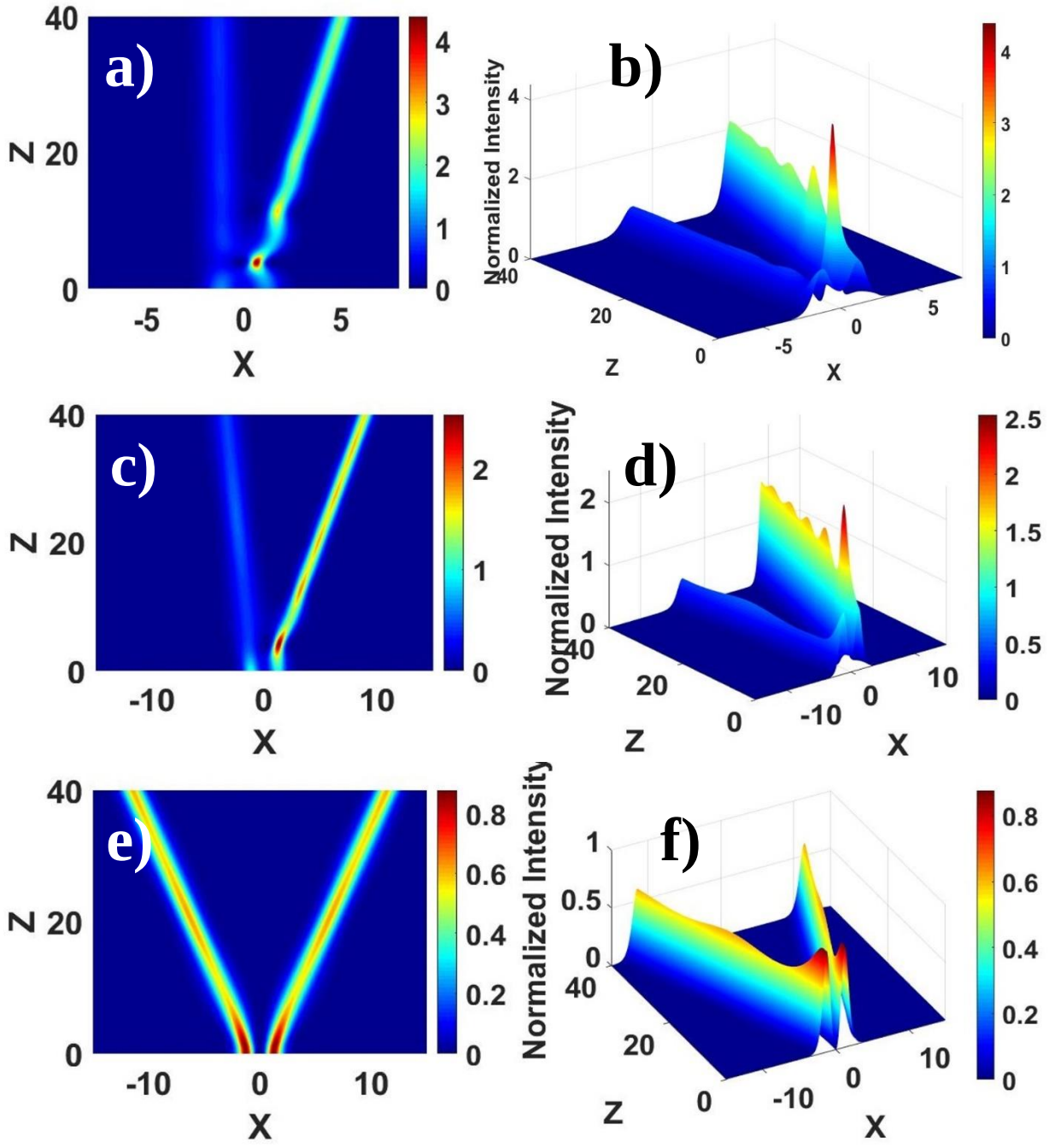

Figure 3-4: Two Sech beam propagation, when their center of beams are at $X = \pm 1.2$ (a) 2-D (b) 3-D for $\Delta\phi = \pi/4$, (c) 2-D (d) 3-D for $\Delta\phi = \pi/2$, and (e) 2-D (f) 3-D for $\Delta\phi = \pi$

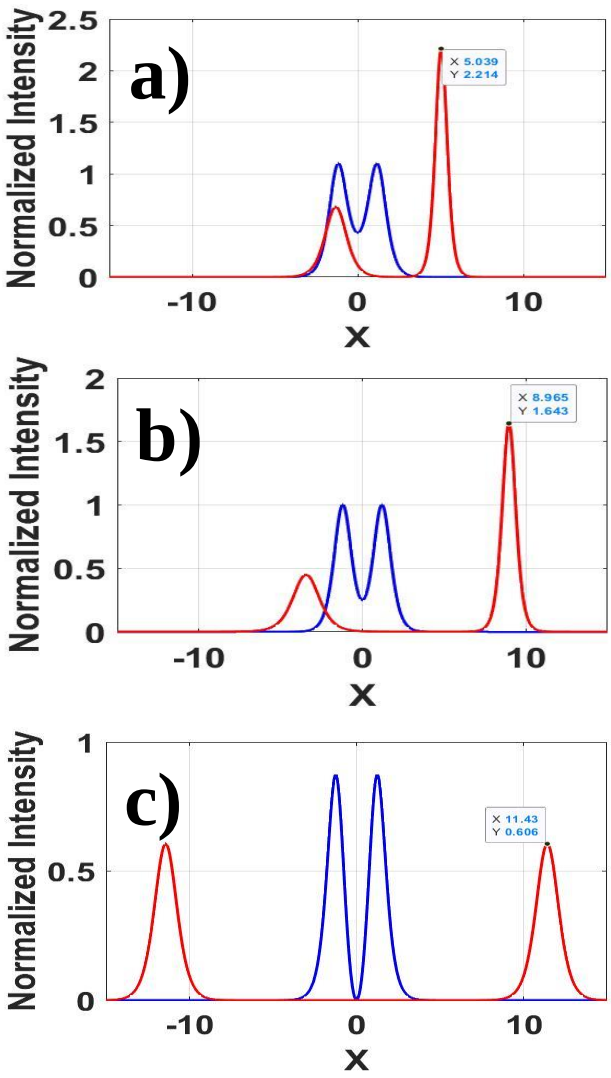

Figure 3-5: Comparison between initial normalized intensity profile and propagated intensity profile of two Sech beam, after 40Z, with initial center of beams at $X = \pm 1.2$ for (a) $\Delta\phi = \pi/4$, (b) $\Delta\phi = \pi/2$, and (c) $\Delta\phi = \pi$

3.2 Collision between two symmetric bright spatial solitons in Kerr medium

Soliton interaction between two coherent bright spatial solitons in Kerr media were investigated and it was proved that it is possible to control a weak beam [84,94,95] and even obtain an optical switching according to the phase difference between the solitons [96,97]. Soliton interactions were demonstrated experimentally for (1+1)-D glass waveguides in 1991 by Aitchison et al [86,98]. They reported that in a Kerr medium in-phase solitons are attracted to each other, whereas out-of-phase solitons repelled one another. Solitons propagate and interact with one another while

displaying properties that are normally associated with real particles. Collisions between solitons are fully elastic in Kerr media, which implies that the number of solitons always is conserved. Collision of two bright spatial solitons with initial condition mentioned in equation (3.4), is simulated in this section. Consider two initial beams having 2C separation distance.

$$A(X) = A_0\,\mathrm{Sech}\left(\sqrt{2}\,(X + C)\right) * \exp(-i\Delta\phi) * \exp(iV.X) + A_0\,\mathrm{Sech}\left(\sqrt{2}\,(X - C)\right) * \exp(i(-V).X) \quad (3.4)$$

Where $A_0 = 1$ is the amplitude of both beams, $\Delta\phi$ the relative phase, C the initial separation distance between the two initial Sech beams at $X = \pm C$, and $V = 1$ the initial angle of beam path. In this work, in the collision process, various relative phases $\Delta\phi = 0, \pi/4\,, \pi/2,\ \pi$ and 2π are considered. Figure 3-6 shows the two Sech normalized intensity beam propagating in Kerr medium with some angles in which they finally collide each other. In Figure 3-6a) the considered relative phase is zero. Since both beam profiles are symmetric and have the same initial phase, the collision takes place exactly at X=0. In the colliding point, the two beams give a high intensity I=4.002, and after colliding, both beams again get their own intensity profile and continue the propagation. By increasing the relative phase to $\Delta\phi = \pi/4$ as simulated in Figure 3-6b, the colliding point still is in the center. The left-hand side beam with $\pi/4$ retardant relative phase, transfers the energy to the right-hand side beam, and increases the normalized intensity of right-hand side beam around I=3.69, at X=+0.2344. After the collision, both beams retake their own initial intensity profile. If the relative phase continues changing till $\Delta\phi = \pi/2$ (see Figure 3-6c) transferring energy happens to I=3.29, at X=+0.4688. By increasing the relative phase, the transferring energy decay until reach to the critical point $\Delta\phi = \pi$ (see Figure 3-6d), the two beams no more absorb each other and they completely repel. The symmetric points X=-0.8203 and X= +0.8203 gives lowest energy to the medium I=1.781, and as in previous cases, after collision the two beams collect their own intensity profile and continue their own propagation path. For the relative phase higher than π, all these issues happen but in the mirror form: the other beam receives energy, until relative phase come to the $\Delta\phi = 2\pi$. At the center point X=0 they absorb each other and gives highest energy to the medium.

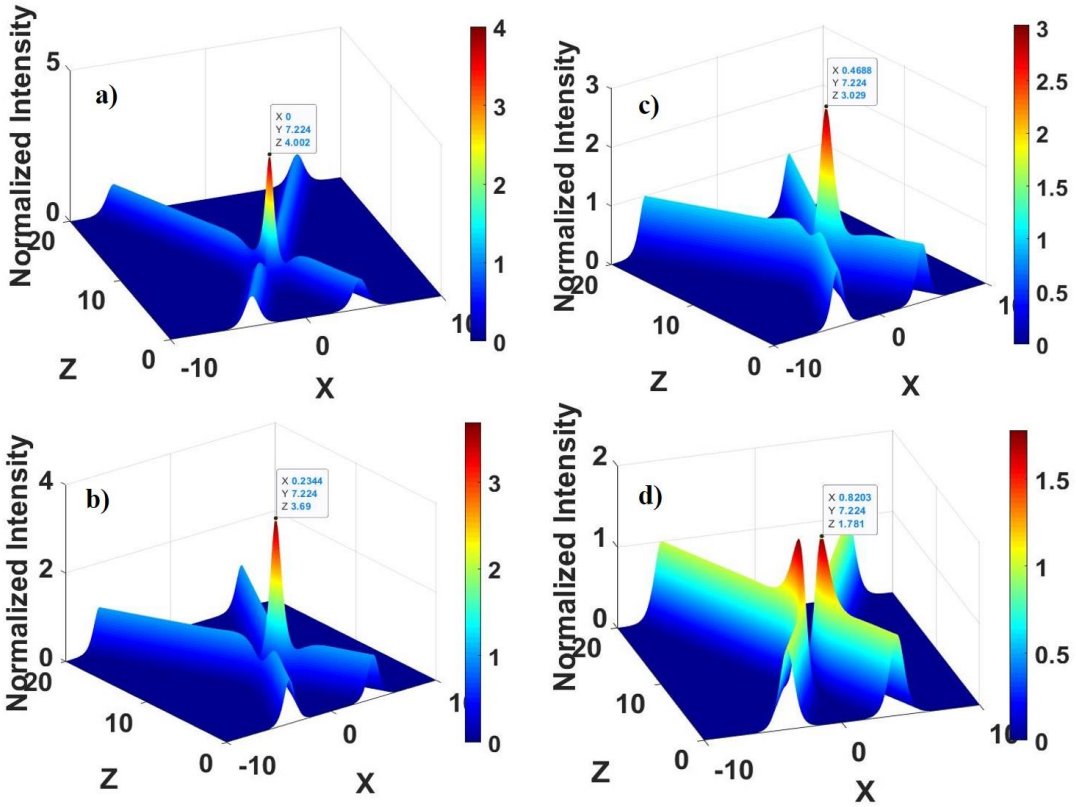

Figure 3-6: Two symmetric Sech beams collision with relative phase a) $\Delta\phi = 0$, b) $\Delta\phi = \pi/4$, c) $\Delta\phi = \pi/2$ and d) $\Delta\phi = \pi$.

After collision between two beams, they do not follow the same path they were following before and they propagate with wider angles. This behavior in displayed in Figure 3-7. The figure compares the initial intensity profile and the center position of the two initial Sech beams, before (blue) and after propagation (red). Also, in this figure we plot in green the position of the two beams when they propagate without any collision. In this simulation the initial position of the two beams are at $X = \pm 4$, and the widening angle of propagation due to collision, has no dependency on their relative phase.

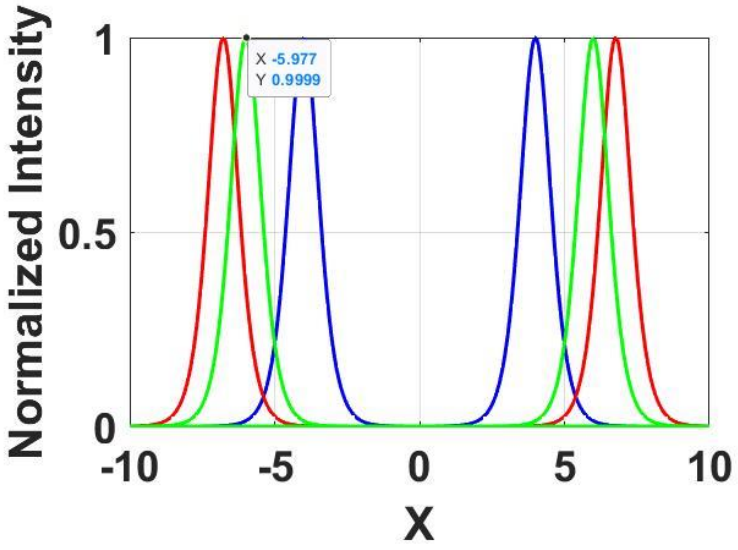

Figure 3-7: Two Sech beam collision, before collision (blue), after collision (red) and without collision (green)

3.2.1 Dark soliton interaction in Kerr medium

Dark soliton is referred to an area of intense beam having a hole at the center with zero intensity. "Dark solitons, which have an intensity profile in the form of a dip in an otherwise uniform background, are topological objects because of their nontrivial phase structure" [99]. Interaction between two dark solitons (Tanh) which are initially in parallel trajectory, is investigated in this part. The main parametric equation that is used for interaction of two dark soliton is mentioned in the general case in Equation (3.5). In this equation A(X) is the total amplitude of two dark solitons, $2C$ the separation distance between the two beams, A_0=1 the amplitude of each beam with their center are located at $X = \pm C$, $\Delta\phi$ the relative phase between the two beams. So that, the beam located at $X = -C$ receives $\Delta\phi$ retardant phase. In equation (3.5), expression $\exp\left(-\left(\frac{X}{0.80*X_f}\right)^{20} \right)$, which is a super Gaussian, is multiplied to initial beam profile to avoid reflection from boundaries in the MATLAB program. And X_f is the distance from X=0 to the right or left side of the boundary.

$$A(X) = \left\{\left[Tanh\left(\sqrt{2}\,(X+C)\right) * \exp(-i\Delta\phi)\right] * \left[Tanh\left(\sqrt{2}\,(X-C)\right)\right]\right\} * \exp\left(-\left(\frac{X}{0.80 * X_f}\right)^{20}\right) \quad (3.5)$$

Dark soliton is the solution of Nonlinear Schrödinger Equation with negative Kerr coefficient [87]. The numerical Split-Step method in a MATLAB program has been used to solve and simulate the interaction of two dark solitons. First, we consider a high separation distance (C =4) in comparison with the width of the beams, in such a way that they do not feel their presence. The initial on-phase $\Delta\phi = 0$ and out-of-phase $\Delta\phi = \pi$ is considered. In Figure 3-8 (a, b & c) appears the initial real part, imaginary part, and normalized initial intensity respectively, for the case of on-phase (up row), and out-of-phase $\Delta\phi = \pi$ (down row). Figure 3-9 shows the simulation for propagation of two parallel Tanh beams for 30Z, where their initial center of beams are located at $X = \pm 4$, for both cases of on-phase and out-of-phase beams. Since their separation is large, they do not feel each other, and the result is the same by considering any relative phase. More confirmation that they do not feel each other is demonstrated by Figure 3-10 in which the comparison between initial (blue line) and propagated (red points) normalized intensity of two parallel Tanh beams is simulated for both case of in-phase or out-of-phase.

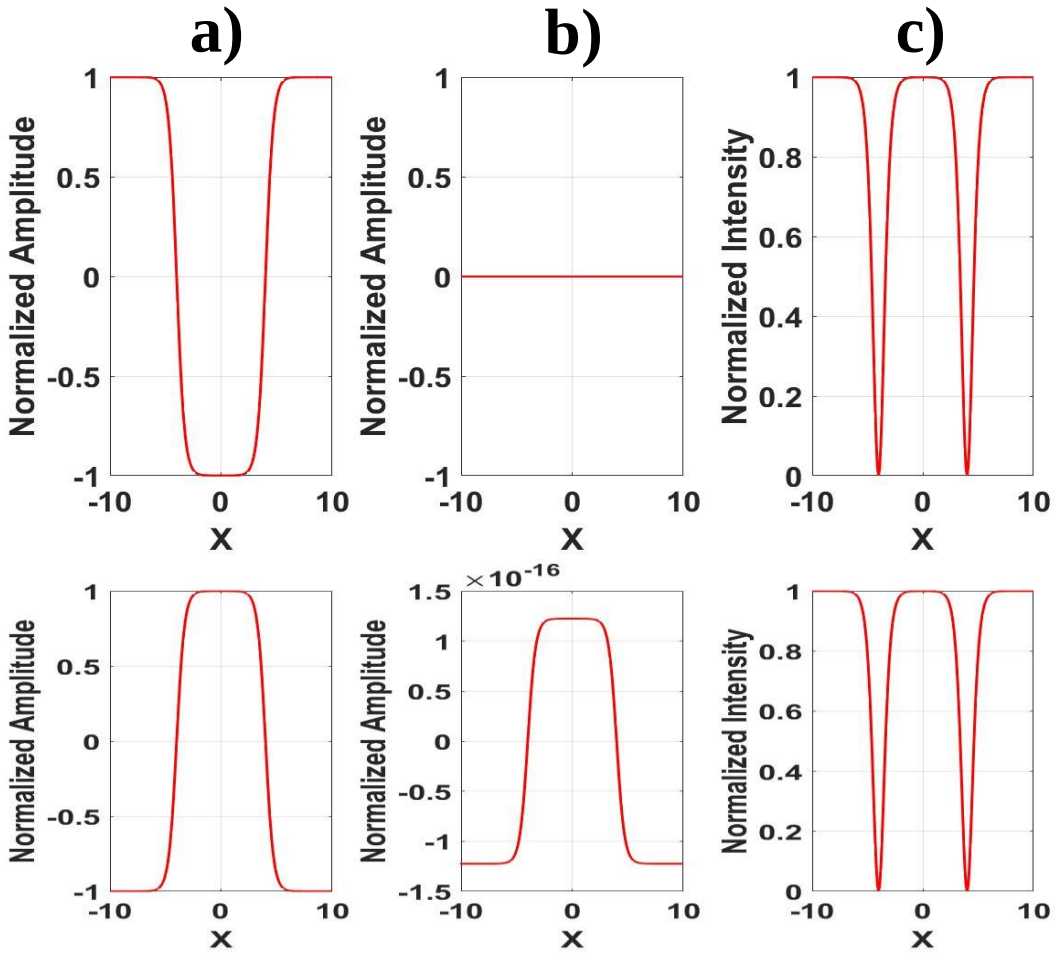

Figure 3-8: Initial two tanh beams located at $X = \pm 4$ with relative phase $\Delta\phi = 0$ (up row), and $\Delta\phi = \pi$ (down row). (a) amplitude, (b) imaginary part, and (c) intensity of two beams.

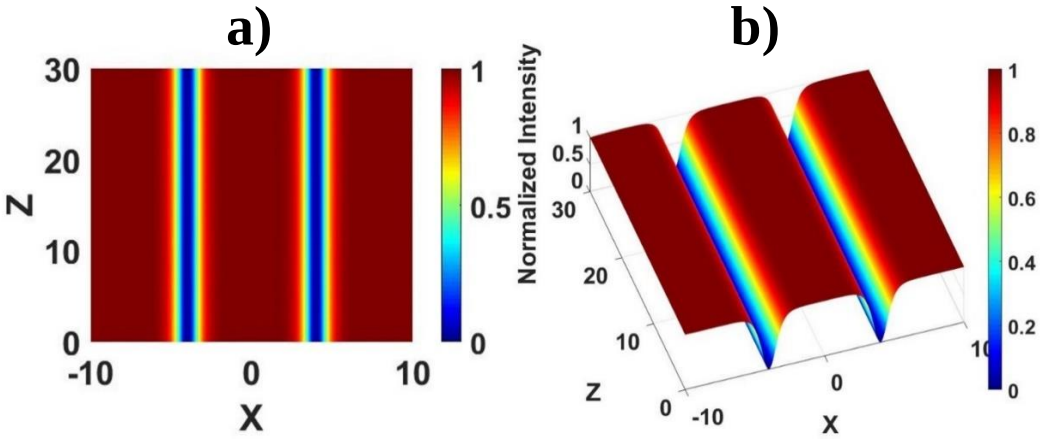

Figure 3-9: Simulation of the propagation for two parallel Tanh beams when their initial center of beam are located at $X = \pm 4$, (a) 2-D and (b) 3-D.

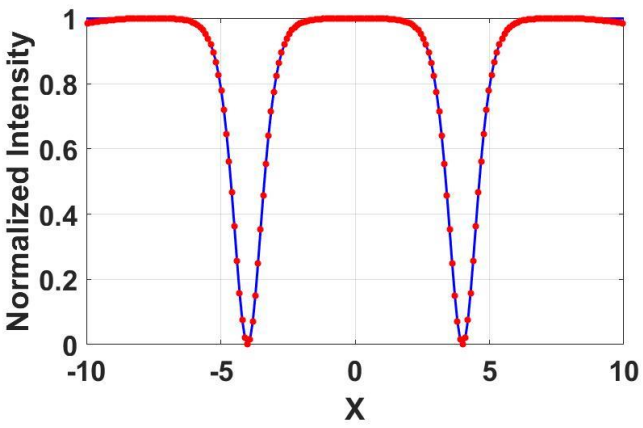

Figure 3-10: Comparison between initial (blue line) and propagated (red points) normalized intensity of two-parallel Tanh beam propagation when their initial center of beam are located at $X = \pm 4$

However, if smaller separation distance is used (i.e. C=1.2), they have effect over each other. In Figure 3-11 we plot two initial tanh beams located at $X = \pm 1.2$ with relative phase $\Delta\phi = 0$ (up row), and $\Delta\phi = \pi$ (down row). In this figure appear, (a) the amplitude, (b) the imaginary part, and (c) the normalized intensity. Figure 3-12 shows the normalized intensity for propagation and interaction of two Tanh beams, for (a) the two-dimensional view, and (b) the three-dimensional view. The Figure 3-12 is valid for both cases of in-phase ($\Delta\phi = 0$), or out of phase ($\Delta\phi = \pi$), and the figure shows that always the solitons repel each other and has no relation with their relative phase. For more confirmation on repelling issue between two dark solitons, Figure 3-13 compares the initial intensity profile (blue line), and the propagated intensity profile after 30Z (red line) for both cases of on-phase and out-of-phase (any value of $\Delta\phi$). we observe that the two intensity profiles don't match, and the final intensity profile has shifted to sides. The result from Figure 3-13 shows that, although the initial center point of intensity profile locates $X = \pm 1.2$, the final position is repelled and shifted to the $X = \pm 2.344$ by considering any relative phases. Then it is concluded that, the interaction between two dark solitons, or more precisely the repulsion doesn't have relation to their relative phase.

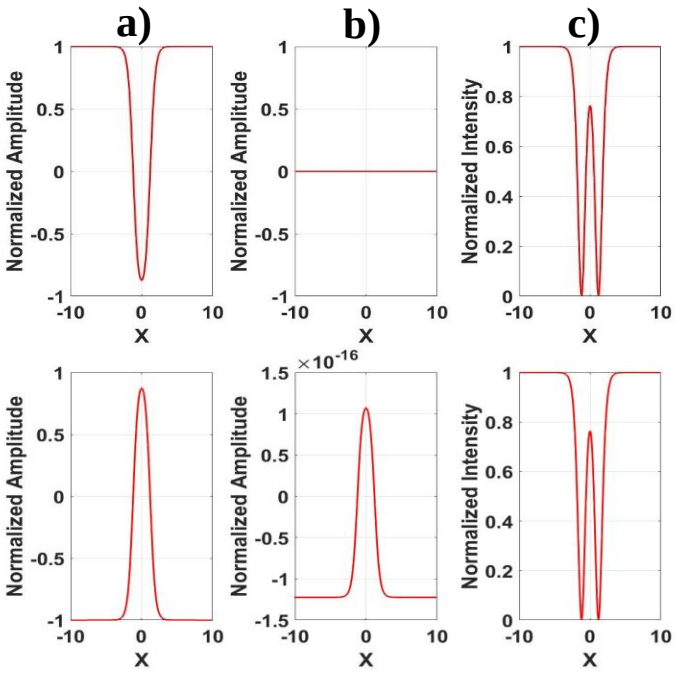

Figure 3-11: Initial two tanh beams located at $X = \pm 1.2$ with relative phase $\Delta\phi = 0$(up row), and $\Delta\phi = \pi$ (down row). (a) Amplitude of two beams, (b) imaginary part, and (c) the normalized intensity.

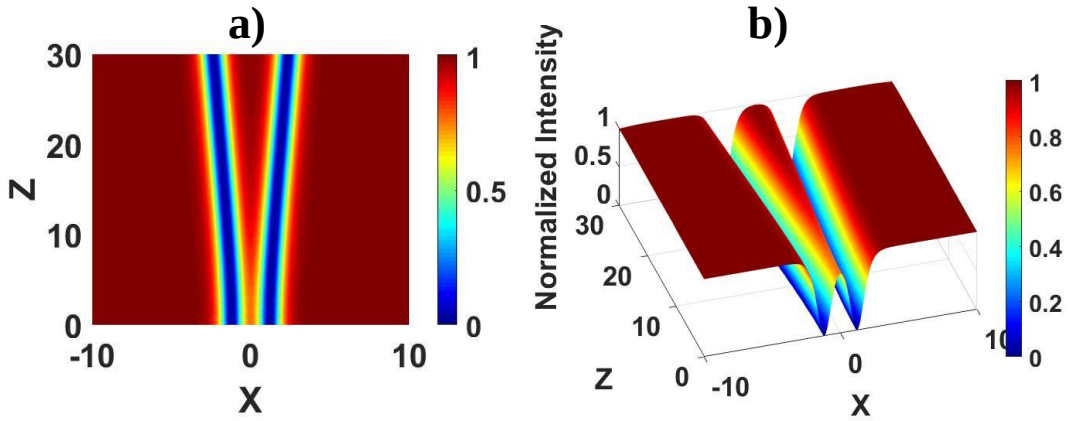

Figure 3-12: Simulation of propagation for two parallel Tanh beams (in-phase and out-of-phase $\Delta\phi = \pi$) when their initial center of beam are located at $X = \pm 1.2$, (a) 2-D, (b) 3-D

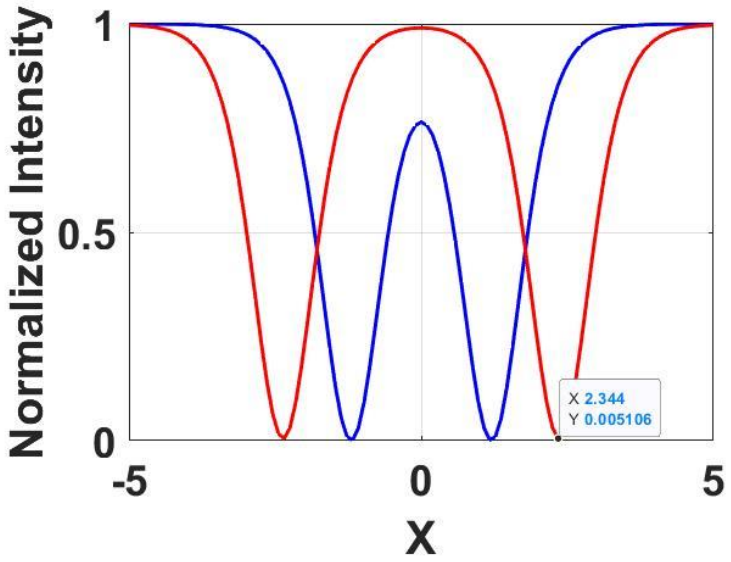

Figure 3-13: Comparison between initial (blue line) and propagated (red line) normalized intensity of two parallel Tanh beams when their initial center of beam are located at $X = \pm 1.2$

3.3 Summary

In this chapter, the interaction of initially parallel trajectory of two bright spatial soliton beams was investigated. We demonstrated that, when the relative phase between two bright solitons is zero $\Delta\phi = 0$, the resulting path of the centroid of each individual soliton is periodic, with the solitons returning to their input condition at the end of each cycle. However, when the relative phase is $\Delta\phi = \pi$, the intensity of two beams interact destructively, in such a way that the intensity between two beam paths is decreased. Since the refractive index in a third order nonlinear medium has a dependency on intensity, by decreasing the induced refractive index in the path between two solitons, the two beams appear to repel each other. For other relative phases, the interaction issue is more complicated. In other viewpoint, the "force" between the solitons varies smoothly from a maximum attractive at $\Delta\phi = 0$, to a maximum repulsive at $\Delta\phi = \pi$. The results show that, when two bright solitons propagate at a big angle, after the colliding point, they never return to each other, and continue their own modified paths. For the interaction of two initially parallel trajectory dark solitons in a third order nonlinear medium, there is no dependency to their initial relative phase, and always they repel each other.

Chapter 4: **Quasi-solitons in nonlocal and local medium**

In this chapter, we study the propagation of an arbitrary initial beam profile in nonlocal and local media. At first the theory of nonlocality using different nonlocal response function of the medium such as Gaussian, Hyperbolic Secant, and Exponential, with different degree of nonlocality will be discussed. In addition, the appropriate NLS equation for nonlocal medium is presented. Propagation of Hyperbolic Secant beam (as bright soliton in local medium) in a nonlocal medium is simulated, and we observe that the beam suffers diffraction if we increase the degree of nonlocality. In order to confine the beam intensity profile as much as possible in the direction of propagation, some initial condition has to be considered, although some intensity oscillation is inevitable, and the beam propagates as the quasi-soliton. In general the quasi-solitons is referred to a soliton-like pulses in laser or fiber optic links, where true soliton cannot exist, and here as spatial soliton discussion the quasi-soliton is used since the intensity profile of the beam is not constant and some oscillation is detected as well as the oscillation on beam-width during the propagation. The propagation of other arbitrary beam profiles in nonlocal media is discussed in order to obtain the quasi-soliton. Then after, the propagation in local medium by an arbitrary initial beam profile (Super-Gaussian, Gaussian, Triangular, Rectangular, Exponential) for obtaining the quasi-soliton is discussed.

4.1 Propagation in nonlocal media

Typical of many nonlinear materials, the induced change of refractive index, Δn, ($n = n_0 + \Delta n$ and $\Delta n = n_2 I$) obeys $\Delta n \ll n_0$. The conventional model assumes an idealized local response when, by definition, n at position X is proportional to the beam's intensity at X. This local (Kerr) model admits solitons in two dimensions only [38]. Spatial nonlocality, which is already an established concept in plasma physics, means that the response of the medium at a particular point is not determined solely by the wave intensity at that point (as in local media), but also depends on the wave intensity in its vicinity [57]. The nonlocal nature often results from a transport process, such as atom diffusion [35], heat transfer [100], or drift of electric charges [101]. It can also be

induced by a long-range molecular interaction as in dipolar Bose Einstein Condensate[102], or Nematic liquid crystals [26]. Nonlocality is, thus, a generic feature of a large number of nonlinear systems. It has also recently become important in optics [38]. Although nonlocality can have a considerable impact on many nonlinear phenomena, studies of nonlocal nonlinear effects are still in their infancy. Consider a model of nonlinearity whose response is highly nonlocal. Then, by definition, a light beam of characteristic radius ρ creates a circularly symmetrical refractive index change Δn whose characteristic spatial extent is much larger than ρ and whose axis is set by the beam center and its initial direction. Consequently, Δn_2 depends on the integrated intensity of the beam, or power *P*. The situation of high nonlocality is analogous to observing distant point sources through a badly blurred lens. When the point sources (light beams) are sufficiently close to the lens axis, the shape of the blur circle (nonlocal response) is indistinguishable from that due to one-point source alone. At the other extreme, a local response is analogous to having a delta-function blur circle. Various materials exhibit a highly nonlocal response, including photorefractive materials, liquid crystalline materials, and materials that exhibit laser-induced thermal nonlinearities [38]. Even though it is quite apparent in some physical situations that the nonlinear response in general is nonlocal (as in the case of thermal lensing), the nonlocal contribution to the refractive index change was often neglected. This is justified if the spatial scale of the beam is large compared to the characteristic response length of the medium (given by the width of the response function). However, for very narrow beams the nonlocality can be of crucial importance and has to be taken into account [33], [103]. The nonlinear response of various materials extends beyond the illuminating beam. According to the degree of the nonlocality determined by the relative width of the response kernel and the optical beam (or the other wave packets for more general cases), there are four categories of the nonlocality[3],[49],[104]: local, weakly nonlocal, generally nonlocal, and strongly nonlocal. In local media (as till now it was the case) we present the Nonlinear Schrodinger equation (NLS) as below:

$$-i\frac{\partial q(r,Z)}{\partial Z}=\frac{1}{4}\left(\frac{\partial^2 q(r,Z)}{\partial X^2}+\frac{\partial^2 q(r,Z)}{\partial Y^2}\right)\pm\frac{Z_R}{L_{NL}}|q(r,\mathrm{Z})|^2 q(\mathrm{r},Z) \qquad (4.1)$$

The following scalar electric field as an optical beam for propagation in nonlinear medium, is considered.

$$U(r,t)=A(r,\mathrm{Z})e^{in_0\vec{K}_0.\vec{r}}e^{-i\omega t}+\mathrm{C.C}$$

That ω is optical frequency and $A(\vec{r},Z)=\sqrt{I_m}q(\vec{r},Z)$ is slowly varying amplitude with I_m the maximum value of intensity, and $q(\vec{r},Z)$ the normalized amplitude by $\sqrt{I_m}$.

As is mentioned in many articles [57] the NLS equation for the nonlocal case can be written as,

$$-i\frac{\partial q(r,z)}{\partial Z}=\frac{1}{4}\left(\frac{\partial^2 q(r,z)}{\partial X^2}+\frac{\partial^2 q(r,z)}{\partial Y^2}\right)\pm\Delta n(\mathrm{I})*q(r,z) \tag{4.2}$$

Where the positive (negative) signs correspond to a focusing (defocusing) nonlinearity and r and Z denote transverse and propagation normalized coordinates, respectively. It is assumed, that the refractive index change $\Delta n(I)$, induced by the beam, with intensity $I(r,z)=|q(r,z)|^2$ can be described by the phenomenological nonlocal model according to,

$$\Delta n(I)(r,Z)=\int_{-\infty}^{+\infty}R(r'-r)I(r',Z)dr' \tag{4.3}$$

In equation (4.3), the induced refractive index change $\Delta n(I)$ is the convolution between local intensity and $R(r)$, the response function of the medium. And the integral $\int dr'$ is over all transverse dimension. The response function $R(r)$ is assumed to be real, localized and symmetric (i.e. $R(\vec{r})=R(r)$, where $r=|\vec{r}|$) and satisfies the normalization condition as following.

$$\int_{-\infty}^{+\infty}R(X)dX=1 \tag{4.4}$$

The width of the response function $R(r)$ determines the degree of nonlocality. For a singular response, $R(x)=\delta(x)$ –delta Dirac– the refractive index change in equation (4.3) becomes same as the local case, equal to light intensity, $\Delta n(I)(x,z)=I(x,z)$ i.e., the refractive index change at a given point is solely determined by the light intensity at that very point [26]. By increasing width of $R(r)$,which is done by increasing the value of α in equation (4.5) and (4.6), the light intensity in the vicinity of the point r, also contributes to the refractive index change at that point. While equation (4.3) is a phenomenological model, it nevertheless adequately describes several physical situations of the nonlocal nonlinear response, such as various transport effects where the nonlocal response is manifested: heat conduction, diffusion of molecules or atoms. We propose various nonlocal response functions, such as Hyperbolic Secant (Sech), Gaussian and Exponential function and the considered functions are:

$$R_g(X)=R_{0g}\exp\left(-\left(\frac{X}{\alpha_g}\right)^2\right) \qquad \rightarrow \text{Gaussian Nonlocal response} \tag{4.5}$$

$R_S(X) = R_{0s}\, Sech\left(\frac{X}{\alpha_s}\right)$ → Sech Nonlocal response

$R_e(X) = R_{0e} \exp\left(-\frac{|X|}{\alpha_e}\right)$ → Exponential Nonlocal response

In this package of equations, R_{0s}, R_{0g}, R_{0e} are the amplitude and $\alpha_s, \alpha_g, \alpha_e$ represent the width or degree of nonlocality of Sech, Gaussian and Exponential nonlocal response functions respectively. If we normalize the equations according to equation (4.4), they can be written as,

$$R_g(X) = \frac{1}{\alpha_g\sqrt{\pi}} \exp\left(-\left(\frac{X}{\alpha_g}\right)^2\right) \quad \text{→Normalized Gaussian Nonlocal response}$$

$$R_S(X) = \frac{1}{\int_{-\infty}^{+\infty} Sech\left(\frac{X}{\alpha_s}\right) dX}\, Sech\left(\frac{X}{\alpha_s}\right) \quad \text{→Normalized Hyperbolic Secant Nonlocal response} \qquad (4.6)$$

$$R_e(X) = \frac{1}{2*\alpha_e} \exp\left(-\frac{|X|}{\alpha_e}\right) \quad \text{→Normalized Exponential Nonlocal response}$$

In the NLS equation, the term $i\frac{\partial q(r,z)}{\partial Z}$ shows the change over the beam profile by propagation in direction of z. $\frac{1}{4}\left(\frac{\partial^2 q(r,z)}{\partial X^2} + \frac{\partial^2 q(r,z)}{\partial Y^2}\right)$ gives the information about diffraction, however $\frac{Z_R}{L_{NL}}|q(r,\mathrm{Z})|^2 q(r,Z)$ in equation (4.1) demonstrate the nonlinear effect (self-focusing or self-defocusing). When the diffraction effect and nonlinear effect are equal the beam propagates as a soliton, i.e. the beam intensity profile does not change by propagation in medium. The bright soliton profile is one solution of NLS equation in the local medium, in the form of hyperbolic secant as follows:

$$q(X) = Sech\left(\sqrt{2}X\right) = Sech\left(\frac{X}{b_s}\right) = Sech\left(\frac{X}{0.7071}\right) \qquad (4.7)$$

First, we study the propagation behavior of an initial bright soliton, hyperbolic Secant (Sech) in a nonlocal medium with different nonlocal responses and different degrees of nonlocality. To obtain the effect of the nonlocal response over the beam propagation, the convolution between the nonlocal response function and the local intensity of beam is required. The related Nonlinear Schrodinger Equation (NLS) for nonlocal medium, equation (4.2), is solved numerically by MATLAB using the Split-Step method. The MATLAB program is written for (1+1)-Dimensional NLSE, where 1 dimension is for transversal axis (X), and another dimension is for propagation direction (Z). In figures Figure 4-1, Figure 4-2, and Figure 4-3 we demonstrate the propagation of the Sech as appears in (4.7) as the initial condition in a nonlocal medium. Three different nonlocal response functions (Exponential, Gaussian, and Sech) are considered according to (4.6). In

addition of different nonlocal response functions, different degree of nonlocality has been taken into account, from very weak nonlocality till highly nonlocal case. For a better view, the propagation simulation appears in two different views. Left column of these three figures (Figure 4-1, Figure 4-2, and Figure 4-3) shows the top view of the propagation for a beam launched from down side in the medium, and the color value shows the value of intensity referred to the bar color. The right column in these three figures, shows the similar information, just the intensity value in any point of positions is displayed over another perpendicular axis. In Figure 4-1 we show the propagation of a Sech as initial condition in an Exponential nonlocal medium for different degrees (α_e), of nonlocality where: (a & b) $\alpha_e = 0.1$, (c & d) $\alpha_e = 1$, (e & f) $\alpha_e = 3$, (g & h) $\alpha_e = 5$, (i & j) $\alpha_e = 10$. In Figure 4-2 and Figure 4-3, the same initial condition as Figure 4-1 is considered, the only difference is the nonlocal response function, Gaussian, and Sech respectively. In Figure 4-2, α_g plays the role for degree of nonlocality, and the intensity profile is illustrated in Figure 4-2 corresponding to (a & b) $\alpha_g = 0.1$, (c & d) $\alpha_g = 1$, (e & f) $\alpha_g = 3$, (g & h) $\alpha_g = 5$, (i & j) $\alpha_g = 10$. In Figure 4-3 (a & b) corresponds to $\alpha_s = 0.1$, (c & d) $\alpha_s = 1$, (e & f) $\alpha_s = 3$, (g & h) $\alpha_s = 5$, and (I & j) $\alpha_s = 10$. Form these figures (Figure 4-1, Figure 4-2, and Figure 4-3), it is clear that, when the degree of nonlocality is very low (for example, 0.1) the medium behaves like a local medium, and the Sech beam propagates as a perfect soliton. However, by increasing the degree of nonlocality (for $\alpha = 1, 3, 5, 10$), the medium is highly nonlocal, and the balance between diffraction and self-focusing effect is violated. By increasing the nonlocal degree, the self-focusing effect becomes weaker, and the diffraction is more important. In this case, the beam suffers diffraction rather than self-focusing, and this is the reason why the beam decreases its on-axis intensity and low self-focusing occurs by propagation. Since the nonlocal response functions are different each other, they have different effect. Any of the three different nonlocal responses (4.6), has their own different radius effect over the medium. From Figure 4-1, Figure 4-2, and Figure 4-3 we observe that, when the same degree of nonlocality is considered, the exponential nonlocal response function has the weakest effect while the Gaussian and the Hyperbolic Secant has almost the same effect.

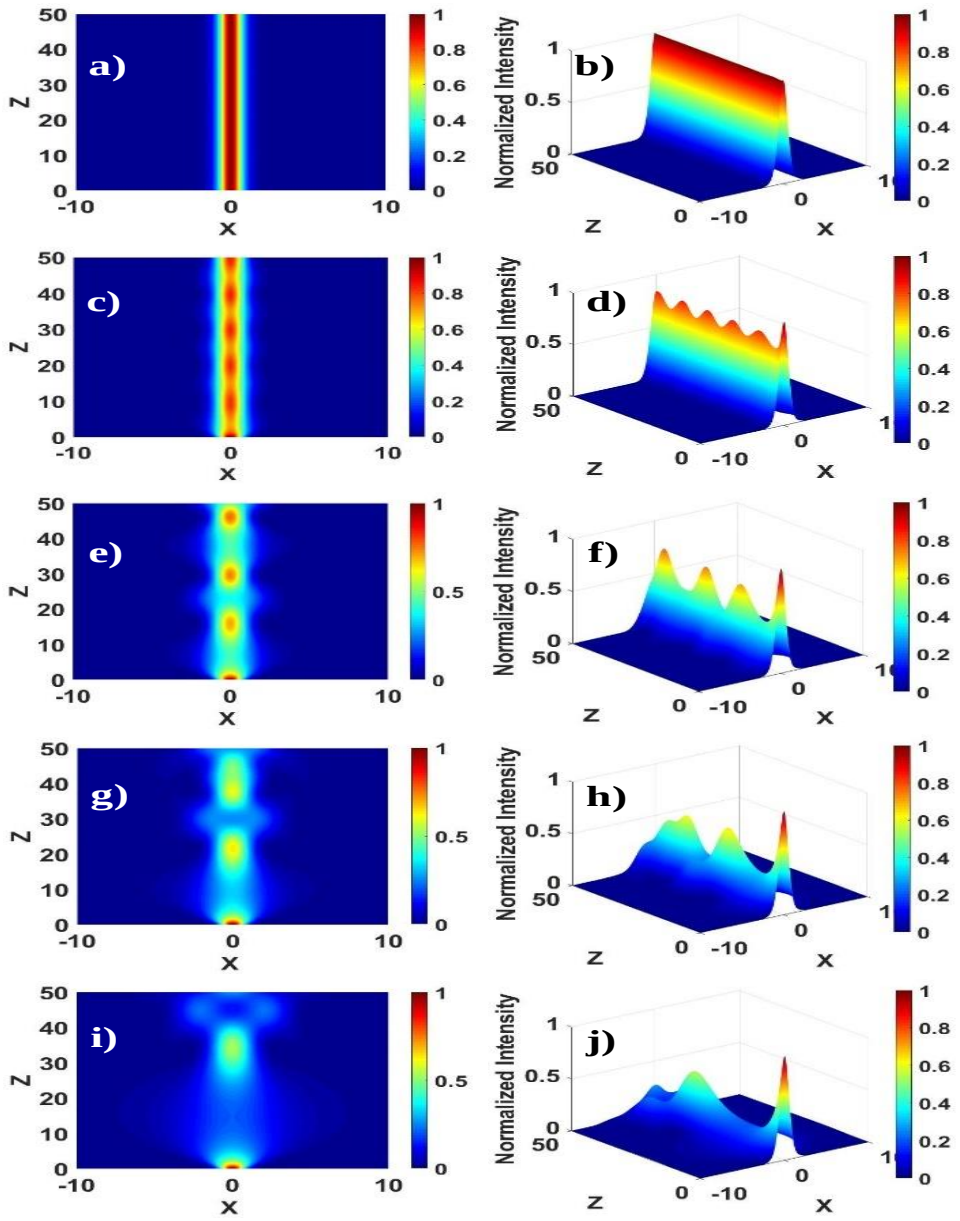

Figure 4-1: Propagation of $Sech\left(\frac{X}{0.7071}\right)$ as initial condition in an Exponential nonlocal medium by different degree, α_e, of nonlocality, (a & b) $\alpha_e = 0.1$, (c & d) $\alpha_e = 1$, (e & f) $\alpha_e = 3$, (g & h) $\alpha_e = 5$, (i & j) $\alpha_e = 10$. (Left column) Top view of the beam propagation from down side, (right colum) Three dimensions view of propagation.

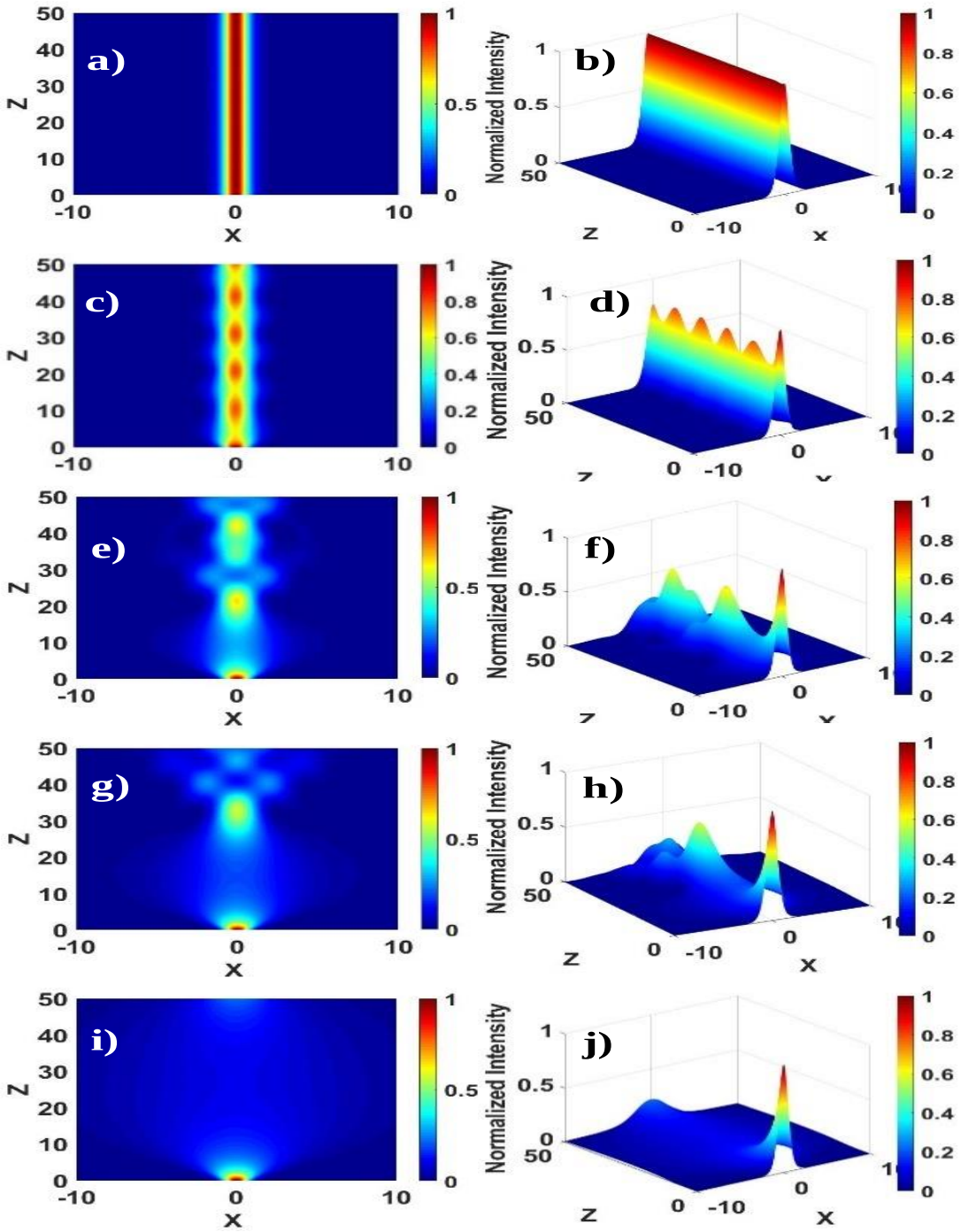

Figure 4-2: Propagation of $Sech\left(\frac{X}{0.7071}\right)$ as initial condition in Gaussian nonlocal medium by different degree, α_g, of nonlocality, (a & b) $\alpha_g = 0.1$, (c & d) $\alpha_g = 1$, (e & f) $\alpha_g = 3$, (g & h) $\alpha_g = 5$, (i & j) $\alpha_g = 10$. (left column) Top view of the beam propagation from down side, (right colum) Three dimensions view of propagation.

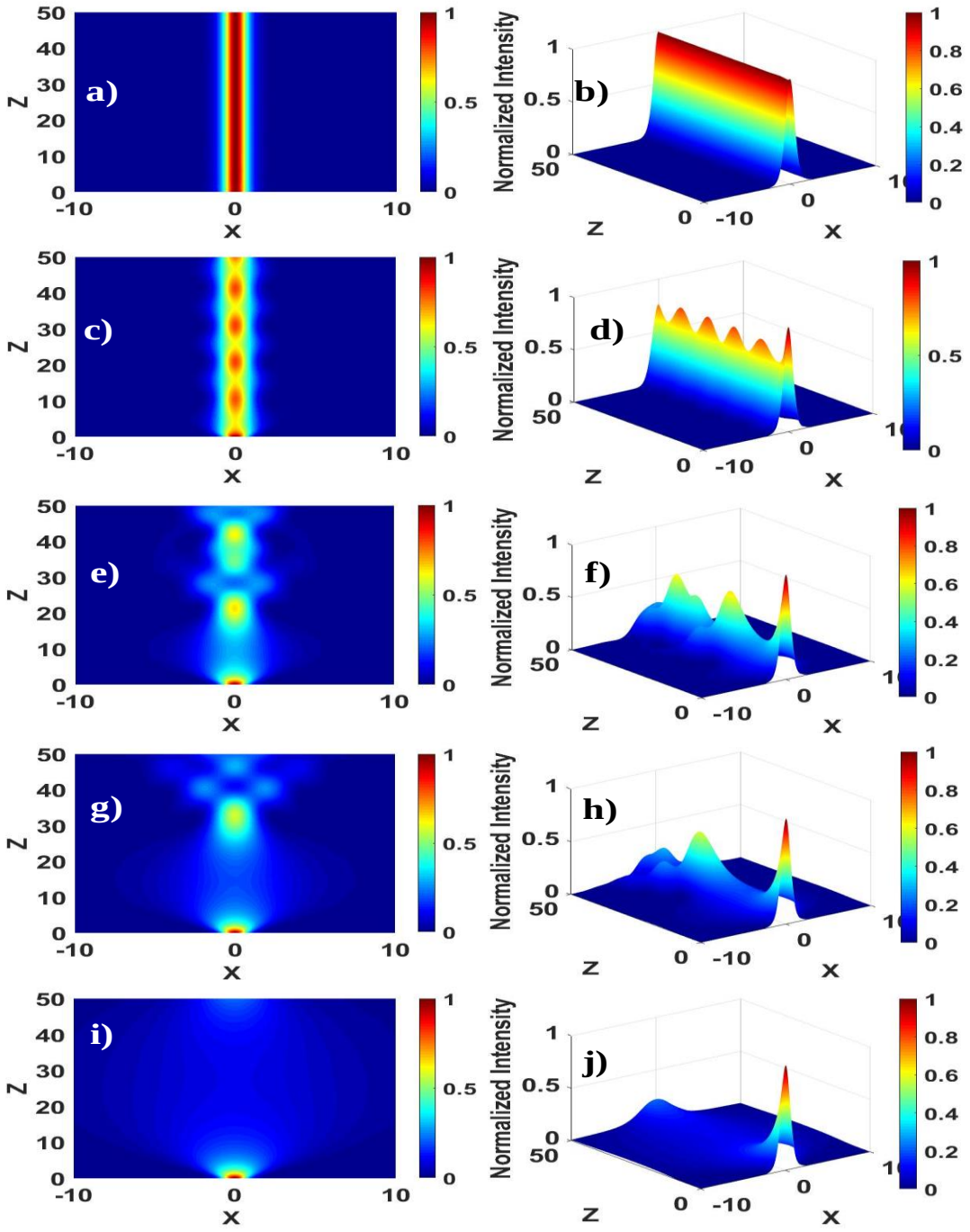

Figure 4-3: Propagation of $Sech\left(\frac{X}{0.7071}\right)$ as initial condition in Sech nonlocal medium by different degree, α_s, of nonlocality, (a & b) $\alpha_s = 0.1$, (c & d) $\alpha_s = 1$, (e & f) $\alpha_s = 3$, (g & h) $\alpha_s = 5$, (i & j) $\alpha_s = 10$. (left column) Top view of the beam propagation from down side, (right colum) Three dimensions view of propagation.

As it was mentioned and displayed in previous three figures, by using the basic Sech profile equation (4.7) since the self-focusing doesn't have enough effect to compensate the diffraction effect, by increasing the degree of nonlocality, Sech initial beam profile no more propagates such as a bright spatial soliton, and its intensity profile cannot be confined properly in direction of propagation.

Here, it is worth to mention that there are not too much differences if we consider different nonlocal response functions. The only difference is, for a nonlocal medium defined by any of an exponential, a Sech, or a Gaussian nonlocal response, with same value of degree of nonlocality ($\alpha_e = \alpha_s = \alpha_g$), by increasing the degree of nonlocality, for an exponential case the effect of nonlocality grows smaller in comparison with the two other nonlocal functions, Sech and Gaussian (see previous three figures and Figure 4-8).

In order to increase the effect of self-focusing in the nonlocal medium, we considered higher value for initial beam-width. Note that, till this part of the thesis the normalized basic initial beam-width ($b_s = 0.7071$) for Sech beam profile has been considered as mentioned in equation (4.7). As it was demonstrated in three previous figures, for propagation in nonlocal medium, if we consider the basic initial beam-width value of Sech (suitable initial condition in local medium case $b_s = 0.7071$ to produce bright soliton), the intensity profile suffers diffraction. The effect of diffraction in nonlocal medium depends on the value of α , from very low till high value, that the beam profile can be diffracted smoothly or strongly, since the initial power is not enough to abandon the diffraction and reinforce the self-focusing effect. By increasing the initial beam-width, initial power increases, so that the self-focusing effect can gain force until overcome the diffraction. By more increase over the initial beam-width, the self-focusing effect can be overwhelming and big value of oscillation is observed by propagation. So that, precise value for initial beam-width must be adjusted, until lowest on-axis intensity oscillation and consequently lowest beam-width change during propagation is detected. In other words, the best initial beam-width is required, to almost confine the beam intensity in direction of propagation, since some intensity oscillation is inevitable, and the beam intensity cannot be confined 100 percent. In the next section the best initial condition to find the best solitary behavior for beam propagation with small intensity oscillation, called quasi-soliton, is explained. Then after, the quasi soliton is discussed for two different media; quasi-soliton in local, and nonlocal medium with arbitrary beam profiles rather than Sech.

4.2 Quasi-Soliton in Nonlocal medium

It was already mentioned that in the Nonlinear Schrodinger Equation for nonlocal medium (4.2), the change of refractive index $\Delta n(I)$ (4.3) is measured by the convolution between intensity profile and the nonlocal response function. In order to demonstrate that the numerical solution of NLS equation (4.2) produces quasi-solitons when any initial field is considered, the maximum I_{max} and minimum I_{min} on-axis intensity was monitored for 100 propagation lengths. The width of the initial field was carefully increased until the smallest variations $\Delta I = I_{max} - I_{min}$ were obtained. As representative examples of the different initial conditions, we present the numerical simulation considering the following three functions as initial conditions:

$$A_g = 1 * \exp\left(-\left(\frac{X}{b_g}\right)^2\right)$$
$$A_s = 1 * Sech\left(\frac{X}{b_s}\right) \qquad (4.8)$$
$$A_e = 1 * Exp\left(-\frac{|X|}{b_e}\right)$$

where A_g represents a Gaussian having width b_g, A_s a Sech function of width b_s and A_e an exponential of width b_e. First, we present the results obtained with the Sech nonlocal response function $R_s(X)$ given by (4.6) and using the hyperbolic secant (4.8), as initial field profile. We observe that for degrees of nonlocality α_s smaller than one and b_s=0.7071 the initial profile is slightly affected during the propagation and its solitonic behavior is kept. Degrees of nonlocality equal or larger than 1, requires the increasing in the width of the initial profile in order to get the quasi-soliton behavior, therefore we can say that the initial power must be increased as we increase the degree of nonlocality. In Figure 4-4, the propagation, initial and final intensity profiles for this field distribution and response function are plotted for different degrees of nonlocality. When $\alpha_s = 1$ the quasi-soliton behavior was obtained for $b_s = 0.87$. The on-axis intensity present variations smaller than 1.5%. For $\alpha_s = 5$, the adequate width for quasi-soliton behavior was of $b_s = 1.6$. In this case the on-axis variations are smaller than 16%. Finally, for $\alpha_s = 10$ the adequate quasi-soliton width was $b_s = 2.19$, with variations in the on-axis intensity of 18%. Then as the degree of nonlocality increases, the variation in the on-axis intensity increases and the beam propagates as an oscillating soliton. This type of behavior is also called breather.

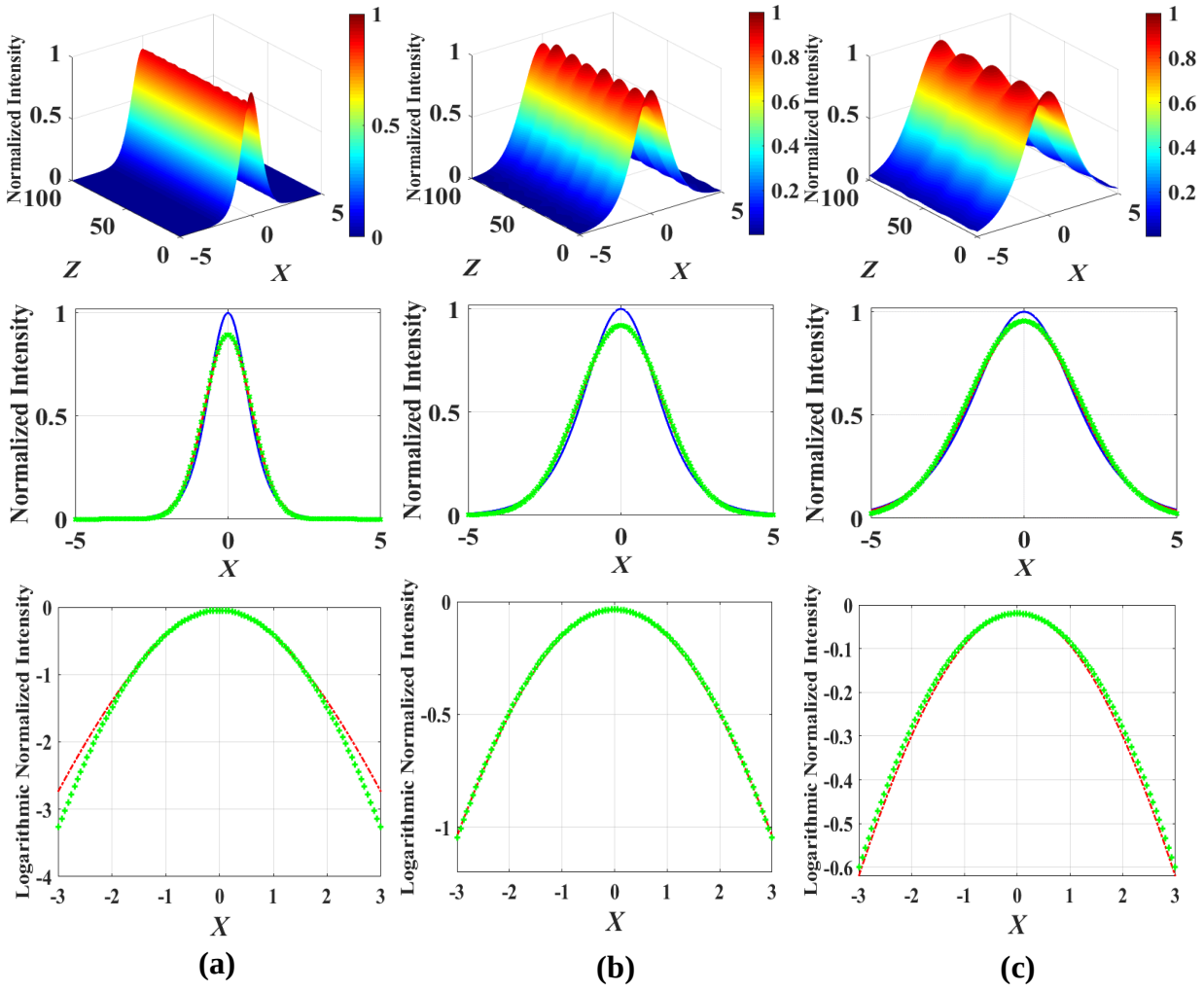

Figure 4-4: Numerical propagation (top) and intensity profiles in linear (middle) and logarithmic (bottom) scale for a hyperbolic secant initial field in a media with Sech nonlocal response and nonlocal degrees α_s of: (a) 1, (b) 5 and (c) 10. Input profile (blue), Final profile (red) and Gaussian-Test (green marks)

In Figure 4-5 we plot the initial power as a function of the degree of non-locality. We observe that, in order to obtain best quasi-soliton behavior, it is necessary to increase the power if the degree of non-locality is increased. Similar behavior of the critical power was obtained considering the hyperbolic secant initial condition with different response functions, Exponential and Gaussian (4.6), with different degrees of nonlocality. When the exponential response function, is considered, low initial powers are needed. Intermediate values of initial power are needed when a Gaussian response function is considered.

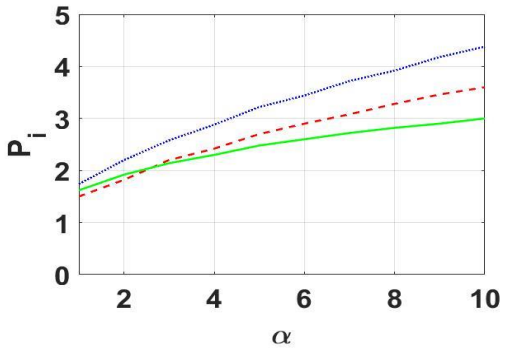

Figure 4-5: Initial power to obtain quasi-soliton propagation when a Sech initial field distribution is used in media with different degrees of nonlocality and nonlocal response function of: Sech (blue, dotted line), Gaussian (red, dashed line) and Exponential (Green, solid line).

The behavior of the initial power when other initial field distributions were used is plotted in Figure 4-6 and Figure 4-7. We can observe that, as in the previous case, the same tendency with the degree of nonlocality and the response function is obtained. The most important difference is that the exponential response function requires the smallest initial powers to generate the quasi-soliton behavior while the Gaussian response function requires the highest. This fact can be due to the spatial extension of the different response functions for the same value of α, (see Figure 4-8). In Figure 4-8 the three nonlocal response functions are plotted for $\alpha_s = \alpha_e = \alpha_g = 5$, where we can observe that the Gaussian nonlocal response gives the lowest spatial extension, while Sech and Exp have the largest spatial extension.

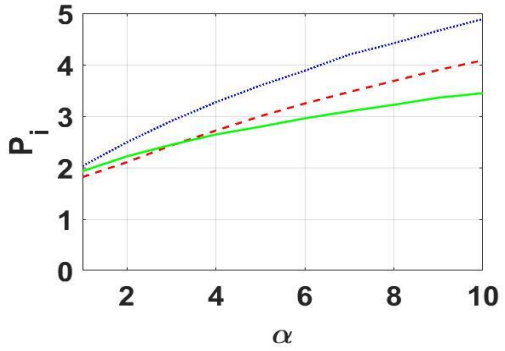

Figure 4-6: Initial power to obtain quasi-soliton propagation when a Gaussian initial field distribution is used in media with different degree of nonlocality and different nonlocal response function of: Sech (blue, dotted line), Gaussian (red, dashed line) and Exponential (green, solid line).

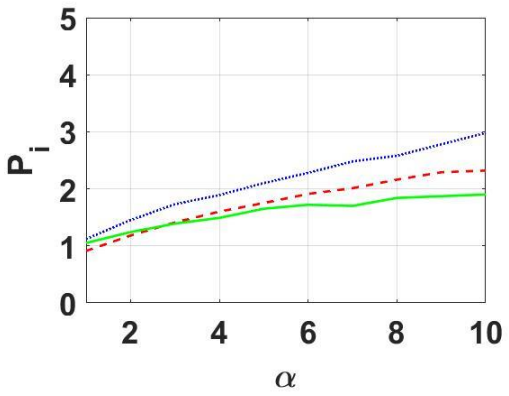

Figure 4-7: Initial power to obtain quasi-soliton propagation when an exponential initial field distribution is used in media with different degrees of nonlocality and nonlocal response function of: Sech (blue dotted line), Gaussian (red, dashed line) and Exponential (green, solid line).

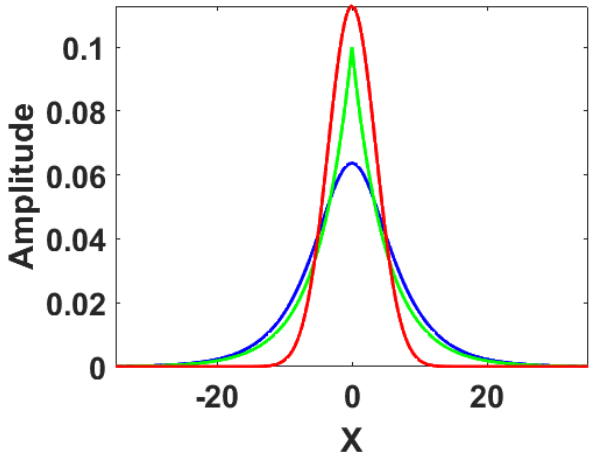

Figure 4-8: Amplitude of the following nonlocal response function: Sech (blue), Exponential (green) and Gaussian (red) for $\alpha = 5$

Another interesting point is that, for all initial field distributions propagating in nonlocal media, described by any nonlocal response function and degree of nonlocality, after some propagation distance the beam intensity profile is reshaped to a Gaussian. This Gaussian-Test can be obtained from the on-axis amplitude, $A_0(Z)$, and the initial power, P_i, using the following expression:

$$I_G(X) = \left[|A_0(Z)|\, exp\left(-\left(\sqrt{\frac{\pi}{2}} \frac{|A_0(Z)|^2}{P_i} \mathrm{X} \right)^2 \right) \right]^2 \tag{4.9}$$

The Gaussian-Test has the form of $A_0(Z)\, exp\left(-\left(\frac{X}{b_x}\right)^2\right)$ and b_x is the width of Gaussian-Test which is found from:

$$P_i = \int_{-\infty}^{+\infty} \left[A_0(Z)\, exp\left(-\left(\frac{X}{b_x}\right)^2 \right) \right]^2 dX = \int_{-\infty}^{+\infty} A_0^2(Z) exp\left(-2\left(\frac{X}{b_x}\right)^2 \right) dX = A_0^2(Z) b_x \sqrt{\frac{\pi}{2}}$$

$$\Rightarrow b_x = \frac{P_i \sqrt{2}}{A_0^2(Z)\sqrt{\pi}}$$

To demonstrate this fact, in Figure 4-4 (middle and bottom row), the final propagated intensity profiles for different degrees of nonlocality, when a sech initial field profile and sech response function are considered, are plotted in a linear and logarithmic intensity scale and compared with Gaussian-Test obtained from equation (4.9) (green marks). Notice the good match obtained between them in the central part of the profile. In order to demonstrate that the same profile is acquired after propagation in nonlocal media, in Figure 4-9, the propagation and intensity profiles are plotted when a Gaussian and an Exponential initial field distributions are propagated in a medium with a Sech response function with $\alpha_s = 5$. Note that in the case of the Gaussian initial condition the beam propagation presents very small variations, almost as a perfect soliton. The conclusion of this part of the study is that any initial field distribution propagated in a nonlocal nonlinear media, with arbitrary degree of nonlocality and response function, after some propagation distance the intensity profile tends to be modified to a Gaussian. With the adequate initial width in some cases the propagated profile generates a quasi-soliton.

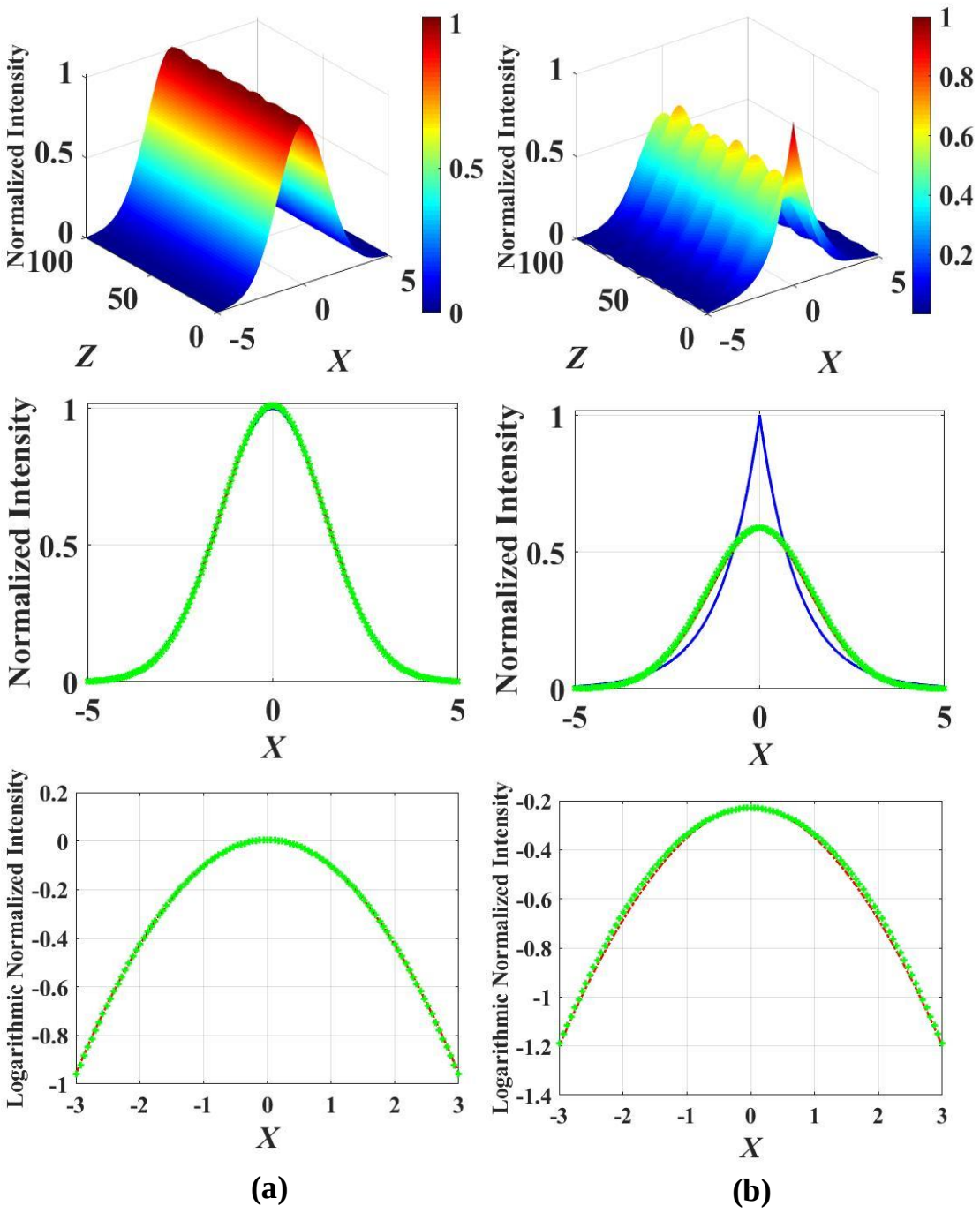

Figure 4-9: Numerical propagation (top) and intensity profiles in linear (middle) and Logarithm (bottom) intensity scale for Gaussian (a) and Exponential (b) initial field distribution propagated in a media with Sech nonlocal response function for $\alpha = 5$. Initial profile (blue, solid line), final profile (red, dash line) and Gaussian test (green marks).

4.3 Quasi-Soliton in local medium

As already mentioned, the paraxial evolution of a (1+1)-Dimensional beam, with field amplitude $\mathrm{E} = \mathrm{E}(\mathrm{x},\mathrm{z})\exp(\mathrm{ikz})$ propagating along the z-direction in a local Kerr medium ($\Delta n(I) = n_2 I$) is described by the Nonlinear Schrodinger Equation NLSE given by:

$$-i\frac{\partial q(X,Z)}{\partial Z} = \frac{1}{4}\frac{\partial^2 q(X,Z)}{\partial X^2} + \frac{Z_R}{L_{NL}}|q(X,Z)|^2 q(X,Z) \qquad (4.10)$$

where $\mathrm{q}(X,Z)$ is the field amplitude normalized to the maximum intensity $I_{\mathrm{m}}^{1/2}$, $Z_R = (n_0 \mathrm{k}_0 \mathrm{x}_0^2)/2$ is the Rayleigh distance or diffraction length, n_0 the linear refractive index, $k_0 = 2\pi/\lambda$ the wave vector, λ the wavelength, x_0 is the initial beam width, $\mathrm{L_{NL}} = (n_2 \mathrm{k}_0 \mathrm{I_m})^{-1}$ the self-focusing distance, positive n_2 the nonlinear refractive index, $X = x/\mathrm{x}_0$ and $Z = z/\mathrm{L_D}$ are the normalized lengths along transversal axis and direction of propagation. When $\mathrm{L_D}/\mathrm{L_{NL}} = 1$ and n_2 is positive, equation (4.10) allows one analytical solution known as a fundamental soliton described by Hyperbolic Secant (Sech) profile called bright spatial soliton. Equation (4.10) was solved numerically using the split-step method. The numerical bright spatial soliton is obtained when the following initial field distribution is used:

$$q(X,Z) = 1 * Sech\left(\sqrt{2}\,X\right) = 1 * Sech\left(\frac{X}{0.7071}\right) = 1 * Sech\left(\frac{X}{b_s}\right) \qquad (4.11)$$

In order to demonstrate that the numerical solution of (4.10) produces quasi-solitons when any initial field is used, the on-axis intensity was monitored for 100 propagation lengths. The width of the initial field was carefully increased in small amount until the smallest variations were obtained. As representative examples of the different initial conditions tested, we present the numerical propagation considering the following five functions as initial conditions:

$$A_{sg} = \exp\left(-\left(\frac{X}{b_{sg}}\right)^{10}\right)$$

$$A_g = \exp\left(-\left(\frac{X}{b_g}\right)^{2}\right)$$

$$A_{tang} = Triangularpulse\left(-\left(\frac{X}{b_{tang}}\right)\right) \tag{4.12}$$

$$A_R(X) = Rectpulse\left(\frac{X}{b_R}\right)$$

$$A_e = \exp\left(-\left(\frac{|X|}{b_e}\right)\right)$$

where A_{sg} represents a Super-Gaussian having width b_{sg}, A_g a Gaussian of width b_g, A_{tang} a Triangular of width b_{tang}, A_R a Rectangular of width b_R, and A_e an exponential of width b_e. It is important to mention that; to obtain quasi-soliton behavior it is necessary to consider an adequate width that depends on the initial function. In Figure 4-11, Figure 4-12, and Figure 4-13, we plot the evolution of each distribution along a 100 Z, together with its initial and final intensity profile. The adequate width for quasi-soliton propagation for the Super-Gaussian, Gaussian, Exponential, Rectangular, and Triangular are $b_{sg} = 1.16, b_g = 1.2, b_e = 1.1, b_R = 2.30,$ and $b_{tang} = 2.22$ respectively. For Sech, a width of $b_s = 0.7071$ produces a perfect soliton. Smaller width values produce a diffracted beam, while higher values produce a beam, with a remarkable intensity oscillatory behavior. Compared with the total power of the fundamental soliton, the supper Gaussian is 1.45 times, the Gaussian is 1.06 times, the exponential is 0.78 times, the rectangular and Triangular is 1.58 and 1.04 times respectively. Then the power of the fundamental soliton cannot be used to obtain the adequate width of the initial field distribution that generates quasi-solitons. The criteria used to determine when the propagation produces a quasi-soliton can be understood with the help of the on-axis intensity behavior, (see Figure 4-10). At the beginning the beam is reshaped and the on-axis intensity can increase (Super Gaussian, Rectangular, Triangular and Gaussian) or decrease (exponential), but after almost 10Z the beam tends to reach a profile, and on-axis intensity propagates with minimum changes. During the propagation maximum, I_{max}, and minimum, I_{min}, on-axis intensity was measured. Small changes over initial beam-width were done until lowest relative intensity, ΔI, was obtained ($\Delta I = I_{max} - I_{min}$). In the case of the Super-

Gaussian distribution, the on-axis intensity reaches an average value of 1.78 with variations less than 1%. In the case of the Gaussian and triangular distribution, the on-axis average intensity is 1.12 and 1.06 with variations lower than 6% and 1.3% respectively. Finally, for the Exponential and Rectangular profile, the on-axis average intensity is of 0.6 and 1.86 with variations lower than 3% and 2% correspondingly. The best initial beam-width for different initial beam profiles (4.12), their relative oscillated intensity ΔI, and average intensity during propagation are written in Table 4-1. In our simulation initial symmetric intensity profile, symmetrically located on x=0, is propagated in the perpendicular direction in positive Z. On-axis intensity is the calculated intensity value on x=0 for all the positive z values.

b	I_{max}	I_{min}	ΔI	Average I
b_{sg}=1.1675	1.7920	1.7733	0.0187	1.7827
b_g=1.2	1.1547	1.0913	0.0633	1.123
b_{tang}=2.22	1.0714	1.0570	0.0145	1.064
b_R=2.30	1.8792	1.8439	0.0352	1.8616
b_e=1.1	0.5993	0.5860	0.0134	0.592

Table 4-1: Beast initial beam-widths for Super-Gaussian, Gaussian, Triangular, Rectangular and exponential beam profile

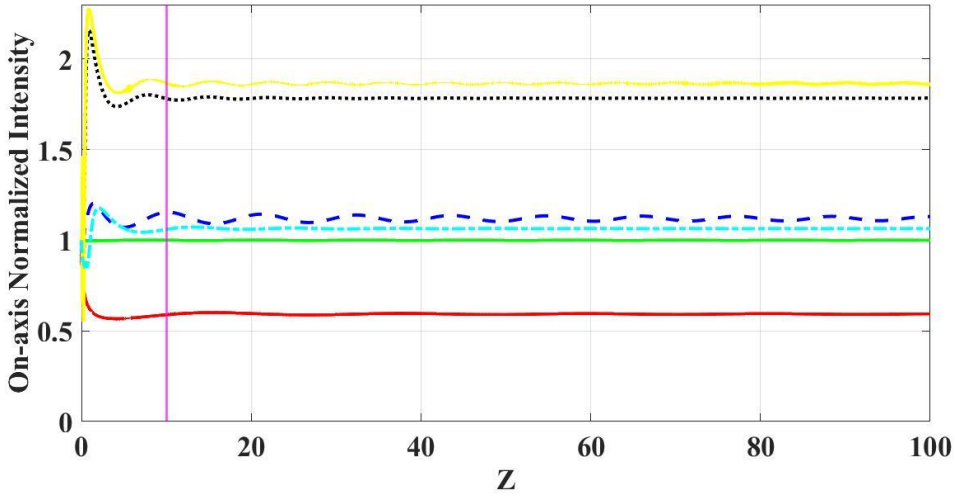

Figure 4-10: On-axis intensity along 100Z for the following initial fields: Rectangular (Yellow, Solid line), Super-Gaussian (Black, Dotted line), Gaussian (Blue, Dashed line), Triangular (Cyan, Dash-dot line), Sech (Green, Solid line), and Exponential (Red, Solid line) with the best initial beam-width mentioned in Table 4-1. As reference, vertical line (pink solid line) at 10Z.

As we mention, at the beginning of the propagation, the beam is reshaped. The interesting point is that, after some propagation distance in a local medium, the beam intensity transforms to Hyperbolic Secant profile. To verify this fact, we compare the profile at different propagation distances Z with an intensity obtained by the expression (4.13) (we call it Sech-Test). where $\mathrm{A_0(Z)}$ is the on-axis amplitude of the propagated beam at the position Z. $\mathrm{P_i} = \int_{-\infty}^{+\infty} |\mathrm{A}(X, Z=0)|^2 \mathrm{d}X$ is the initial power. Note that even that $\mathrm{P_i}$ is used to adjust the propagated intensity profile this does not means that all the initial power is contained in it. In Figure 4-11, Figure 4-12, and Figure 4-13 the final profiles are compared with that obtained through (4.13), plotted as green marks, both in linear (c) and logarithmic (d) scale. We can see that the correspondence between both intensity profiles is very good in the central portion. (4.13) is adequate when the beam propagates with the minimum variations, however the square Sech profile is reached always after a few propagated distances even if the width is smaller than the adequate to generate quasi-soliton. For obtaining Sech-Test, it is considered that the Sech-Test in the form of $A_s(X) = A_0(Z)Sech\left(\frac{X}{b_x}\right)$, where the width b_x is calculated from:

$$P_i = \int_{-\infty}^{+\infty} \left[A_0(Z)Sech\left(\frac{X}{b_x}\right)\right]^2 dX = \int_{-\infty}^{+\infty} A_0^2(Z)b_x Sech^2(u)\, du = A_0^2(Z)b_x Tanh\left(\frac{X}{b_x}\right)|_{-\infty}^{+\infty}$$

$$= 2A_0^2(Z)b_x \Rightarrow b_x = \frac{P_i}{2A_0^2(Z)}$$

$$I_s(X,z) = \left[|A_0(Z)| * Sech\left(\frac{2|A_0(Z)|^2}{P_i}\, X\right)\right]^2 \qquad (4.13)$$

As conclusion of this part of the study is that symmetric initial field profiles are reshaped into a hyperbolic secant when they are propagated in a local nonlinear media, with the adequate initial width, and these profiles can propagate as quasi-solitons.

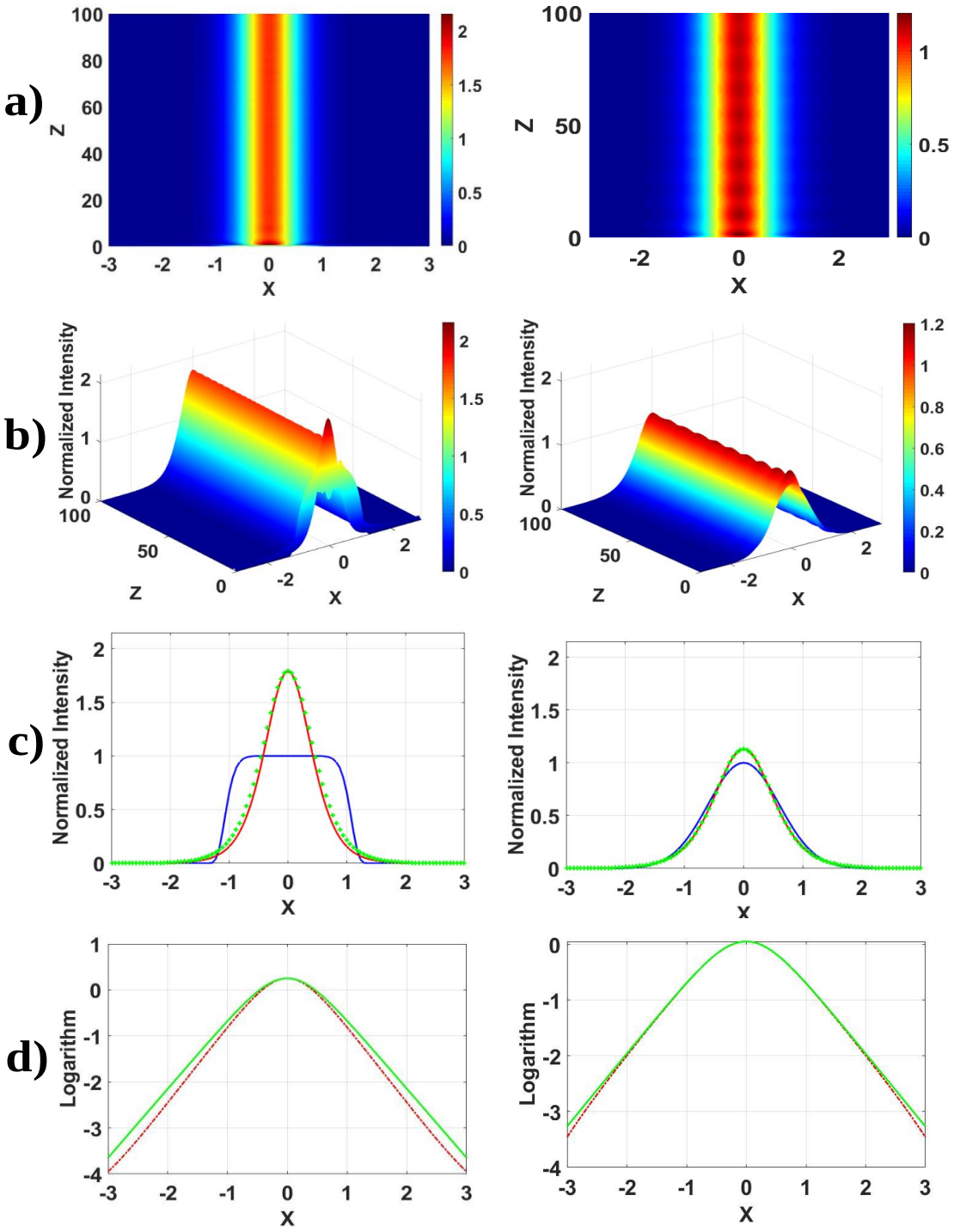

Figure 4-11: Super-Gaussian (left column), Gaussian (right column), beam propagation for two-dimensional (a), and three-dimensional (b) view. Intensity profile comparison (c) between initial (blue line), propagated (red line), and Sech-Test (green point), comparison for logarithms (d) of propagated intensity (red points) and Sech-Test (green line).

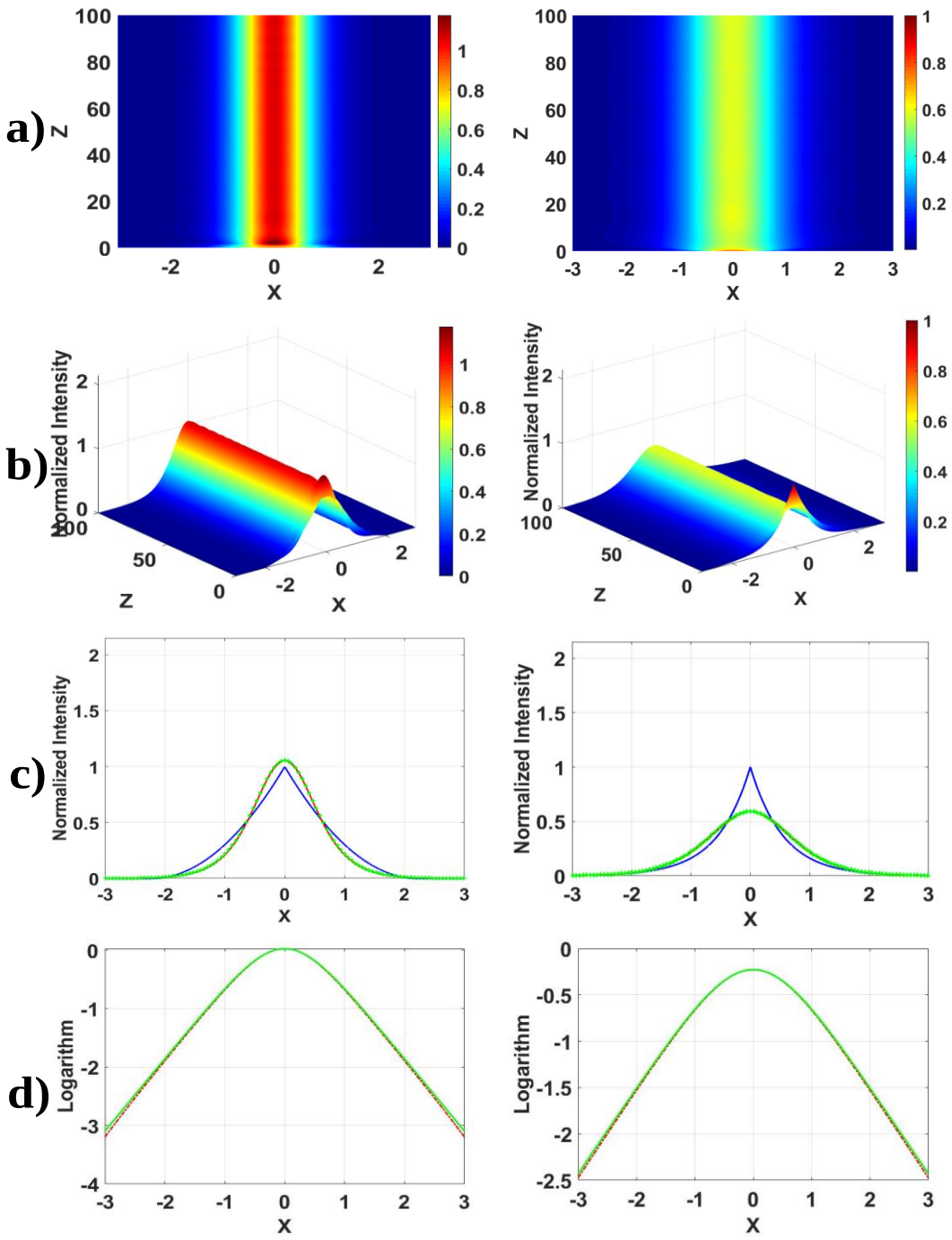

Figure 4-12: Triangular (left column), Exponential (right column), beam propagation for two-dimensional (a), and three-dimensional (b) view. Intensity profile comparison (c) between initial (blue line), propagated (red line), and Sech-Test (green point), comparison for logarithms (d) of propagated intensity (red points) and Sech-Test (green line).

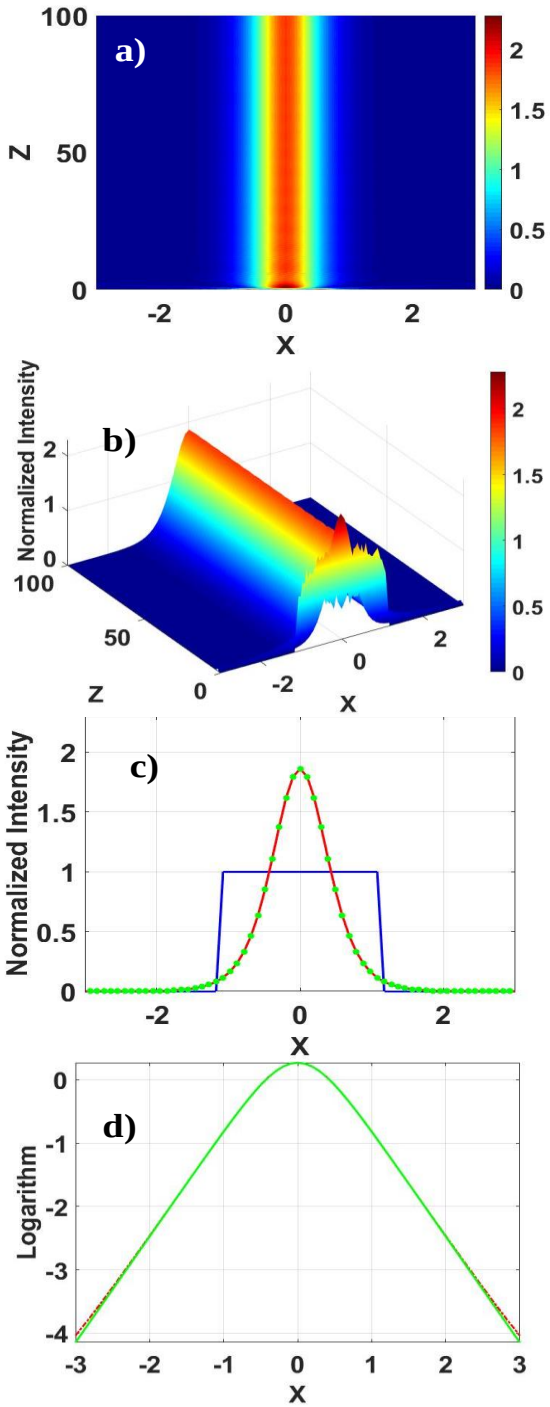

Figure 4-13: Rectangular beam Propagation for (a) two and (b) three -dimensional view for 100 Z propagation distance. Intensity profiles comparison (c) between initial (blue line), propagated (red line), and Sech-Test (green point), comparison for logarithms (d) of propagated intensity (red points) and Sech-Test (green line).

4.4 Summary

As conclusion of this chapter, we have studied the numerical propagation of arbitrary initial field distributions in positive local and nonlocal nonlinear media described by the (1+1)-Dimensional Nonlinear Schrodinger Equation. In the local part, we demonstrated that any symmetric and arbitrary initial beam profiles far from hyperbolic secant distribution, but with an adequate beam-width, can propagate as a soliton or more precisely a quasi-soliton, since small oscillations can be detected. As evidence, two extreme initial profiles were presented: Super-Gaussian and Rectangular (as a very wide beam) and Exponential (with sharp central amplitude). After propagation, all the initial arbitrary profiles evolve to a hyperbolic secant intensity profile. A formula to obtain the propagated profile was given. Furthermore, the numerical propagation of arbitrary initial field profiles was analyzed in nonlocal media, with particular response functions and any degree of nonlocality. The behavior observed was similar to the local case: the arbitrary initial beam profiles, with the adequate width, can propagate as a quasi-soliton after some propagation distance. In the nonlocal case, independently of the response functions of the media and the initial field considered, the intensity profile tends to acquire a Gaussian distribution. A formula for the propagated intensity profile was given. The behavior reported can be extended to asymmetric initial distributions that give rise to one beam. For negative nonlinear materials, it is necessary to do the analysis.

Chapter 5: **Conclusions**

5.1 Summary of research

The main goal of this thesis focuses over the way a beam profile propagates and occupies the transversal space, in different medium, third order nonlinear (Kerr) medium (local medium), and even third order nonlinear nonlocal medium. For any of these three media, we have obtained an equation that governs the propagation of a beam in the medium. In a linear medium the Helmholtz equation has been obtained, which governs the medium, for propagation of a beam and the occupied space. In this equation, just diffraction takes place by propagation and there are not any other opposite phenomena. The results of simulation show that, for one Rayleigh range propagation, the maximum normalized intensity of (1+1)-D and (2+1)-D Gaussian beam, is reduced to 0.7071 and 0.5 respectively. We observe that due to the diffraction effect, the beam occupies the wider transversal space as it propagates. In third order nonlinear medium (Kerr), the Nonlinear Schrodinger Equation (NLS) has been obtained, and it controls all the aspects of beam propagation. The NLS equation is solved analytically and two solitary solutions, hyperbolic secant (bright spatial soliton), and hyperbolic tangent (dark spatial soliton) have been obtained. The NLS equation contains the self-focusing or self-defocusing phenomena which is in contradict with diffraction effect. The required criteria to make a balance between these two effects has been obtained. It is demonstrated, by applying the criteria, that the initial beam profile (solutions of NLS equation) does not take the wider transversal space (due to diffraction) nor become narrower, as propagates. Then, the interaction of initially parallel trajectory of two bright spatial soliton beams, were investigated, which showed strong relation to their relative phase. We demonstrated that, when the relative phase between two bright solitons is zero $\Delta\phi = 0$, the resulting path of the centroid of each individual soliton is periodic, with the solitons returning to their input condition at the end of each cycle. However, when the relative phase is $\Delta\phi = \pi$, the intensity of two beams interact destructively, and the intensity between two beam paths, is decreased. Since the refractive index in a third order nonlinear medium has dependency on intensity, by decreasing the induced refractive index in the path between two solitons, two beams appear to repel each other. For other relative phases, the interaction is more complicated. In other viewpoint, the force between the solitons varies smoothly from maximum attractive at $\Delta\phi = 0$, to maximum repulsive at $\Delta\phi = \pi$.

The results from collision show, when two bright solitons propagate with a big angle, after the colliding point, they never return to each other, and continue their own modified paths. The result of interaction between two initially parallel trajectory dark solitons demonstrates no dependency to initial relative phase, and always two dark solitons repel each other. For the case of the nonlocal medium, a modified NLS equation is used to define the medium, and since the intensity response of medium is not just related to the illuminated points, but some effects from vicinity also contribute to that illuminated points, some modifications over NLS equation are required. We have used the mathematical convolution over local intensity and nonlocal response of the medium. In this thesis, different kinds of nonlocal response functions have been used such as Gaussian, Exponential and hyperbolic Secant. We demonstrate that there is not much difference behavior by using one of them instead of another. For all the nonlocal response functions different degrees of nonlocality were used, from weak till highly nonlocality. We observe that by increasing the degree of nonlocality, propagated beam tends to more diffraction. Since propagating the conventional Hyperbolic Secant (Sech) in the nonlocal medium is not behaving like a spatial soliton, we modified the initial beam-width of Sech to reinforce the self-focusing part to compete with the diffraction effect and confine the beam in direction of propagation. By adjusting the initial beam-width, the result shows that, the intensity profile is confined by propagation, although some intensity oscillation over on-axis was inevitable. This is the reason to call spatial quasi-soliton. Afterwards we didn't limit our self just to Sech initial beam profile, and we have tested some other profiles such as Gaussian and exponential profile as initial beam. The propagation was simulated and in the same manner to defeat the diffraction effect by changing their initial beam-width until we confined the beam intensity in direction of propagation and observe the quasi-soliton. By testing many kinds of initial beam profiles in nonlocal medium, where the medium is defined by different nonlocal response functions with any degree of nonlocality, we conclude that, it is possible to confine any initial symmetric kinds of beam profiles, with adequate initial beam-width in nonlocal medium and produce the quasi-solitons. Then, a variety of initial beam profiles far from Sech (Sech is the exact answer of NLS equation) were tested to propagate in third order (Kerr) nonlinear local medium, and interestingly, confinement of intensity profile in direction of propagation happened just by purely changing the initial beam-width and produce the quasi-soliton. So that as main conclusion, we can assure that, it is possible to confine a beam profile in the direction of propagation, with any initial beam profile in a local medium or nonlocal medium

defined by any symmetric nonlocal response function with any degree of nonlocality, just the adequate initial beam-width is required. Another interesting conclusion is that, by propagating any initial beam profile in local medium, and fitting adequate initial beam-width in order to obtain the quasi-soliton, after some initial step of propagation, the beam profile reshapes to a hyperbolic Secant profile. However, in a nonlocal medium, by choosing any initial beam profiles in a nonlocal medium defined by any nonlocal response function and any degree of nonlocality, the beam intensity after some initial distance of propagation, reshapes to a Gaussian profile, as mentioned in equation (4.9).

5.2 Publications:

5.2.1 Article in Journals

1- Evolution of rectangular and triangular initial beam profiles in positive Kerr local medium, Majid Hesami, Mahrokh Avazpour, Marcela. Maribel Méndez Otero, J. Jesús Arriaga Rodríguez, Suplemento de la Revista Mexicana de Física, 2019.
2- Generation of Bright spatial quasi-solitons by arbitrary initial beam profiles in local and nonlocal (1+1)-Dimensional nonlinear media, Majid Hesami, Mahrokh Avazpour, Marcela. Maribel Méndez Otero, J. Jesús Arriaga Rodríguez, M. D. Iturbe Castillo, Optik-International Journal for Light and Electron Optics, 2019.
3- Transforming higher order bright and dark solitons to the first order solitons in Kerr medium: A review, Majid Hesami, Mahrokh Avazpour, M.M. Méndez Otero, Optik - International Journal for Light and Electron Optics, 2019.
4- Dark soliton by arbitrary initial beam profiles in negative Kerr local and nonlocal nonlinear medium, Majid Hesami, Mahrokh Avazpour, M.M. Méndez Otero, M. D. Iturbe Castillo, Optik - International Journal for Light and Electron Optics, 2019.

5.2.2 Participating in Congresses, workshops and Seminars

1- (First award for poster presentation II-CILCA, Second International Conference , LUZ. CIENCIA. ARTE, 14-17 May 2019, Puebla, México) Numerical study over propagation of Super-Gaussian and Exponential initial beam profile in Kerr type local medium, **Majid Hesami,** Mahrokh Avazpour, Marcela. Maribel Méndez Otero, J. Jesús Arriaga Rodríguez, Marcelo David Iturbe Castillo.
2- (Oral presentation II-CILCA, Second International Conference , LUZ. CIENCIA. ARTE, 14-17 May 2019, Puebla, México) Generation of Solinotic pulse with NPR mode locked fiber laser, Mahrokh Avazpour, **Majid Hesami,** Georgina Beltran Perez, Evgeny Kuzin.

3- (Academic Talk, University of Guanajuato, Guanajuato, Mexico, 11th February 2019) Numerical and Analytical study, over behavior of spatial optical soliton beams, when they are propagating in the same Kerr medium, **Majid Hesami**,

4- (Poster presentation in 61th physics national conference, LXI Congreso Nacional de Física, SMF, Puebla, México, October 2018). Spatial Behavior of Bright solitons in nonlinear nonlocal medium, (Comportamiento espacial del haz Secante Hiperbólico en un medio No-lineal y No-Local), **Majid Hesami**, Mahrokh Avazpour, Marcela. Maribel Méndez Otero, J. Jesús Arriaga Rodríguez, Marcelo David Iturbe Castillo.

5- (Oral presentation in 61th physics national conference, LXI Congreso Nacional de Física, SMF, Puebla, México, October 2018). Experimental and theoretical study of soliton spectral compression obtained of pulse laser based on fiber optics, Mahrokh Avazpour, **Majid Hesami**, Gerogina Beltrán Pérez, Juan Castillo Mixcoatl, Severino Muñoz Aguirre, Evgeny Kuzin

6- (Student seminar- IFUAP-28-August-2018). Numerical and Analytical study of Propagation, interaction & Collision of spatial solitons in 3rd order Nonlinearity (Kerr) medium, with Split-Step and Fourier Scattering method by MATLAB.

7- Participation in IX school of Bio-photonics, Tonantzintla, Puebla, México (4 to 6 of July 2018).

8- (student Seminar in academic group of quantum and nonlinear optics, 2018, IFUAP, BUAP university), Numerical and Analytical study of beam propagation and interaction for Gaussian, Secant and Tangent Hyperbolic beams in linear medium.

Bibliography

[1] Boyd R W, Lukishova S G and Shen Y R, 2009, Self-Focusing: Past and Present Topics in Applied Physics.

[2] Segev M and Christodoulides D N, 2001, Spatial Solitons ed S Trillo and W Torruellas

[3] Królikowski W and Bang O, 2000, Solitons in nonlocal nonlinear media: Exact solutions *Phys. Rev. E* **63,** 16610.

[4] Shabat A and Zakharov V, 1972, Exact theory of two-dimensional self-focusing and one-dimensional self-modulation of waves in nonlinear media, *Sov. Phys. JETP* **34,** 62.

[5] Mitchell D J and Snyder A W, 1999, Soliton dynamics in a nonlocal medium *JOSA B* **16** 236–9.

[6] Duque E I and Lopez-Aguayo S, 2019, Generation of solitons in media with arbitrary degree of nonlocality using an optimization procedure, *Phys. Rev. A*, **99,** 13831.

[7] Kaminer I, Rotschild C, Manela O and Segev M, 2007, Periodic solitons in nonlocal nonlinear media *Opt. Lett.* **32,** 3209.

[8] Conti C, Peccianti M and Assanto G 2004 Observation of Optical Spatial Solitons in a Highly Nonlocal Medium *Phys. Rev. Lett.* **92,** 113902–1.

[9] Ultanir E A 2004 EA Ultanir, GI Stegeman, CH Lange, and F. Lederer, Opt. Lett. 29, 283 (2004). *Opt. Lett.* **29,** 283.

[10] Dalfovo F, Giorgini S, Pitaevskii L P and Stringari S 1999 Theory of Bose-Einstein condensation in trapped gases *Rev. Mod. Phys.* **71,** 463.

[11] Pecseli H L and Rasmussen J J, 1980, Nonlinear electron waves in strongly magnetized plasmas, *Plasma Phys.* **22,** 421.

[12] Assanto G, Peccianti M and Conti C, 2003, Nematicons: optical spatial solitons in nematic liquid crystals *Opt. Photonics News* **14,** 44–8.

[13] Sackett C A, Gerton J M, Welling M and Hulet R G, 1999, Measurements of collective collapse in a Bose-Einstein condensate with attractive interactions *Phys. Rev. Lett.* **82,** 876.

[14] Rotschild C, Cohen O, Manela O, Segev M and Carmon T, 2005, Solitons in nonlinear media with an infinite range of nonlocality: first observation of coherent elliptic solitons and of vortex-ring solitons *Phys. Rev. Lett.* **95,** 213904.

[15] Shi X, Guo Q and Hu W, 2008, Propagation properties of spatial optical solitons in different nonlocal nonlinear media with arbitrary degrees of nonlocality *Optik (Stuttg).* **119,** 503–10.

[16] Duque E I and Lopez-Aguayo S, 2019, Generation of solitons in media with arbitrary degree of nonlocality using an optimization procedure *Phys. Rev. A,* **99,** 13831.

[17] Ablowitz M J and Musslimani Z H, 2005, Spectral renormalization method for computing self-localized solutions to nonlinear systems *Opt. Lett.* **30,** 2140–2.

[18] Bahaa E. A. Saleh M C T, 1991, *Fundamentals of photonics.*

[19] Boyd R W, 2003, *Nonlinear optics* (Elsevier).

[20] Chiao R Y, Garmire E and Townes C H, 1964, Self-trapping of optical beams *Phys. Rev. Lett.* **13,** 479.

[21] Maiman T H and others, 1960, Stimulated optical radiation in ruby.

[22] Peters P A F A E H C W and Weinreich G, 1961, Generation of optical harmonics *Phys. Rev. Lett* **7,** 118–9.

[23] Boyd R W, 1992, Nonlinear Optics (Boston, MA: Academic).

[24] Kelley P L, 1965, Self-focusing of optical beams *Phys. Rev. Lett.* **15,** 1005.

[25] Yariv A, 1997, Optical Electronics in Modern Communications, Oxford Series in Electrical and Computer Engineering.

[26] Krolikowski W, Bang O, Nikolov N I, Neshev D, Wyller J, Rasmussen J J and Edmundson D, 2004, Modulational instability, solitons and beam propagation in spatially nonlocal nonlinear media *J. Opt. B quantum semiclassical Opt.* **6,** S288.

[27] Conti C, Ruocco G and Trillo S, 2005, Optical spatial solitons in soft matter *Phys. Rev. Lett.* **95,** 183902.

[28] Parola A, Salasnich L and Reatto L, 1998, Structure and stability of bosonic clouds: Alkali-metal atoms with negative scattering length *Phys. Rev. A* **57,** R3180.

[29] Pedri P and Santos L, 2005, Two-dimensional bright solitons in dipolar Bose-Einstein condensates *Phys. Rev. Lett.* **95,** 200404.

[30] Ván P and Fülöp T, 2005, Weakly non-local fluid mechanics: the Schrödinger equation *Proc. R. Soc. A Math. Phys. Eng. Sci.* **462,** 541–57.

[31] Conti C, Peccianti M and Assanto G, 2003, Route to Nonlocality and Observation of Accessible Solitons *Phys. Rev. Lett.* **91,** 073901.

[32] Litvak A G, 1966, Self-focusing of powerful light beams by thermal effects *Sov. J. Exp.*

Theor. Phys. Lett. **4,** 230.

[33] Rotschild C, Cohen O, Manela O, Segev M and Carmon T, 2005, Solitons in Nonlinear Media with an Infinite Range of Nonlocality: First Observation of Coherent Elliptic Solitons and of Vortex-Ring Solitons *Phys. Rev. Lett.* **95,** 1–4.

[34] Tam A C and Happer W, 1977, Long-range interactions between cw self-focused laser beams in an atomic vapor *Phys. Rev. Lett.* **38,** 278.

[35] Suter D and Blasberg T, 1993, Stabilization of transverse solitary waves by a nonlocal response of the nonlinear medium *Phys. Rev. A* **48,** 4583.

[36] Ultanir E A, Stegeman G I, Lange C H and Lederer F, 2004, Coherent interactions of dissipative spatial solitons *Opt. Lett.* **29,** 283–5.

[37] Conti C, Peccianti M and Assanto G, 2003, Route to nonlocality and observation of accessible solitons *Phys. Rev. Lett.* **91,** 73901.

[38] Snyder A W and Mitchell D J, 1997, Accessible solitons *Science (80-.).* **276,** 1538–41.

[39] Nikolov N I, Neshev D, Królikowski W, Bang O, Rasmussen J J and Christiansen P L, 2004, Attraction of nonlocal dark optical solitons *Opt. Lett.* **29,** 286–8.

[40] Xu Z, Kartashov Y V and Torner L, 2006, Stabilization of vector soliton complexes in nonlocal nonlinear media *Phys. Rev. E* **73,** 55601.

[41] Pérez-Garc\'\ia V M and Vekslerchik V, 2003, Soliton molecules in trapped vector nonlinear Schrödinger systems *Phys. Rev. E* **67,** 61804.

[42] Kartashov Y V, Torner L, Vysloukh V A and Mihalache D, 2006, Multipole vector solitons in nonlocal nonlinear media *Opt. Lett.* **31,** 1483–5.

[43] Desyatnikov A S, Neshev D, Ostrovskaya E A, Kivshar Y S, McCarthy G, Krolikowski W and Luther-Davies B, 2002, Multipole composite spatial solitons: theory and experiment *JOSA B* **19,** 586–95.

[44] Dreischuh A, Neshev D N, Petersen D E, Bang O and Krolikowski W, 2006, Observation of attraction between dark solitons *Phys. Rev. Lett.* **96,** 43901.

[45] Segev M, Crosignani B, Yariv A and Fischer B, 1992, Spatial solitons in photorefractive media *Phys. Rev. Lett.* **68,** 923.

[46] Peccianti M, De Rossi A, Assanto G, De Luca A, Umeton C and Khoo I C, 2000, Electrically assisted self-confinement and waveguiding in planar nematic liquid crystal cells *Appl. Phys. Lett.* **77,** 7–9.

[47] Peccianti M, Conti C, Assanto G, De Luca A and Umeton C, 2004, Routing of anisotropic spatial solitons and modulational instability in liquid crystals *Nature* **432,** 733.

[48] Wyller J, Krolikowski W, Bang O and Rasmussen J J, 2002, Generic features of modulational instability in nonlocal Kerr media *Phys. Rev. E* **66,** 66615.

[49] Bang O, Krolikowski W, Wyller J and Rasmussen J J, 2002, Collapse arrest and soliton stabilization in nonlocal nonlinear media *Phys. Rev. E* **66,** 46619.

[50] Peccianti M, Brzd\kakiewicz K A and Assanto G, 2002, Nonlocal spatial soliton interactions in nematic liquid crystals *Opt. Lett.* **27,** 1460–2.

[51] Xu Z, Kartashov Y V and Torner L, 2005, Upper threshold for stability of multipole-mode solitons in nonlocal nonlinear media *Opt. Lett.* **30,** 3171–3.

[52] Méndez-Otero M M, Iturbe-Castillo M D, Rodr\íguez-Montero P and Mart\í-Panameño E, 2001, High order dark spatial solitons in photorefractive Bi12TiO20 crystal *Opt. Commun.* **193** 277–82.

[53] Otero M M M, Pérez G B, Carrasco M L A, Panameño E M, Castillo M D I and Cerda S C, 2006, Interferometric generation of dark spatial solitons in a photorefractive Bi12TiO20 crystal *Opt. Commun.* **258,** 280–7.

[54] Guo Q, Luo B, Yi F, Chi S and Xie Y, 2004, Large phase shift of nonlocal optical spatial solitons *Phys. Rev. E* **69,** 16602.

[55] Skupin S, Bang O, Edmundson D and Krolikowski W, 2006, Stability of two-dimensional spatial solitons in nonlocal nonlinear media *Phys. Rev. E* **73,** 66603.

[56] Kartashov Y V and Torner L, 2007, Gray spatial solitons in nonlocal nonlinear media *Opt. Lett.* **32,** 946–8.

[57] Krolikowski W, Bang O, Briedis D, Dreischuh A, Edmundson D, Luther-Davies B, Neshev D, Nikolov N, Petersen D E, Rasmussen J J and Wyller J, 2005, Nonlocal soliton *Proc. SPIE* **5949,** 59490B – 1.

[58] Suarez P, 2016, An introduction to the split step Fourier method using MATLAB.

[59] Fisher R A and Bischel W K, 1975, Numerical studies of the interplay between self-phase modulation and dispersion for intense plane-wave laser pulses *J. Appl. Phys.* **46,** 4921–34.

[60] López-Aguayo S, Ochoa-Ricoux J P and Gutiérrez-Vega J C, 2006, Exploring the behavior of solitons on a desktop personal computer *Rev. Mex. Fis. E* **52,** 28–36.

[61] Govind P A and others, 2001, Nonlinear fiber optics *Opt. Photonics, Acad. Press. San*

Diego, Calif.

[62] González-Gaxiola O and Biswas A, 2018, W-shaped optical solitons of Chen--Lee--Liu equation by Laplace--Adomian decomposition method *Opt. Quantum Electron.* **50,** 314.

[63] Wazwaz A-M and Kaur L, 2019, Optical solitons for nonlinear Schrödinger (NLS) equation in normal dispersive regimes *Optik (Stuttg).* **184,** 428–35.

[64] Samiullah M, 2015, *A first course in vibrations and waves* (Oxford University Press).

[65] Chaurasiya H and Kaur A, 2013, Multi-humped pulses interaction resulting in temporal spreading, *Int. J. Adv. Eng. Technol.* **6,** 1237.

[66] Shkunov V V and Anderson D Z, 1998, Radiation transfer model of self-trapping spatially incoherent radiation by nonlinear media *Phys. Rev. Lett.* **81,** 2683.

[67] Chiao R Y, Garmire E and Townes C H, 1965, Self-Trapping of Optical Beams. *Phys. Rev. Lett.* **14,** 1056.

[68] Martinez D R, Otero M M M, Carrasco M L A and Castillo M D I, 2012, Waveguide properties of the asymmetric collision between two bright spatial solitons in Kerr media. *Opt. Express* **20,** 27411–8.

[69] Tabiryan N V, 1986, NV Tabiryan, AV Sukhov, and B. Ya. Zel'dovich, Mol. Cryst. Liq. Cryst. 136, 1 (1986). *Mol. Cryst. Liq. Cryst.* **136,** 1.

[70] Jánossy I ,1994, Molecular interpretation of the absorption-induced optical reorientation of nematic liquid crystals *Phys. Rev. E* **49,** 2957.

[71] Karpierz M A, Domanski A W, Sierakowski M, Swillo M and Wolinski T R, 1999, Optical nonlinearity in liquid crystalline optical waveguides *Acta Phys. Pol. A Gen. Phys.* **95,** 783–92.

[72] Karpierz M A 2001 Soliton Driven Photonics, eds. AD Boardman and AP Sukhorukov.

[73] Warenghem M, Henninot J F and Abbate G, 1998, Bulk optical fréedericksz effect: Non linear optics of nematics liquid crystals in capillaries *Mol. Cryst. Liq. Cryst. Sci. Technol. Sect. A. Mol. Cryst. Liq. Cryst.* **320,** 207–30.

[74] Taylor J R, 1992, *Optical solitons: theory and experiment* vol 10 (Cambridge University Press).

[75] Peccianti M, 2002, M. Peccianti and G. Assanto, Phys. Rev. E 65, 035603 (R). *Phys. Rev. E* **65,** 35603.

[76] Peccianti M, 2001, M. Peccianti and G. Assanto, Opt. Lett. 26, 1791, (2001). *Opt. Lett.* **26,**

1791.

[77] Kashyap R, 2009, *Fiber bragg gratings* (Academic press).

[78] Meltz G, Morey W and Glenn W H, 1989, Formation of Bragg gratings in optical fibers by a transverse holographic method *Opt. Lett.* **14,** 823–5.

[79] Segev M, 1998, Optical spatial solitons *Opt. Quantum Electron.* **30,** 503–33.

[80] Kivshar Y S and Luther-Davies B, 1998, Dark optical solitons: physics and applications *Phys. Rep.* **298,** 81–197.

[81] Aitchison J S, Al-Hemyari K, Ironside C N, Grant R S and Sibbett W, 1992, Observation of spatial solitons in AlGaAs waveguides *Electron. Lett.* **28,** 1879–80.

[82] Kewitsch A S and Yariv A, 1996, Self-focusing and self-trapping of optical beams upon photopolymerization *Opt. Lett.* **21,** 24–6.

[83] Stegeman, George I and Segev M, 1999, Optical Spatial Solitons and Their Interations: Universality and Diversity *Science (80-.).* **286,** 1518–22.

[84] Luther-Davies B and Yang X, 1992, Steerable optical waveguides formed in self-defocusing media by using dark spatial solitons *Opt. Lett.* **17,** 1755–7.

[85] Barthelemy A 1988 Opt. Com-mun. 55, 201 (1985); S. Maneuf, R. Desailly, and C. Froehly *Opt. Commun* **65,** 193.

[86] Aitchison J S, Weiner A M, Silberberg Y, Leaird D E, Oliver M K, Jackel J L and Smith P W E, 1991, Experimental observation of spatial soliton interactions *Opt. Lett.* **16,** 15–7.

[87] Kivshar Y S and Agrawal G, 2003, *Optical solitons: from fibers to photonic crystals* (Academic press).

[88] Królikowski W and Bang O, 2001, Solitons in nonlocal nonlinear media: Exact solutions *Phys. Rev. E - Stat. Nonlinear, Soft Matter Phys.* **63,** 1–6.

[89] Anderson D and Lisak M, 1985, Bandwidth limits due to incoherent soliton interaction in optical-fiber communication systems *Phys. Rev. A* **32** 2270.

[90] Gordon J P, 1983, Interaction forces among solitons in optical fibers *Opt. Lett.* **8** ,596–8.

[91] Shalaby M, Reynaud F and Barthelemy A, 1992, Experimental observation of spatial soliton interactions with a $π$/2 relative phase difference *Opt. Lett.* **17,** 778–80.

[92] Snyder A W and Sheppard A P, 1993, Collisions, steering, and guidance with spatial solitons *Opt. Lett.* **18,** 482–4.

[93] Gatz S and Herrmann J, 1992, Soliton collision and soliton fusion in dispersive materials

with a linear and quadratic intensity depending refraction index change *IEEE J. Quantum Electron.* **28,** 1732–8.

[94] Miller P D and Akhmediev N N, 1996, Transfer matrices for multiport devices made from solitons *Phys. Rev. E* **53,** 4098.

[95] Akhmediev N and Ankiewicz A, 1993, Spatial soliton X-junctions and couplers *Opt. Commun.* **100** ,186–92.

[96] Shalaby M and Barthelemy A, 1992, Ultrafast photonic switching and splitting through cross-phase modulation with a spatial solitons couple *Opt. Commun.* **94** ,341–5.

[97] Kodama Y and Hasegawa A, 1991, Effects of initial overlap on the propagation of optical solitons at different wavelengths *Opt. Lett.* **16,** 208–10.

[98] Aitchison J S, Silberberg Y, Weiner A M, Leaird D E, Oliver M K, Jackel J L, Vogel E M and Smith P W E, 1991, Spatial optical solitons in planar glass waveguides *JOSA B* **8,** 1290–7.

[99] Nikolov N I, Neshev D, Królikowski W, Bang O, Rasmussen J J and Christiansen P L, 2004, Attraction of nonlocal dark optical solitons *Opt. Lett.* **29,** 286.

[100] Gordon J P, Leite R C C, Moore R, Porto S P S and Whinnery J R, 1965, Long-transient effects in lasers with inserted liquid samples *J. Appl. Phys.* **36,** 3–8.

[101] Gatz S and Herrmann J, 1998, Anisotropy, nonlocality, and space-charge field displacement in (2+ 1)-dimensional self-trapping in biased photorefractive crystals *Opt. Lett.* **23,** 1176–8.

[102] Griesmaier A, Werner J, Hensler S, Stuhler J and Pfau T, 2005, Bose-Einstein condensation of chromium *Phys. Rev. Lett.* **94,** 160401.

[103] Sic H Y and Austra T, 2003, Optical Beams in Nonlocal Nonlinear Med ia **3.**

[104] Krolikowski W, Bang O, Rasmussen J J and Wyller J, 2001, Modulational instability in nonlocal nonlinear Kerr media *Phys. Rev. E* **64,** 16612.

[105] Arfken G B, Weber H J and Harris F E, 2013, *Mathematical Methods for Physicists*

Chapter 6: **Appendix**

6.1 **Fourier Transform of derivatives** [105]

In the case that $g(\omega)$ if Fourier transform of $f(x)$, we have:

$$g(\omega) = F.T\big(f(x)\big) = \frac{1}{\sqrt{2\pi}}\int_{-\infty}^{+\infty} f(x)e^{-i\omega x}dx \tag{6.1}$$

And Fourier transform for $\frac{df(x)}{dx}$:

$$g_1(\omega) = \frac{1}{\sqrt{2\pi}}\int_{-\infty}^{+\infty} \frac{df(x)}{dx}e^{-i\omega x}dx \tag{6.2}$$

Integrating by parts, results: $u = e^{-i\omega x}, dv = \frac{df(x)}{dx}dx$

$$g_1(\omega) = \frac{e^{-i\omega x}}{\sqrt{2\pi}}f(x)|^{+\infty}{}_{-\infty} - \frac{-i\omega}{\sqrt{2\pi}}\int_{-\infty}^{+\infty} f(x)e^{-i\omega x}dx \tag{6.3}$$

If $f(x)$ vanishes as $x \to \pm\infty$, then we have:

$$g_1(\omega) = i\omega g(\omega) = i\omega \times F.T\big(f(x)\big) \tag{6.4}$$

$g_1(\omega)$, the transform of the derivative is $-i\omega$ times the transform of the original function.

This may readily be generalized to the nth derivative to yield

$$g_n(\omega) = (i\omega)^n * g(\omega) = (i\omega)^n * F.T\big(f(x)\big) \tag{6.5}$$

Another way of calculating the Fourier transform of derivative function:

$$g(v_x) = F.T[f(x)] = \int_{-\infty}^{+\infty} f(x)e^{-i2\pi v_x x}dx \to Fourier\ transform \tag{6.6}$$

$$f(x) = I.F.T[g(v_x)] = \int_{-\infty}^{+\infty} g(v_x)e^{+i2\pi v_x x}dv_x \to Inverse\ Fourier\ transform \tag{6.7}$$

$$\frac{d}{dx}f(x) = \frac{d}{dx}\int_{-\infty}^{+\infty} g(v_x)e^{+i2\pi v_x x}dv_x = \int_{-\infty}^{+\infty} g(v_x)i2\pi v_x\, e^{+i2\pi v_x x}dv_x = I.F.T[g(v_x)i2\pi v_x]$$

$$F.T\left[\frac{d}{dx}f(x)\right] = F.T\left[I.F.T[g(\nu_x)i2\pi\nu_x]\right] = g(\nu_x)i2\pi\nu_x \qquad (6.8)$$

And in the same way it is possible to demonstrate that:

$$F.T\left[\frac{d^n}{dx^n}f(x)\right] = F.T\left[I.F.T[g(\nu_x)(i2\pi\nu_x)^n]\right] = g(\nu_x)(i2\pi\nu_x)^n \qquad (6.9)$$

6.2 MATLAB Programs

```
% this program is going to simulate one dimensional Gaussian beam
% propagation, in linear medium, in z-direction, started in z=0.
clc, clearvars, close all % to clear all previous information
Xi=-30; Xf=30;          % initial and final Normalized points X=x/w0
Numdata=(2^10);         % Number of points which are even and a power of 2
X=linspace(Xi,Xf,Numdata+1);  % Zero included X range
X=X(1:Numdata);      % Zero included X range with even number of points
Deltax=Xf-Xi;           % whole width in space
delta_nu=1/Deltax;         % increment of spatial frequency
Angular=(-Numdata/2: Numdata/2-1)*2*pi*delta_nu; % Range of Angular frequencies
XL=5;     % X limitation for limiting the figure demonstration
lambda=600*1e-6;       % wavelength in free space 600 nm
w0=1;                % beam width (millimeter) w0=10^3 micrometer
n=1.5;               % refractive index of medium
Zr=(n*pi*(w0^2))/lambda;  % Rayleigh range in medium
   L_d=1;  % if we consider L_d as Rayleigh range
   L_nl=1; % if we consider L_nl is nonlinear diffraction length
eta=L_d/L_nl ;   % eta is relation between (L_d & L_nl)
%% Initial Beam Profile
AX=1*exp(- ((X).^2));     % initial Gaussian beam
I_AX=abs(AX).^2;          % Intensity of initial beam
```

```
figure(1)     % real part of initial beam is figured
  plot(X,real(AX),'r'),  title('Real part of Incident beam')
     xlabel('X axis'), ylabel('Normalized Amplitude'), xlim([-XL,XL]);
figure(2)    % imaginary part of incident beam
  plot(X,imag(AX),'r') , xlabel('X axis'), ylabel('Normalized Amplitude'),
 title('Imaginary part of Incident  beam'),  xlim([-XL,XL]);
figure(4)     % initial intensity is figured
  plot(X,I_AX,'r' ),     title('Intensity of incident beam')
     xlim([-XL,XL]),   xlabel('X axis'),  ylabel('Normalized Intensity')
ang1=unwrap(angle(AX))/(2*pi);   % phase of Initial beam
figure(5) % for plotting the initial phase
  plot(X,ang1,'r'),     title('Phase of initial beam Sech')
     ylim([-0.1,0.55]), xlim([-XL,XL]), xlabel('X axis'), ylabel('Phase/(2*pi)')
dZ=(0.01)*Zr;   % increments on Z direction
H=fftshift(exp(-1i*(dZ/Zr)*(Angular.^2)/4 ));%Shifted version of Transfer function
Numstep=100;
Rayleigh_Rang_Num=1; % number of Rayleigh Range
Z=linspace(0,Rayleigh_Rang_Num,Rayleigh_Rang_Num*Numstep); % Z axis
Zeromatrix=zeros(Rayleigh_Rang_Num*Numstep,Numdata); %defining zero matrix
TotalIntensity = Zeromatrix; % defining a matrix for whole intensity
TotalIntensity(1 ,:) =I_AX; % first column of Total Intensity is filled
for ii=2:Rayleigh_Rang_Num*Numstep %started from 2, since first column
                              %of Total Intensity is filled
   AXdZ=ifft(H.*fft(AX)).* exp(-( X/(0.99*Xf) ).^50 ); % diffraction in linear
   I_AXdZ=abs(AXdZ).^2;    % Intensity of diffracted beam
   TotalIntensity(ii,:)=I_AXdZ; % whole intensity matrix
   AX=AXdZ; %repeating the loop
end
%% Intensity Calculation
figure(6) % two dimensional view for intensity
```

```
  surf(X, Z, TotalIntensity),  set(gca,'fontweight','bold','FontSize',26);
shading interp, view(2), title('Beam propagation for 100*Z_R'),
          colormap jet, colorbar, xlim([-XL,XL]), xlabel('X'), ylabel('Z')
figure(7) % three dimensional view on intensity propagation
  surf(X, Z, TotalIntensity),     set(gca,'fontweight','bold','FontSize',26);
     shading interp, title('Beam propagation for 100*Z_R')
  colormap jet, colorbar, xlim([-XL,XL]), xlabel('X'), ylabel('Z'), zlabel('Normalized Intensity')
figure(8) %on-axis intensity
  plot(Z,TotalIntensity(:,(Numdata/2)+1),'r','LineWidth',2),
set(gca,'fontweight','bold','FontSize',26),       title('On-axis Intensity plot')
       xlabel('Z') ,  ylabel('Nomalized Intensity'),  ylim([0.5,2]),
figure(11)
  plot(X,I_AX,'b',X,I_AXdZ,'r','LineWidth',2),  set(gca,'fontweight','bold','FontSize',26);
     title('Comparing Initia, Final Intensity'),     legend(' Initial',' Propagated')
        xlabel('X'), ylabel('Normalized Intensity'),  xlim([-XL,XL]);
```

Program 6-1: MATLAB program for simulation on propagation of one-dimensional transverse gaussian beam.

```
% this program is going to simulate two-dimensional Gaussian beam
% propagation, in linear medium, in z-direction, started in z=0.
clc, clearvars, close all % to clear all previous information
x0=3;            % a value to define X limitation
Xi=-x0; Xf=x0;    %  initial and final points over x-axis.
Yi=-x0; Yf=x0;    %  initial and final points over y-axis.
Numdata=(2^10);   % Number of points which are even and a power of 2
X=linspace(Xi,Xf,Numdata+1);  % Zero included X range
X=X(1:Numdata);  % Zero included X range with even number of points
Y=linspace(Yi,Yf,Numdata+1);  % Zero included Y range
Y=Y(1:Numdata);  % Zero included Y range with even number of points
deltaX=Xf-Xi;       % whole width on X axis
```

```
  deltaY=Yf-Yi;       % whole width on Y axis
    delta_nuX=1/deltaX; % % increment of spatial frequency for X axis
      delta_nuY=1/deltaY; % increment of spatial frequency for Y axis
nuX=(-(Numdata/2): (Numdata/2)-1)*2*pi*delta_nuX; %Angular frequencies range for X axis
nuY=(-(Numdata/2): (Numdata/2)-1)*2*pi*delta_nuY; %Angular frequencies range for Y axis
[x,y]=meshgrid(X,Y); % mesh grid over X and Y
[nux,nuy]=meshgrid(nuX,nuY); % mesh grid over spatial frequencies
lambda=600*1e-6;        % wavelength in free space 600 nm=600*1e-6 mm
w0=1;                   % beam width (millimeter) w0=10^3 micrometer
A0=1;                   % a constant
n=1.5;                  % refractive index
Zr=(n*pi*w0^2) /lambda; % Rayleigh range
Axy=A0*exp(- x.^2- y.^2);    %Initial Gaussian beam profile
I_Axy=abs(Axy).^2;            % Intensity of initial beam
figure(1)  % Three dimensional view over initial intensity
  mesh(x,y,I_Axy);  shading interp,   title ('Initial Intensity')
       set(gca,'fontweight','bold','FontSize',26);
colorbar, colormap jet, xlim([-x0,x0]), ylim([-x0,x0]), xlabel('X'),  ylabel('Y'),
zlabel('Normalized Intensity')
figure(2)    % Two dimensional view over initial intensity
  imagesc(X,Y,I_Axy),  shading interp,   title('Initial Gaussian beam')
       set(gca,'fontweight','bold','FontSize',26);
        colorbar, colormap jet, xlim([-x0,x0]), ylim([-x0,x0]), xlabel('X '), ylabel('Y')
dZ=0.01*Zr;    % increments on Z direction
H=fftshift(exp(-1i*(dZ/Zr)*(nux.^2+nuy.^2)/4)); % Shifted version of Transfer function
Numstep=100;
for ii=1:Numstep
   Axydz=ifft2(H.*fft2(Axy));    % diffraction in linear
   I_Axydz=abs(Axydz).^2;        % Intensity of propagated beam
   Axy=Axydz;                    %repeating the loop
```

```
end
figure(3)  % Three dimensional view for propagated intensity
  mesh(x,y,I_Axydz),  shading interp, colorbar, colormap jet
        title('Output Gaussian beam after Z_R'),   set(gca,'fontweight','bold','FontSize',26);
  xlim([-x0,x0]), ylim([-x0,x0]), zlim([0,1]), xlabel('X'), ylabel('Y')
                  zlabel('Normalized Intensity')
figure(4) % Two dimensional view for propagated intensity
imagesc(X,Y,I_Axydz),  shading interp,   title('output Gaussian beam after Z_R')
colorbar, colormap jet, set(gca,'fontweight','bold','FontSize',26);
           xlim([-x0,x0]), ylim([-x0,x0]), xlabel('X'), ylabel('Y')
```

Program 6-2: MATLAB program for simulation on propagation of two-dimensional transverse gaussian beam.

```
% one dimensional Secant Hyperbolic beam propagation in third order nonlinear media
clc, clearvars, close all % to clear all previous information
Xi=-30; Xf=30;            % initial and final Normalized points X=x/w0
Numdata=(2^10);           % Number of points which are even and a power of 2
X=linspace(Xi,Xf,Numdata+1);  % Zero included X range
X=X(1:Numdata);     % Zero included X range with even number of points
stepx=X(2)-X(1);
Deltax=Xf-Xi;             % whole width in space
delta_nu=1/Deltax;          % increment of spatial frequency
Angular=(-Numdata/2: Numdata/2-1)*2*pi*delta_nu; % Range of Angular frequencies
XL=5;     % X limitation for limiting the figure demonstration
lambda=600*1e-6;        % wavelength in free space 600 nm
w0=1;                % beam width (millimeter) w0=10^3 micrometer
n=1.5;               % refractive index of medium
Zr=(n*pi*(w0^2))/lambda;  % Rayleigh range in medium
   L_d=1;  % if we consider L_d as Rayleigh range
   L_nl=1; % if we consider L_nl is nonlinear diffraction length
```

```
eta=L_d/L_nl ;   % eta is relation between (L_d & L_nl)
% eta value be positive or negative
A0=1;           % normalized initial amplitude
%% Initial Beam Profile
AX=A0*sech(sqrt(2)*X);    % initial Secant Hyperbolic beam
%  AX=A0*tanh(sqrt(2)*X);    % initial Tangent Hyperbolic beam
I_AX=abs(AX).^2;            % Intensity of initial beam
Pi=0;  % Pi is the initial power that is constant during propagation
for n=1:Numdata
   Pi=(stepx * I_AX(n))+Pi;
end
Pi
figure(1)     % real part of initial beam is figured
  plot(X,real(AX),'r'),   title('Real part of Incident beam')  % title of figure
     xlabel('X axis') , ylabel('Normalized Amplitude'), xlim([-XL,XL]);
figure(2)    % imaginary part of incident beam
  plot(X,imag(AX),'r'), xlabel('X axis') , ylabel('Normalized Amplitude'),
title('Imaginary part of Incident  beam') ,   xlim([-XL,XL]);
figure(3)     % initial intensity is figured
  plot(X,I_AX,'r' ), title('Intensity of incident beam'), xlim([-XL,XL]);
       xlabel('X axis'),   ylabel('Normalized Intensity'  )
ang1=unwrap(angle(AX))/(2*pi);   % phase of Initial beam
figure(4)  % for plotting the initial phase
  plot(X,ang1,'r'),  title('Phase of initial beam')
ylim([-0.1,0.55])  , xlim([-XL,XL]),  xlabel('X axis'), ylabel('Phase/(2*pi)')
dZ=(0.01)*Zr;   % increments on Z direction
H=fftshift(exp(-1i*(dZ/Zr)*(Angular.^2)/4 ));%Shifted version of Transfer function
Numstep=100;
Rayleigh_Rang_Num=100;  % number of Rayleigh Range
Z=linspace(0,Rayleigh_Rang_Num , Rayleigh_Rang_Num*Numstep); % Z axis
```

```
Zeromatrix=zeros(Rayleigh_Rang_Num*Numstep , Numdata); %defining zero matrix
TotalIntensity = Zeromatrix; % total intensity matrix
TotalIntensity(1 ,:) =I_AX;
for ii=2:Rayleigh_Rang_Num * Numstep % started from 2, since first column
                                % of Total Intensity is filled
   AXdZ=ifft(H.*fft(AX)).* exp(-( X/(0.99*Xf) ).^50 ); % diffraction in linear
   I_AXdZ=abs(AXdZ).^2;    % Intensity of diffracted beam
   %% local media
   N=I_AXdZ;    % N is Nonlinear Operator
   AXdZN=AXdZ.*exp(  1i*eta*N*(  dZ/Zr )  ); % applying self-focusing
   I_AXdZN=abs(AXdZN).^2;
   TotalIntensity(ii,:)=I_AXdZN; % developing whole intensity matrix
   AX=AXdZN;  %repeating the loop
end
%% Intensity Calculation
figure(5) % two dimensional view for intensity propagation
  surf(X, Z, TotalIntensity),  set(gca,'fontweight','bold','FontSize',26);
shading interp, view(2), title('Intensity') , colormap jet,  colorbar, xlim([-XL,XL]),
xlabel('X'),  ylabel('Z')
figure(6)  % three dimensional view on intensity propagation
  surf(X, Z, TotalIntensity), set(gca,'fontweight','bold','FontSize',26);
shading interp, title('Intensity') , colormap jet, colorbar,  xlim([-XL,XL]);
  xlabel('X'),  ylabel('Z'),   zlabel('Normalized Intensity')
```

Program 6-3: Simulation of Sech or Tanh initial beam profile propagating by MATLAB in Kerr medium.